National Library
of Canada

Bibliothèque nationale
du Canada

Canadian Theses Service

Services des thèses canadiennes

Ottawa, Canada
K1A 0N4

CANADIAN THESES

THÈSES CANADIENNES

NOTICE

The quality of this microfiche is heavily dependent upon the quality of the original thesis submitted for microfilming. Every effort has been made to ensure the highest quality of reproduction possible.

If pages are missing, contact the university which granted the degree.

Some pages may have indistinct print especially if the original pages were typed with a poor typewriter ribbon or if the university sent us an inferior photocopy.

Previously copyrighted materials (journal articles, published tests, etc.) are not filmed.

Reproduction in full or in part of this film is governed by the Canadian Copyright Act, R.S.C. 1970, c. C-30.

AVIS

La qualité de cette microfiche dépend grandement de la qualité de la thèse soumise au microfilmage. Nous avons tout fait pour assurer une qualité supérieure de reproduction.

S'il manque des pages, veuillez communiquer avec l'université qui a conféré le grade.

La qualité d'impression de certaines pages peut laisser à désirer, surtout si les pages originales ont été dactylographiées à l'aide d'un ruban usé ou si l'université nous a fait parvenir une photocopie de qualité inférieure.

Les documents qui font déjà l'objet d'un droit d'auteur (articles de revue, examens publiés, etc.) ne sont pas microfilmés.

La reproduction, même partielle, de ce microfilm est soumise à la Loi canadienne sur le droit d'auteur, SRC 1970, c. C-30.

THIS DISSERTATION
HAS BEEN MICROFILMED
EXACTLY AS RECEIVED

LA THÈSE A ÉTÉ
MICROFILMÉE TELLE QUE
NOUS L'AVONS REÇUE

Canada

NL-339 (r.86/06)

THE UNIVERSITY OF ALBERTA

SOLVENT EXTRACTION / FLOW INJECTION ANALYSIS FOR THE DETERMINATION OF ANIONIC SURFACTANTS

by

EDUARDO CASTANEDA SALDIVAR

A THESIS SUBMITTED TO
THE FACULTY OF GRADUATE STUDIES AND RESEARCH
IN PARTIAL FULFILMENT OF THE REQUIREMENTS FOR THE
DEGREE OF MASTER OF SCIENCE

DEPARTMENT OF CHEMISTRY

EDMONTON, ALBERTA
SPRING 1986

Permission has been granted to the National Library of Canada to microfilm this thesis and to lend or sell copies of the film.

The author (copyright owner) has reserved other publication rights, and neither the thesis nor extensive extracts from it may be printed or otherwise reproduced without his/her written permission.

L'autorisation a été accordée à la Bibliothèque nationale du Canada de microfilmer cette thèse et de prêter ou de vendre des exemplaires du film.

L'auteur (titulaire du droit d'auteur) se réserve les autres droits de publication; ni la thèse ni de longs extraits de celle-ci ne doivent être imprimés ou autrement reproduits sans son autorisation écrite.

ISBN 0-315-30137-6

THE UNIVERSITY OF ALBERTA

RELEASE FORM

NAME OF AUTHOR EDUARDO CASTANEDA SALDIVAR
TITLE OF THESIS SOLVENT EXTRACTION / FLOW INJECTION ANALYSIS FOR THE DETERMINATION OF ANIONIC SURFACTANTS
DEGREE FOR WHICH THESIS WAS PRESENTED M. Sc.
YEAR THIS DEGREE GRANTED 1986

Permission is hereby granted to THE UNIVERSITY OF ALBERTA LIBRARY to reproduce single copies of this thesis and to lend or sell such copies for private, scholarly or scientific research purposes only.

The author reserves other publication rights, and neither the thesis nor extensive extracts from it may be printed or otherwise reproduced without the author's written permission.

Eduardo
(Signed)

PERMANENT ADDRESS:
PRIV. DE LAS FLORES # 3
COL. SAN ANTON,
CUERNAVACA, MOR., 62020
MEXICO

DATE : March 18, 1986

THE UNIVERSITY OF ALBERTA

FACULTY OF GRADUATE STUDIES AND RESEARCH

The undersigned certify that they have read, and recommend to the Faculty of Graduate Studies and Research, for acceptance, a thesis entitled SOLVENT EXTRACTION / FLOW INJECTION ANALYSIS FOR THE DETERMINATION OF ANIONIC SURFACTANTS submitted by EDUARDO CASTANEDA SALDIVAR in partial fulfilment of the requirements for the degree of MASTER OF SCIENCE

Frederick F. Cantwell
F. F. CANTWELL, SUPERVISOR

Byron Kratochvil
B. KRATOCHVIL

Loren G. Hepler
L. G. HEPLER

P Fedorak
P. FEDORAK

DATE: March 18, 1986

This thesis is dedicated to Juan and Marta, my parents, for their encouragement during my student years; and to Maria Luisa, my wife, for her support and understanding.

ABSTRACT

The objective of the present work is the automation of a manual method for the determination of anionic surfactants by ion pair formation with ethyl violet. A solvent extraction/flow injection analysis apparatus is described and characterized, utilizing sodium lauryl sulfate as a model compound, in terms of variables such as ethyl violet concentration, buffer concentration, added electrolyte concentration, injection volume, and extraction coil length. The ethyl violet-anionic surfactant ion pairs are extracted into the organic phase and detected spectrophotometrically at 546 nm. In the final procedure, an acetate buffer is used to control the pH at 4.6 and sodium sulfate is used to facilitate the extraction of the ion pairs into the organic phase.

Several problems arising from the properties of surface active samples are discussed. Among these problems are the formation of a charged colloid of the ethyl violet-anionic surfactant precipitate; interfacial adsorption of dye, surfactant, and ion pair; and micellization of the surfactant. The system is designed in such a manner as to avoid these problems.

Variations of solubility in toluene were observed among several batches of ethyl violet. The batches were characterized by UV-VIS, IR, proton NMR, and mass spectroscopy as well as by melting point and thin layer chromatography. It was concluded that the batches were chemically identical and differed only in crystal structure.

Several common anionic surfactants such as sodium lauryl sulfate, sodium alkyl aryl sulfonate, and sodium dodecyl benzene sulfonate are examined and their calibration curves obtained. Also, some surface active agents utilized in the enhanced recovery of oil are analyzed and the results compared to the values obtained via a two-phase titration method. Determinations are performed with a sample frequency of 30 samples/hour and a precision of 2% in contrast to the manual method where the sample frequency is about 5 samples/hour and the precision is about the same. The dynamic range of the method is about 1 to 100 ppm, thereby allowing the determination of low levels of surfactants in environmental samples or of more concentrated samples upon appropriate dilution.

Finally, some of the advantages and disadvantages of the present method are discussed, and some future studies are suggested.

ACKNOWLEDGEMENTS

I would like to express my gratitude to Dr. F. F. Cantwell for his invaluable assistance and guidance throughout the various stages of this work, and for his understanding during my studies.

Thanks are extended to M.Luisa Castaneda and to Veronica de la Mora for their help in typing and drafting this thesis; as well as to James Nolan for proofreading the entire manuscript.

The author would like to acknowledge E. Isaacs and C. McCarthy from the Oil Sands Research department in the Alberta Research Council for kindly providing samples and information.

TABLE OF CONTENTS

CHAPTER PAGE

1. INTRODUCTION 1
    1.1 SURFACTANTS 1
        1.1.1 DEFINITION 1
        1.1.2 PROPERTIES 2
        1.1.3 CLASSIFICATION 4
        1.1.4 USES 5
        1.1.5 ANALYSIS 7
    1.2 FLOW INJECTION ANALYSIS 9
        1.2.1 DESCRIPTION 9
        1.2.2 DEVELOPMENT OF FIA 11
        1.2.3 APPLICATIONS 15
2. OPTIMIZATION OF THE SE/FIA SYSTEM FOR SURFACTANT ANALYSIS 17
    2.1 INTRODUCTION 17
    2.2 EXPERIMENTAL 18
        2.2.1 CHEMICALS AND SOLVENTS 18
        2.2.2 APPARATUS 20
    2.3 RESULTS AND DISCUSSION 23
        2.3.1 VERIFYING THE MANUAL METHOD 23
        2.3.2 DYE CONCENTRATION 28
        2.3.3 BUFFER CONCENTRATION 33
        2.3.4 SODIUM SULFATE CONCENTRATION 38
        2.3.5 EXTRACTION COIL LENGTH 41

2.3.6 EFFECT OF ADDED ELECTROLYTE 52
2.3.7 SAMPLE INJECTION VOLUME 55
2.3.8 CALIBRATION CURVES WITH SLS 68
2.3.9 ETHYL VIOLET.. 96
3. DETERMINATION OF ANIONIC SURFACTANTS 127
3.1 INTRODUCTION.. 127
3.2 EXPERIMENTAL.. 127
3.2.1 CHEMICALS AND SOLVENTS 127
3.2.2 APPARATUS.. 128
3.2.3 PROCEDURE.. 132
3.3 RESULTS AND DISCUSSION.. 133
3.3.1 TRS 10-80.. 133
3.3.2 ENORDET.. 134
3.3.3 SUNTECH IV.. 140
3.3.4 COMMENTS... 153
BIBLIOGRAPHY.. 155

LIST OF TABLES

PAGE

Table I. Calibration curve data for the absorbance of the sodium dodecyl sulfate-ethyl violet ion pair.. 25

Table II. Peak height as a function of dye concentration in the absence of buffer and sodium sulfate.. 30

Table III. Peak height as a function of acetic acid concentration.......... 35

Table IV. Peak height as a function of sodium sulfate concentration....... 39

Table V. Absorbance values of blanks for various concentrations of dye, acetate buffer, and sodium sulfate.. 42

Table VI. "Raw data" of peak heights and peak widths at half-height as a function of variable extraction coil length.. 44

Table VII. "Raw data" of peak heights and peak widths at half-height as a function of variable extraction coil length in the absence of sodium sulfate.. 45

Table VIII. "Raw data" of peak heights and peak widths at half-height as a function of variable extraction coil length in the absence of sodium sulfate and buffer.. 46

Table IX. Corrected peak heights and peak areas as a function of variable extraction coil length.. 47

Table X. Corrected peak heights and peak areas as a function of variable extraction coil length in the absence of sodium sulfate.. 48

Table XI. Corrected peak heights and peak areas as a function of variable extraction coil length in the absence of sodium sulfate and buffer............ 49

Table XII. Effect of added electrolyte.. 54

Table XIII. Variations of peak area, height, and width with injection volume for "high" surfactant concentrations utilizing the dye dissolved in water........ 57

Table XIV. Variations of peak area, height, and width with injection volume for "low" surfactant concentrations utilizing the dye dissolved in water........ 60

Table XV. Variation of peak area, height, and width with injection volume for "medium" surfactant concentrations utilizing the dye dissolved in toluene........ 63

Table XVI. Calibration curve #1........ 69

Table XVII. Calibration curve #2........ 71

Table XIII. Calibration curve #3........ 73

Table XIX. Calibration curve #4........ 75

Table XX. Calibration curve data for ethyl violet........ 80

Table XXI. Beer's law plot for one dye-surfactant ion pair solution........ 84

Table XXII. Beer's law plot for several dye-surfactant ion pair solutions... 87

Table XXIII. "Raw data" of peak heights and peak widths as a function of variable extraction coil length using the dye dissolved in toluene........ 92

Table XXIV. Corrected peak heights and peak areas as a function of variable extraction coil length utilizing the dye dissolved in toluene........ 93

Table XXV. Thin layer chromatography retention factors of ethyl violet batches 0-1 and N-2........ 101

Table XXVI. Solubility of ethyl violet batch N-2........ 115

Table XXVII. Sodium lauryl sulfate calibration curve data........ 118

Table XXVIII. Sodium alkyl aryl sulfonate calibration curve data........ 122

Table XXIX. Sodium dodecyl benzene sulfonate calibration curve data.... 125

Table XXX. TRS 10-80 calibration curve data........ 135

Table XXXI. Sodium lauryl sulfonate calibration curve data.................... 138
Table XXXII. Interfacial adsorption data... 143
Table XXXIII. Assay values under non-stirring/stirring conditions.......... 144
Table XXXIV. Avoiding micellization of Suntech IV.............................. 151
Table XXXV. Assay data of samples.. 152

LIST OF FIGURES

PAGE

Figure 1. Velocity profiles of carrier.. 12

Figure 2. Block diagram of the SE/FIA apparatus utilized for the optimization of the system.. 21

Figure 3. Absorption spectra of the ethyl violet-dodecyl sulfate ion pair in toluene.. 24

Figure 4. Calibration curve for the dodecyl sulfate-ethyl violet ion pair (manual method)... 26

Figure 5. Calibration curve for the dodecyl sulfate-ethyl violet ion pair over a wider concentration range (manual method)........................ 27

Figure 6. Replicate injections of a sodium dodecyl sulfate solution.......... 29

Figure 7. Peak height as a function of dye concentration........................ 31

Figure 8. Peak height as a function of acetic acid concentration.............. 36

Figure 9. Peak height as a function of sodium sulfate concentration......... 40

Figure 10. Corrected peak heights as a function of variable extraction coil length.. 50

Figure 11. Corrected peak areas as a function of variable extraction coil length... 51

Figure 12. Normalized peak area versus injection volume for "high" surfactant concentrations and the dye dissolved in water................ 58

Figure 13. Peak width and normalized peak height versus injection volume for "high" surfactant concentrations and the dye dissolved in water.. 59

Figure 14. Normalized peak area versus injection volume for "low" surfactant concentrations and the dye dissolved in water.......................... 61

Figure 15. Peak width and normalized peak height versus injection volume for "low" surfactant concentrations and the dye dissolved in water.. 62
Figure 16. Normalized peak area versus injection volume for "medium" surfactant concentrations and the dye dissolved in toluene........ 64
Figure 17. Peak width and normalized peak height versus injection volume for "medium" surfactant concentrations and the dye dissolved in toluene.. 65
Figure 18. Calibration curve #1.. 70
Figure 19. Calibration curve #2.. 72
Figure 20. Calibration curve #3.. 74
Figure 21. Calibration curve #4.. 76
Figure 22. Calibration curve for ethyl violet obtained in a spectrophotometer.. 81
Figure 23. Calibration curve for ethyl violet obtained in a flow-through detector.. 82
Figure 24. Beer's law plot for one dye-surfactant ion pair solution........... 85
Figure 25. Beer's law plot for several dye-surfactant ion pair solutions..... 88
Figure 26. VIS spectra of ethyl violet solutions..................................... 89
Figure 27. VIS spectra of dye-surfactant ion pair solutions..................... 90
Figure 28. Corrected peak heights as a function of variable extraction coil lenght using the dye dissolved in toluene.. 94
Figure 29. Corrected peak areas as a function of variable extraction. coil length using the dye dissolved in toluene.. 95
Figure 30. UV-VIS absorption spectra of ethyl violet.............................. 99
Figure 31. IR absorption spectrum of ethyl violet batch 0-1 in methanol.. 102

Figure 32. IR absorption spectrum of ethyl violet batch N-2 in methanol.. 103
Figure 33. IR absorption spectrum of ethyl violet batch 0-1 in nujol........ 104
Figure 34. IR absorption spectrum of ethyl violet batch N-2 in nujol....... 105
Figure 35. Electron impact mass spectrum of ethyl violet batch 0-1......... 107
Figure 36. Electron impact mass spectrum of ethyl violet batch N-2........ 108
Figure 37. Fast atom bombardment mass spectrum of ethyl violet batch 0-1.. 109
Figure 38. Fast atom bombardment mass spectrum of ethyl violet batch N-2.. 110
Figure 39. Proton NMR spectrum of ethyl violet batch 0-1....................... 112
Figure 40. Proton NMR spectrum of ethyl violet batch N-2...................... 113
Figure 41. Sodium lauryl sulfate calibration curve (peak heights)............. 119
Figure 42. Sodium lauryl sulfate calibration curve (peak areas)............... 120
Figure 43. Sodium alkyl aryl sulfonate calibration curve......................... 123
Figure 44. Sodium dodecyl benzene sulfonate calibration curve............... 126
Figure 45. Block diagram of the solvent extraction/flow injection analysis system utilized in the determination of surfactant samples............ 129
Figure 46. Diagram of the apparatus used to determine interfacial adsorption.. 131
Figure 47. TRS 10-80 calibration curve.. 136
Figure 48. Sodium lauryl sulfonate calibration curve.............................. 139
Figure 49. Spectrophotometric recorder tracing for the determination of interfacial adsorption.. 142
Figure 50. Block diagram of the modified solvent extraction/flow injection analysis system utilized in the determination of surfactants.......... 149

LIST OF SYMBOLS

Symbol	Description
FIA	Flow injection analysis.
SE/FIA	Solvent extraction/flow injection analysis.
s.d.	Standard deviation.
r.s.d.	Relative standard deviation.
$F_{o,t}$	Total volumetric flow rate of organic phase.
$F_{a,t}$	Total volumetric flow rate of aqueous phase.
F_c	Volumetric flow rate of carrier.
a.i.u.	Arbitrary integrator units.
AUFS	Absorbance units at full scale.
ppm	Parts per million.
SLS	Sodium lauryl sulfate.
SLSN	Sodium dodecane sulfonate (sodium lauryl sulfonate).
SAAS	Sodium alkyl aryl sulfonate.
SDBS	Sodium dodecyl benzene sulfonate.
nm	Nanometers.
M	Molar (moles/liter).
a.m.u.	Atomic mass units.
e.s.u.	Electrostatic units.
psig	Pounds per square inch at the gauge.
VIS	Visible region of the spectrum.
UV-VIS	Ultraviolet-visible region of the spectrum.
IR	Infra-red region of the spectrum.
NMR	Nuclear magnetic resonance.

CHAPTER 1

INTRODUCTION

1.1 Surfactants

1.1.1 Definition

The word surfactant is a condensation of the descriptive phrase "surface active agent". Since the meaning that this phrase implies is too broad, surfactants are often characterized by the following fundamental properties [1,2]:

(a) Amphipathic structure. Amphipathy is the occurrance in a single molecule or ion of one or more groups which have affinity ("sympathy") for the phase in which the molecule or ion is dissolved, together with one or more groups which are antipathetic to the medium. Thus, a surfactant is an organic compound that encompasses in the same molecule two groups with opposing solubility tendencies, i.e. a water-soluble and a water-insoluble moiety.

(b) Adsorption at interfaces. The equilibrium concentration of a surfactant solute at a phase interface is greater than its concentration in the bulk of the solution. This condition is caused by adsorption of the surfactant molecules onto the various phase interfaces of the system (liquid-liquid, liquid-gas, and liquid-solid). The adsorption process may involve chemical interactions (e.g. ion-exchange, hydrogen bond formation) and/or occur through van der Waals' forces between adsorbent and adsorbate.

(c) Orientation at interfaces. Due to their amphipathic nature, surfactant molecules tend to accumulate at the phase interfaces in such an orientation as to satisfy the solubility requirements of each part of the molecule. In the specific case of an oil-water-air system, for example, the hydrophobic portion of the molecule extends into the gaseous or oil phases; whereas the hydrophilic portion remains in contact with the water. A consequence of this orientation pattern is that at the interfaces some of the water molecules are replaced by non-polar groups. Since the forces of intermolecular attraction between water molecules and non-polar groups are of smaller magnitude than those existing between water molecules alone, the contracting power of the interface is reduced, and so is the interface tension.

(d) Micelle formation. Surfactants form aggregates of molecules or ions called micelles when the concentration of the solute in the bulk of the solution exceeds a limiting value that is a fundamental characteristic of each solute-solvent system (critical micelle concentration, CMC). In aqueous systems, a micelle can be thought of as a conglomerate of as little as 20 or as many as 500 or more molecules, arranged in such a way as to have a liquid core formed by associated hydrocarbon chains with the fully ionized head groups projecting out into the water. In non-aqueous solvents, an inverted micelle is formed with the polar heads in the center and the hydrocarbon chains extended outwards into the solvent.

1.1.2 Properties

As a consequence of their rather unusual characteristics, surfactants in solution exhibit a combination of the following functional properties [1,2]:

(a) Solubilizing power. The presence of surfactants in aqueous solutions increases the solubility of insoluble or sparingly soluble organic substances. Non-polar compounds are solubilized in water when these compounds are dissolved in the hydrocarbon core of the micelles; whereas semi-polar compounds are solubilized by orienting the molecules radially in the micelle. Conversely, in non-aqueous solvents, small polar molecules and water can be solubilized within the micellar interior. Hydrogen bonding is thought to be a predominant factor in the solubilization of water. In both, aqueous and non-aqueous systems, the amount of a given sustance that can be solubilized is a function of polarity, polarizability, and steric factors.

(b) Emulsifying power. Emulsions, defined as heterogeneous systems of one liquid dispersed in another in the form of droplets, are not thermodynamically stable. Unstabilized emulsions tend to coalesce and form two phases rapidly; whereas stabilized emulsions can retain a highly dispersed internal phase for months or years. An emulsion can be stabilized by the inclusion of a surfactant in the system, which acts by forming a barrier delaying the coalescence of the droplets via a combination of steric, viscous, and elastic effects or by affecting the electrostatic charge of the dispersed droplets causing electrical repulsion.

(c) Dispersing power. As in the case of emulsions, surfactants stabilize suspensions (i.e, dispersions of solid particles in a liquid) and avoid problems of sedimentation, flocculation, etc. The stability of a suspension is governed by the same factors that control emulsions, except that coalescence obviously cannot occur. The surfactant adsorbs onto the interfaces and stabilizes the suspension through basically the same effects as in emulsions.

(d) Wetting power. When an immiscible liquid or a solid is brought together with a liquid, a process in which liquid-air or solid-air interface is replaced by liquid-liquid or solid-liquid interface occurs. This process is called wetting, and the presence of a surfactant, which would adsorb onto the interfaces, is of practical importance in the process due to the resultant changes in interfacial tension.

1.1.3 Classification

Surfactants are classified on the basis of their hydrophilic group into four categories: anionic, cationic, non-ionic, and amphoteric [1,2].

(a) Anionic surfactants. The solubilizing moiety on their hydrophilic group is negatively charged. The anions most commonly found are carboxylates, sulfonates, sulfates, and phosphates. Typical examples are: potassium laurate [$CH_3(CH_2)_{10}COO^{-+}K$] and sodium lauryl sulfate [$CH_3(CH_2)_{11}SO_4^{-+}Na$].

(b) Cationic surfactants. The water-soluble moiety of this type is positively charged. The most frequently encountered cations are primary, secondary, tertiary amines, and quaternary ammonium groups. Typical examples of this type of surfactants are: hexadecyltrimethyl ammonium bromide [$CH_3(CH_2)_{15}N^+(CH_3)_3{}^-Br$] and dodecylamine hydrochloride [$CH_3(CH_2)_{11}NH_3^{+-}Cl$].

(c) Non-ionic surfactants. The hydrophilic moiety in this type bears no charge and usually contains hydroxyl groups or a polyoxyethylene chain. Examples of this type of surfactants are: Polyoxyethylene p-tert octylphenyl ether [C_8H_{17}-C_6H_4-$O(CH_2CH_2O)_{10}H$] and polyoxyethylene monohexadecyl ether [$CH_3(CH_2)_{15}(OCH_2CH_2)_{21}OH$].

(d) Amphoteric surfactants. This type can behave either as anionic, cationic, or non-ionic species depending on the pH of the solution. A classical example is the zwitterionic form of N-dodecyl-N,N dimethylbetain [$C_{12}H_{25}N^+(CH_3)_2CH_2COO^-$], where the positively charged ammonium group behaves as a cation and the carboxylate as an anion.

1.1.4 Uses

Depending upon their properties, surfactants are used in a wide variety of industrial applications and products such as laundry detergents, pharmaceuticals, oil recovery, paints, cosmetics, pesticides, fibres, plastics, foodstuffs, and toilet preparations [1,2]. Laundry detergents represent the largest single use of surfactants. Most detergents contain as a general rule the following ingredients: anionic surfactants, inorganic builders, inorganic fillers, and special purpose additives. Anionic surfactants constitute typically 10-20% of the mixture and are responsible for the cleaning action of detergents. The most widely used are linear alkyl sulfonates and fatty alcohol sulfates. Branched alkyl benzene sulfonates are no longer used due to non-biodegradability and toxicity related problems. Inorganic builders are compounds that enhance the performance of the mixture by contributing alkalinity, by softening the water, or by increasing foaming and emulsifying power. Builders normally constitute 35-50% of the mixture, with phosphates and carbonates being the most widely used. Phosphates have the disadvantage of promoting growth of algae in lakes and rivers due to excessive fertilization. Inorganic fillers are compounds that do not contribute directly to the performance enhancement of the mixture. They are added to the product to make it easily measurable and more attractive in appearance. In the case of liquid detergents water is the main filler; whereas for solid detergents, sodium sulfate is used. The latter has the advantage of reducing the amount of surfactant required to reach the critical micelle concentration, at which maximum detergency is observed. Fillers constitute about 20-50% of the mixture. The most common special purpose additives are bleaching agents, emollients, perfumes, optical brightening agents, bactericides, abrasive agents, and enzymes.

Surfactants are widely used in the pharmaceutical industry as emulsifying agents, solubilizers, and suspension stabilizers. Emulsions, traditionally prepared with naturally occurring gums such as acacia and tragacanth, have been used in pharmacies for centuries. Surfactant-stabilized emulsions are extensively used today when insoluble drugs must be formulated, especially for intravenous feeding, where it is vital that particles remain below 1 micrometer in diameter to avoid complications. Taking advantage of the solubilizing power of surfactant micelles, several insoluble or sparingly soluble drugs can be formulated in solution form. An example of this application is a surfactant-solubilized formulation of vitamins A and D. The number of insoluble drugs that are formulated with surfactants is rather large and includes predominantly steroids, barbiturates, salicylates, antibiotics, and antibacterial compounds [1]. Pharmaceutical suspensions, which are often non-colloidal in nature, are frequently stabilized by the use of surfactants. The objective is to produce a partially deflocculated system, where the particles are not so small as to sediment and form a "cake" of closely packed particles that become irreversibly bound together; or not so big that the particles settle rapidly leaving a preparation that appears unsightly.

Surfactants are also used in oil recovery [1]. Microemulsions represent an intermediate state between micellar solutions and true emulsions. They are distinguished from emulsions by their transparency and by the fact that they represent thermodynamically stable solution phases; and from micellar solutions by the fact that microemulsions have droplet size or diameters ranging from 250 to 10 nanometers whereas micellar solutions have diameters of less than 10 nanometers. Surfactant systems capable of producing microemulsions have attracted attention because of their potential value in increasing the recovery of oil from underground reservoirs. Anionic surfactants, usually alkyl olefin sulfonates or petroleum sulfonates, are used in conjuction with medium chain-length alcohols (co-surfactants) and an electrolyte to form a system with very low interfacial tension. Since the co-surfactant is non-ionic, its adsorption is not impeded by the electrostatic field that acts as a barrier for the further adsorption of more ionic surfactant onto the interface. Thus, the co-surfactant provides the additional lowering of interfacial tension necessary for microemulsion formation. The low viscosities and interfacial tensions of the crude oil-surfactant-cosurfactant mixtures aid the removal of oil from porous rock formations.

1.1.5 Analysis

In this section some general considerations in surfactant analysis are presented. These are sample pre-treatment, determination by surfactant class, and determination of individual surfactants. The sample pre-treatment step can be broadly delineated as the isolation of surfactants as a class (i.e. cationic, anionic, or non-ionic) from the matrix. The amount of pre-treatment required is determined by the origin of the sample. For example, in the production of surfactants, quality control of relatively pure samples will require virtually no pre-treatment. On the other hand, a complex detergent mixture or an environmental water sample to be analyzed for surfactant content will require a totally different approach. There are several schemes to accomplish the separation of non-surfactant material (both organic and inorganic) from the sample and the differentiation of surfactants as a class. Most of the procedures involve predominantly solvent extraction and ion exchange processes but other techniques such as centrifugation, precipitation, and distillation are also utilized [3-6].

After the pre-treatment step, surfactants are often determined as a class. Most commercial applications of surfactants involve the use of mixtures of homologues and isomers but full identification and quantitation of each and every component is not always possible or required. The most common approach to the analysis of surfactants by class (i.e. anionic, cationic, or nonionic) is through antagonistic reactions of the type:

$$R^-M^+ + R^+X^- = R^-R^+ + M^+X^- \qquad (1.1)$$

where R^+X^- can be a cationic surfactant that is being determined with R^-M^+, which may be an anionic dye salt or an anionic surfactant; or, alternatively, R^-M^+ can be an anionic surfactant being determined with a cationic dye or a cationic surfactant (R^+X^-). Depending upon the characteristics of the sample, reagent, and products, as well as the means of detection, this approach gives rise to a variety of techniques such as one-phase titrations [7,8], gravimetric determinations [9-14], two-phase titrations [15-21], and spectrophotometric methods [22-33].

Measurements of total surfactant content in water samples are sometimes performed. Many of the techniques used for this purpose are highly specific, and little or no pre-treatment of the samples is required. The methodology involved in these cases includes mass spectrometry [34], infra-red spectroscopy [35,36], nuclear magnetic resonance spectroscopy [37,38], ion selective electrode potentiometry [39,40], and surface tension measurements [41-43].

When it is desired to know the identity and abundance of individual components in a surfactant mixture (i.e. homologs and/or isomers), separation techniques are employed. The extensive growth of chromatography in all its different forms provides the analyst with a variety of methods that may be adapted to solve the majority of problems in surfactant analysis. Thin layer chromatography techniques are often used because of their ease, speed, and specificity [44-49]. Detection is usually accomplished by spraying the plate with a suitable reagent(s) or by examination under UV light. Surfactants may be analyzed by gas chromatography provided that the components in the sample are converted to thermally stable volatile derivatives [50-58]. Gas chromatography/mass spectrometry has also been utilized [59,60]. High performance liquid chromatographic techniques are probably the most powerful methods to separate, identify, and quantify complex surfactant mixtures [61-81]. Depending upon the characteristics of the analyte, detection can be achieved by UV absorption, fluorescence, refractive index, conductivity, and pre-or post-column reactors. The latter are usually based on an antagonistic reaction. The best separations have been carried out by reverse-phase HPLC but normal phase HPLC and ion exchange techniques have also proved extremely useful.

1.2 Flow injection analysis

1.2.1 Description

The fact that a large number of repetitive tests are performed every day has given rise to a significant amount of research and considerable effort in developing automated analyzers. Two major types of automated analyzers can be readily distinguished: batch and continuous flow. In a typical batch analyzer, the samples pass through a number of stations where manual operations such as grinding, dissolving, diluting, pipetting, adding of reagents, mixing, heating, etc, are performed followed by measurement of a property of the sample such as color, turbidity, electrode potential, absorbance, etc. In a continuous flow analysis, samples are interposed into a stream of fluid which is continuously flowing through the analyzer. At strategic points, reagents are added and the mixing and reactions take place while the sample zone is on its way to a detection device where the signal is continuously monitored.

Flow injection analysis (FIA), pioneered by Ruzicka [82] and Stewart [83], in the early 1970's, is a type of continuous flow analysis that, unlike the Technicon AutoAnalyzer system, does not use air-segmentation of the liquid flow stream. FIA is based on a combination of three principles: sample injection, exact timing, and controlled dispersion. There are some differences in approach between Ruzicka and Stewart. In Ruzicka's approach the sample solution is injected into a flowing reagent solution stream. In contrast, in the Stewart scheme the sample solution is injected into a non-reagent-containing carrier stream and, at a point downstream of the injector, a reagent stream is joined to the carrier stream at a "tee". Although details of mixing of sample component with reagent in the flowing stream differ in the two approaches, nevertheless axial dispersion functions in both cases to bring the sample component in contact with reagent ahead of and behind the initially narrow sample zone. In one case axial dispersion is the only means of contacting sample and reagent (Ruzicka) while in the other case it supplements the mixing achieved at the "tee" (Stewart).

The injection of the sample solution into the liquid stream can be done using a syringe but this technique relies heavily on experimental skill for accuracy and reproducibility. When an injection valve is used, on the other hand, the sample is delivered in a reliable and accurate way in the form of a discrete "slug" of well defined volume and length.

Exact timing of the flow of reagent and sample through the system can be achieved via a constant flow rate pump (reciprocating or syringe-type), with a persistaltic pump, or by the use of a constant pressure pump. Advantages of the latter are that it generates a steady pulse-free flow, and it is relatively inexpensive. If the flow rate is constant, the time between sample injection and detection will be highly reproducible, and successive samples will have the same residence time.

Once the sample has been introduced into the flowing stream, the sample zone disperses and reacts with the components of the stream as they move through a reaction tube. Subsequently, the generated species is monitored by a flow-through detection device. In the reaction tube, the injected sample zone spreads (disperses) along the tube as a result of the parabolic velocity profile characteristic of laminar flow, in which the liquid in the center of the tube moves at twice the mean speed of the fluid, whereas, the layers closer to the walls are progressively more retarded due to frictional drag. This parabolic velocity profile imposed by the liquid is relaxed somewhat in the sample zone by lateral diffusion of sample molecules which results in decreased axial dispersion (see figure1). If the reaction tube is coiled, the profile is relaxed even further due to the induction of a secondary flow in the radial direction [84].

The total axial dispersion of the sample zone is the sum of the contributions from the injector, the reaction tube, and the detector. Therefore, dispersion can be adjusted by carefully selecting parameters such as injection volume, flow rate, length and radius of the reaction tube, and size of the flow-cell in the detector [82]. This adjustment of the total dispersion should be at a certain compromise value, neither so big as to cause problems such as low sensitivity and sampling frequency nor so small as to cause incomplete reaction due to insufficient mixing. The role of dispersion in mixing of sample and reagent is obviously more important when the sample has been injected into the reagent stream (Ruzicka's approach).

1.2.2 Development of FIA

A major difficulty encountered in the development of continous flow analyzers was intermixing of adjacent samples during their passage through the system (carryover). In 1966, Skeggs [85] introduced a flow analyzer that

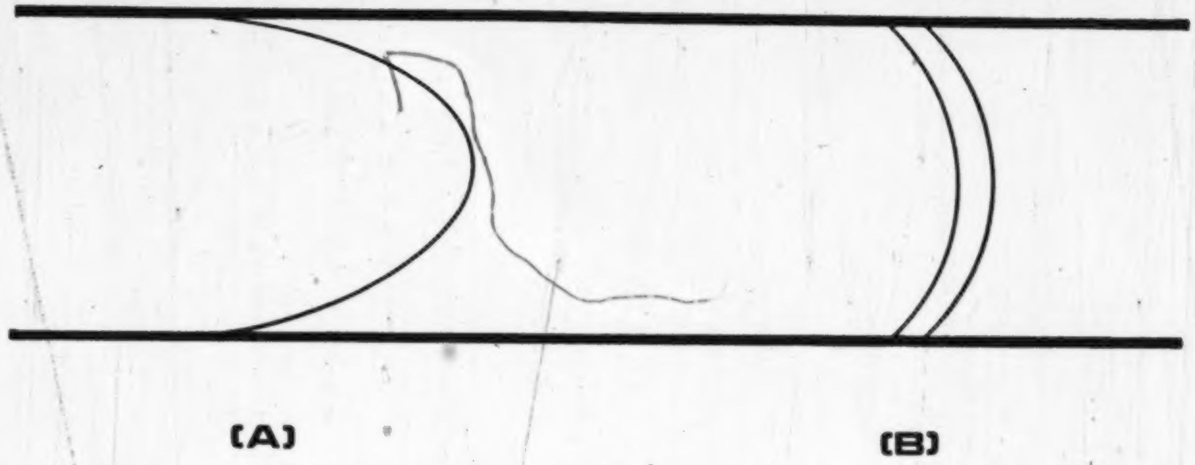

Figure 1. (A) Velocity profile of carrier (characteristic of laminar flow) (B) Sample zone profile after partial relaxation due to lateral dispersion. See text for details.

utilized air segmentation to divide the flowing stream into a number of short segments separated by air bubbles. Air segmentation reduced axial dispersion of the sample zone, and thus minimized carryover. This concept eventually led to a very popular system successfully marketed as the Technicon AutoAnalyzer. However, air-segmented systems had several drawbacks such as the presence of pulsating flow due to the compressibility of air, the fact that air segmentation hinders dispersive mixing of sample and reagent, and the obvious need of an air bubble producing device before the injector and of a debubbler before the detector.

A fundamental difference between the Technicon approach and that of FIA is that in FIA air bubble segmentation is eliminated and the internal diameter of tubing and other components is made smaller in order to reduce the extent of axial dispersion and carryover. As mentioned before, dispersion is adjusted at a compromise value in order to obtain maximum sampling frequency and sensitivity, while allowing the reaction to take place to a significant extent. If the sample zone is permitted to spread too much, it would intermix with the next oncoming sample zone but, on the other hand, an insufficiently dispersed sample zone would not be sufficiently mixed with the reagent causing severe incompleteness of the reaction [82].

FIA methodology has been utilized not only as a very flexible way to perform a number of operations associated with the measurement step in chemical assays, but also in conjunction with separation techniques such as chromatography [144,145], distillation [102], dialysis/gas diffusion [111,112], and solvent extraction [86,87,89,95,104-106] aimed at improving the selectivity of the determinations. The first FIA separation procedures based on solvent extraction were devised independently by Karlberg [86] and Bergamin [87] in 1978 and represented a significant advance in the automation of solvent extraction methodology. In these solvent extraction/flow injection analysis (SE/FIA) systems, the sample was injected into a flowing aqueous reagent stream which was subsequently joined by an organic phase stream at a junction specially designed to produce alternating small segments of organic and aqueous phases, which flowed through the reaction-extraction coil. In this coil an analyte species was generated in the aqueous segments and extracted into the adjoining organic segments by diffusion across the interfaces during its passage through the coil. Finally, most of the organic phase was separated from the aqueous via a phase separation device and carried into a flow-through detector for continous monitoring of a property of the sample (absorbance, fluorescence, etc.)

The creation of a regular pattern of organic and aqueous segments and the rapid and efficient separation of the phases were, obviously, of great importance in these SE/FIA systems. The earliest segmentor, proposed by Kalberg [86], consisted of a modification of a standard Technicon A8 connector where segmentation was achieved by the confluence of the organic stream, via a platinum capillary, with the aqueous stream in a variable-volume Teflon cavity. Later it was realized that a simple "tee" with converging organic and aqueous streams could also produce a well-behaved segmentation pattern [88].

The first on-stream phase separators were either chambers that relied on gravity to accomplish their purpose [87] or modified Technicon "tee" connectors in which the separation took place using gravity and preferential wetting achieved by the use of a phase guide made ad hoc of hydrophobic or hydrophilic materials [86,89]. More sophisticated phase separators were later designed by taking advantage of the selective permeability of microporous membranes towards a particular phase [90-93]. Since these devices can be used at high flow velocities and do not require a density difference between the aqueous and organic phases to achieve separation, they constituted a major development in SE/FIA.

As in any FIA system, dispersion is a very important parameter in SE/FIA systems. It has been observed that one of the consequences of the use of solvent-segmented flow is that sample dispersion and resulting carryover are minimized within the extraction coil. This is due to the fact that the laminar flow profile is interrupted and converted to a "bolus" circulating flow within the segment by the presence of liquid-liquid interfaces stretched across the tube, and thus sample dispersion is limited by the two-phase flow. While there is some intersegment transfer of sample via the wetting layer of solvent on the walls of the coil [89,92,95,96,143], this effect is small. Other consequences of bolus flow within the segments are rapid mixing of reagent and sample within each segment and rapid convective mass transfer of sample to the interfaces [97,98] which increases the rate of solvent extraction.

While only slight sample dispersion occurs in the extraction coil, greater contributions to the total dispersion of the system occur throughout the unsegmented regions of the system, the injection valve, the phase separator (particularly critical because a mixing chamber effect may be generated), and the detector flow-cell. By properly designing these components, dispersion can be controlled and utilized as a tool in conjunction with sample injection and exact timing, in the same manner as in FIA, to obtain reproducible and accurate analyses.

1.2.3 Applications

FIA and SE/FIA systems have been configured into a wide variety of manifolds, coupled with a number of detection methods, and utilized in conjunction with several separation techniques. This has resulted in wide applicability and great versatility in many areas of chemical analysis such as pharmaceutical, agricultural, clinical, environmental, etc. The type of samples that can be analyzed varies greatly, and may include compounds as dissimilar as surfactants [90], acids [99, 100], steroids [101], nitrogen [102], proteins [103] and vitamins [104]; to mention just a few. Spectrophotometry [92-94], atomic absorption [87,110], fluorescence [105], flame photometry [106], potentiometry with ion-selective electrodes [107], and voltammetry [108,109] are among the most widely used detection methods. FIA has been used with some separation techniques such as distillation [102], and dialysis/gas diffusion [111,112]. When coupled to other separation techniques, SE/FIA systems are most often used as post-column reactors or on-stream derivatization devices in conjunction with HPLC [69,70,113-118]. FIA methodology is the subject of a technical journal [146], of a textbook by Ruzicka and Hansen [82], and of numerous reviews [119-125].

CHAPTER 2

OPTIMIZATION OF THE SE/FIA SYSTEM FOR SURFACTANT ANALYSIS

2.1 Introduction

For many years, the determination of anionic surfactants as a class has been done by forming ion pairs with a cationic dye, extracting the ion pairs into an organic solvent, and measuring their absorbances. Among the dyes that have been utilized for this purpose are methylene blue, methyl green, azure A, toluidine blue-O, and many others [22-33]. Of these, methylene blue has been extensively employed in several different versions [126-129], and it is probably the cationic dye most frequently used. It is also the dye recommended in the official methods in many countries for the analysis of water and wastewater [130]. Nevertheless, this method has been reported to have a relatively low sensitivity because of the small extractability of the ion pairs formed, to be susceptible to several interferences, and to be time consuming. Interferences may be positive or negative and can be so serious that the analysis is officially said to determine "Methylene Blue Active Substances" (MBAS) [130] rather than "anionic surfactants".

In 1982, Motomizu et al. [131] reported a manual solvent extraction-spectrophotometric method using ethyl violet as the cationic dye to determine trace amounts of anionic surfactants in water. Ethyl violet was chosen from among malachite green, methylene blue analogues, Bindschedler's green analogues, crystal violet, rosaniline, and others as the most suitable reagent. The selection of ethyl violet was based on stability, sensitivity, specificity, and speed of the procedure involved. Motomizu also examined several extracting solvents, addition of EDTA to reduce interferences, use of a buffer solution, and use of sodium sulfate to accelerate phase separation. The resulting method provided high sensitivity, small blank absorbances, good reproducibility, and only slight interferences. Nevertheless, being a manual method, it is inherently slow.

The objective of the present thesis is the automation of Motomizu's batchwise method by means of a solvent extraction/flow injection analysis approach, aiming for higher analysis rates and better precision. In this adaptation, aqueous surfactant sample solutions are injected into a carrier stream (distilled water) which is merged and mixed with an aqueous reagent stream containing, in addition to ethyl violet, an acetate buffer and sodium sulfate. The resultant aqueous stream is then segmented with an organic stream (toluene) and the surfactant-ethyl violet ion pair is extracted, separated, and sensed by a flow-through absorbance detector. In this chapter, the optimization and characterization of the SE/FIA system is presented. Sodium dodecyl sulfate is utilized as a model anionic surfactant to find the most favorable instrument parameters. Later, in chapter 3, use of the method for the determination of other anionic surfactants is described. The ion pair formed between ethyl violet and dodecyl sulfate is represented in equation 2.1.

2.2 Experimental

2.2.1 Chemicals and solvents

With the exception of water, which was distilled from alkaline permanganate in an all-glass still, all the chemicals and solvents utilized were used as received from the different manufacturers

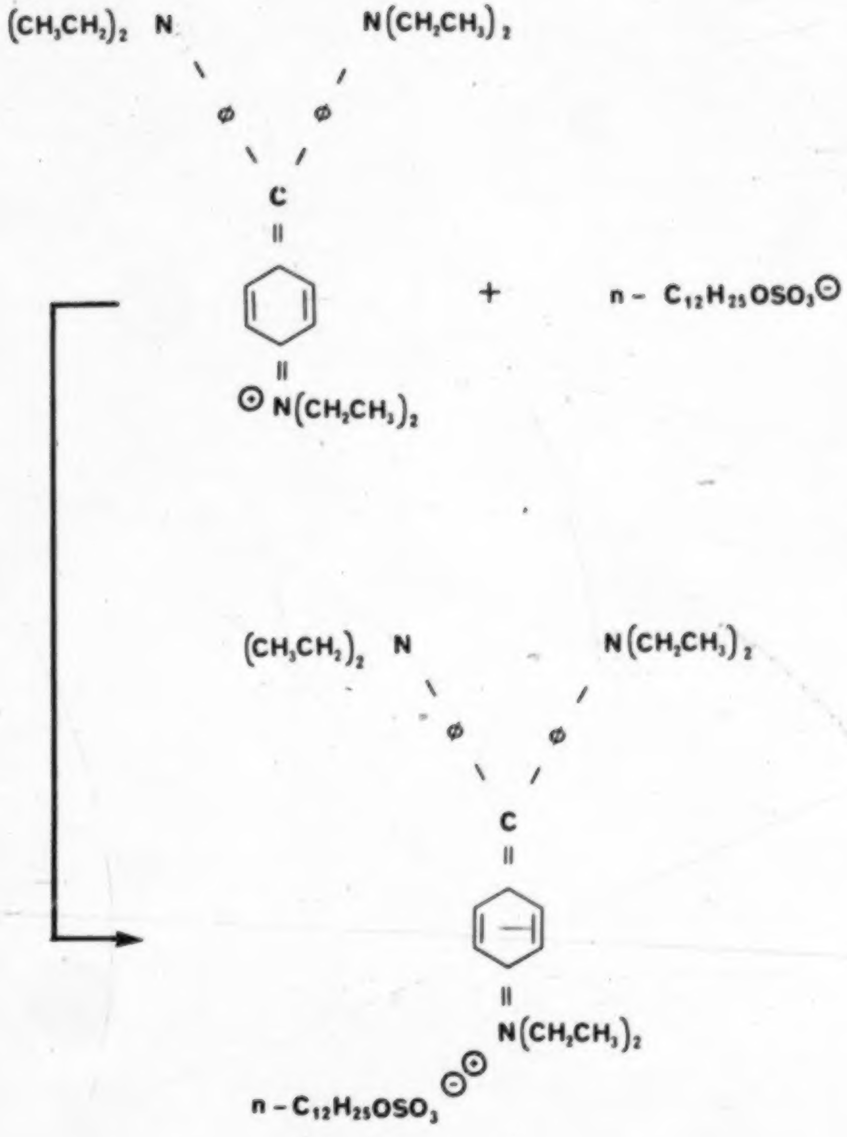
(CH₃CH₂)₂ N
N(CH₂CH₃)₂
ϕ
ϕ
C
⊕ N(CH₂CH₃)₂
+
n - C₁₂H₂₅OSO₃⊖
(CH₃CH₂)₂ N
N(CH₂CH₃)₂
ϕ
ϕ
C
N(CH₂CH₃)₂
⊖⊕
n - C₁₂H₂₅OSO₃

(2.1)

Ethyl violet C. I. 42600, Allied Chem. Co. Catalog number 536. Batch number 14120 (utilized in all the experiments except where otherwise is stated).

Ethyl violet C. I. 42600, Anachemia LTD. Catalog number R-2260. Batch number 380826.

Ethyl violet C. I. 42600, BDH Chemicals LTD. Catalog number 33114. Batch number 9379960E.

Sodium dodecyl sulfate, Aldrich Chemical Co. Catalog number 85192-2.

Sodium alkyl aryl sulfonate, Fisher Scientific Co. Catalog number S-198.

Sodium dodecylbenzene sulfonate, ICN Pharmaceuticals, Inc. Catalog number 311.

Sodium Acetate tri-hydrate, ACS grade, Amachem.

Acetic acid, ACS grade, Fisher Scientific Co.

Toluene, ACS grade, BDH Chemicals LTD.

Methanol, ACS grade, BDH Chemicals LTD.

2.2.2 Apparatus

The SE/FIA system, which employs a membrane phase separator and constant pressure pumps, is schematically represented in figure 2. Nitrogen at 20 psig is used to pressurize four aluminum cylinders in which the liquids to be delivered are contained in glass bottles. The components of the system are interconnected with 0.3 mm i.d. Teflon tubing, except the extraction coil where 0.8 mm i.d. is used. Access of the liquids into the system is controlled by two-way valves, V_1 (part number CAV2031, Laboratory Data Control). Flow rates are regulated by varying the resistance to flow which in turn is governed by the length of the tubing since a constant diameter is being used. V_2 is a three-way valve (part number CAV3031, LDC) that allows the selection of either toluene for the analysis or methanol for washing purposes.

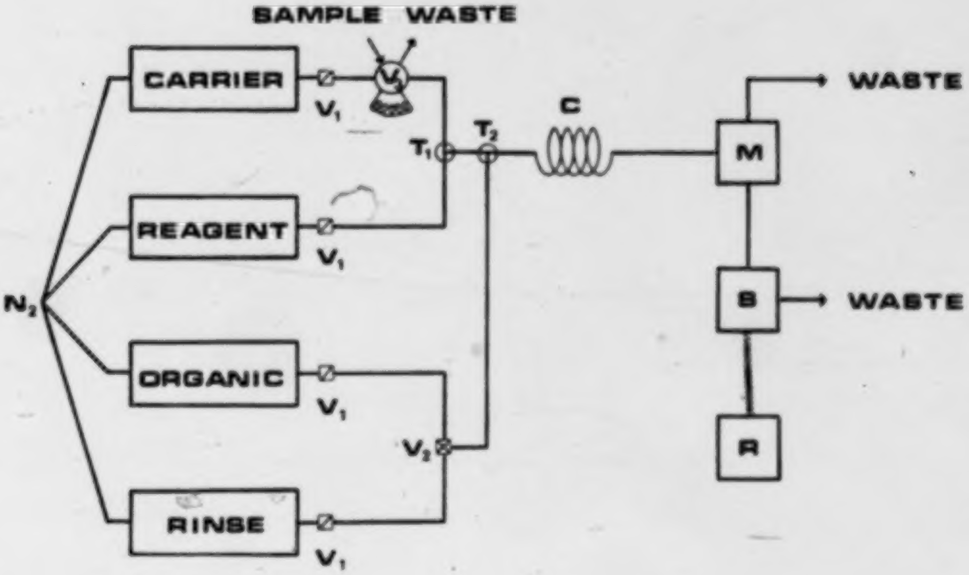
SAMPLE
WASTE
CARRIER
V_1
V_3
T_1
T_2
C
WASTE
M
REAGENT
V_1
N_2
S
WASTE
ORGANIC
V_1
V_2
R
RINSE
V_1

Figure 2. Block diagram of the solvent extraction/flow injection analysis apparatus utilized for the optimization of the system.The contents of the cylinders are: Toluene in the "organic"; distilled water in the "carrier"; ethyl violet, acetate buffer, and sodium sulfate in the "reagent"; and methanol in the "rinse" cylinder. "C" is the extraction coil; "M" the membrane phase separator; "S" a spectrophotometric detector; and "R" is a recorder.

The sample is injected into the aqueous carrier stream via a six-way valve (V_3) equipped with a 50 microliter loop (Cheminert R-6031SWP). The injection loop is filled by placing the inlet filling tube in the solution to be injected and drawing up on the plunger of a syringe attached to the outlet filling tube. The aqueous reagent and the toluene streams are added via "tees" T_1 and T_2 (part number CJ-3031, LDC), respectively. The result is a segmented aqueous-organic stream which then flows through the extraction coil where the ethyl violet- anionic surfactant ion pairs are extracted into the organic segments.

The design of the phase separator is the same as the one previously employed in this laboratory by Fossey and Cantwell [94]. It utilizes two layers of porous Teflon membrane with a pore size of 10-20 microns (Zitex, part number E249-122, Chemplast Inc.) and one with a pore size of 30-60 microns (Zitex, part number K1064-122D, Chemplast Inc.) sandwiched between two main body pieces made of Kel-F. By means of this phase separator a portion of the toluene, free of aqueous phase, flows through the membrane while the remainder of the toluene and all of the aqueous phase is vented to waste. The water-free toluene that has passed through the membrane goes to the flowcell (10-mm optical path length, 20-microliter cell volume) of a UV-VIS absorbance detector (Spectra-Physics 8200). Here the absorbance is continuously monitored at 546 nm and the outcoming signal is fed to a recorder (Fisher series 5000) and/or an integrator (Hewlett-Packard 3390A).

In all cases seven replicate injections were made for each sample and standard. Values of peak heights, areas, and widths reported in tables and figures are averages of the seven replicates. The recorder chart speed in all cases was 0.5 inch/min.

2.3 Results and discussion

2.3.1 Verifying the manual method

First of all, for the sake of gaining familiarity with Motomizu's method and checking that our chemicals were suitably pure, the following standard procedure was tested: "Transfer 100 mL of the sample solution containing sodium dodecyl sulfate into a separatory funnel. Add 5 mL of a solution containing acetate buffer (pH= 5) and sodium sulfate (1 M); 2 mL of ethyl violet solution (10^{-3} M); and 5 mL of toluene. After shaking the funnel for 10 minutes, measure the absorbance in the organic phase at 615 nm" [131]. Several sodium dodecyl sulfate concentrations were utilized resulting in the spectra shown in figure 3 as well as the calibration curves data presented in table I and figures 4 and 5.

At all concentrations, the absorption spectra of the ion pairs obtained do not differ significantly from those reported by Motomizu. In our spectra, two maxima were observed at 613 and 543 nm; whereas in Motomizu's, maxima were seen at 615 and 543 nm. In the present work, the detector used in the optimization of the SE/FIA system was set at 546 nm but the calibration curves presented in this section were obtained at 615 nm. A blank was prepared by shaking distilled water with the reagent, buffer, sodium sulfate, and toluene as indicated in Motomizu's manual method.

Motomizu reported linear calibration curves in the range from zero to 5×10^{7} M for four different surfactants. He estimated the precision of the method (by looking at 9 replicate determinations of the same sample) to be about 1.6%. Our calibration curve (figure 4) was linear. Its slope was 2.03×10^{6} with a relative standard deviation (r.s.d.) of 2.57%, which can be taken as a measure of the precision for the method. The intercept was -0.02 with a standard

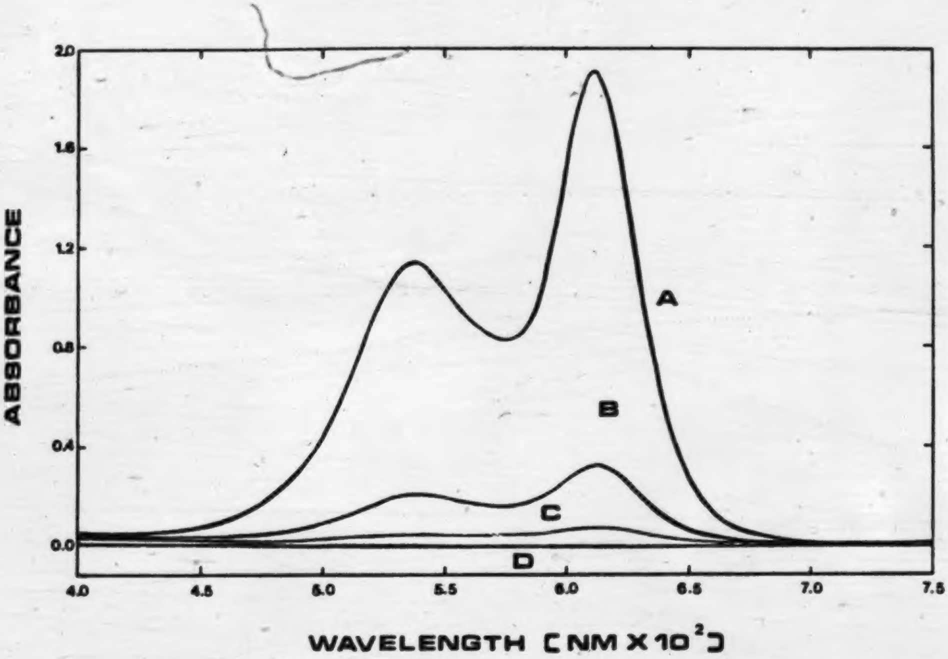

Figure 3. Absorption spectra of the ethyl violet-dodecyl sulfate ion pair in toluene. Spectrograms were recorded on a Cary 118 spectrophotometer (Varian Inc.) from 750 to 400 nm at a speed of 2 nm/sec. The maxima observed were at 613 and 543 nm. Using pure toluene in the reference cell, curve A corresponds to a surfactant sample with a concentration of 93.5 x 10^{-8} M, curve B is for a 9.35 x 10^{-8} M sample, curve C is a blank, and curve D is pure toluene.

Table I. Calibration curve data for the absorbance of the dodecyl sulfate-ethyl violet ion pair (Motomizu's manual method).

[Surfactant] (M)	Absorbance at 615 nm[(a)] (abs. units)
9.35×10^{-9}	1.900
4.67×10^{-9}	0.889
3.74×10^{-9}	0.728
2.80×10^{-9}	0.562
1.87×10^{-9}	0.341
9.35×10^{-8}	0.216

(a) The absorbances were obtained utilizing a blank in the reference cell.

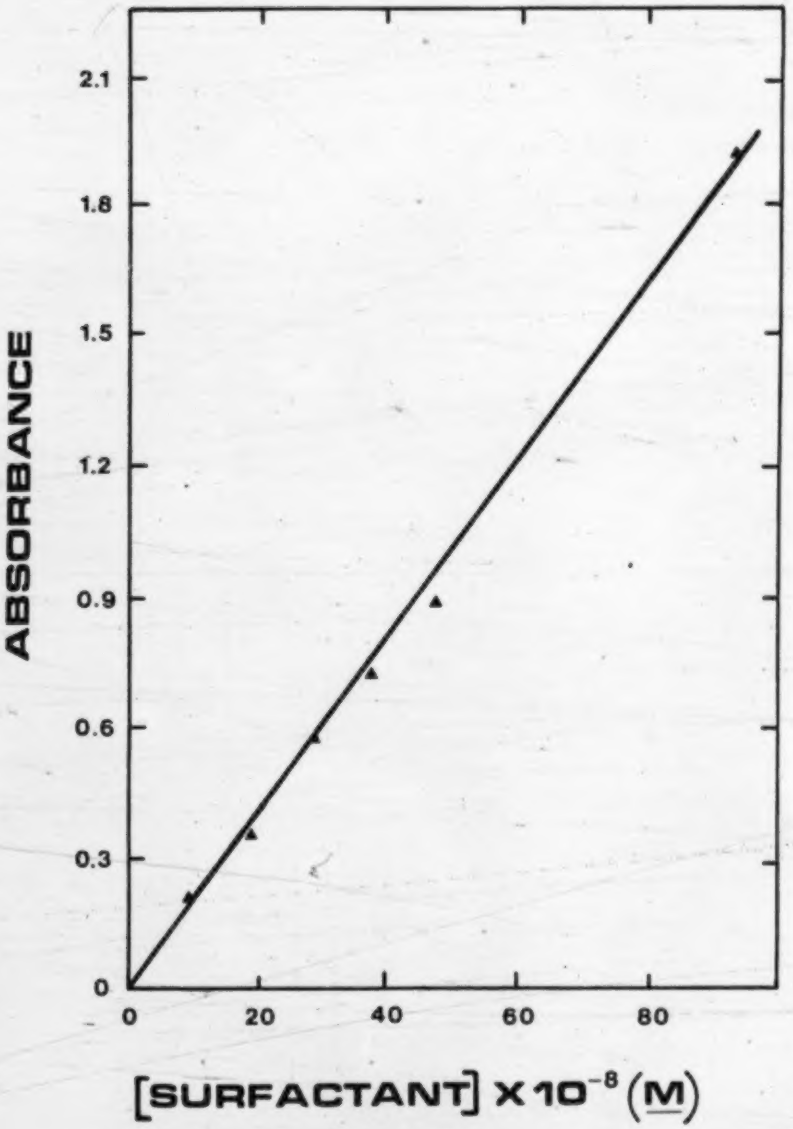

Figure 4. Calibration curve for the dodecyl sulfate-ethyl violet ion pair. The absorbances were obtained at 615 nm utilizing a blank in the reference cell. The blank and the samples were prepared following Motomizu's manual method.

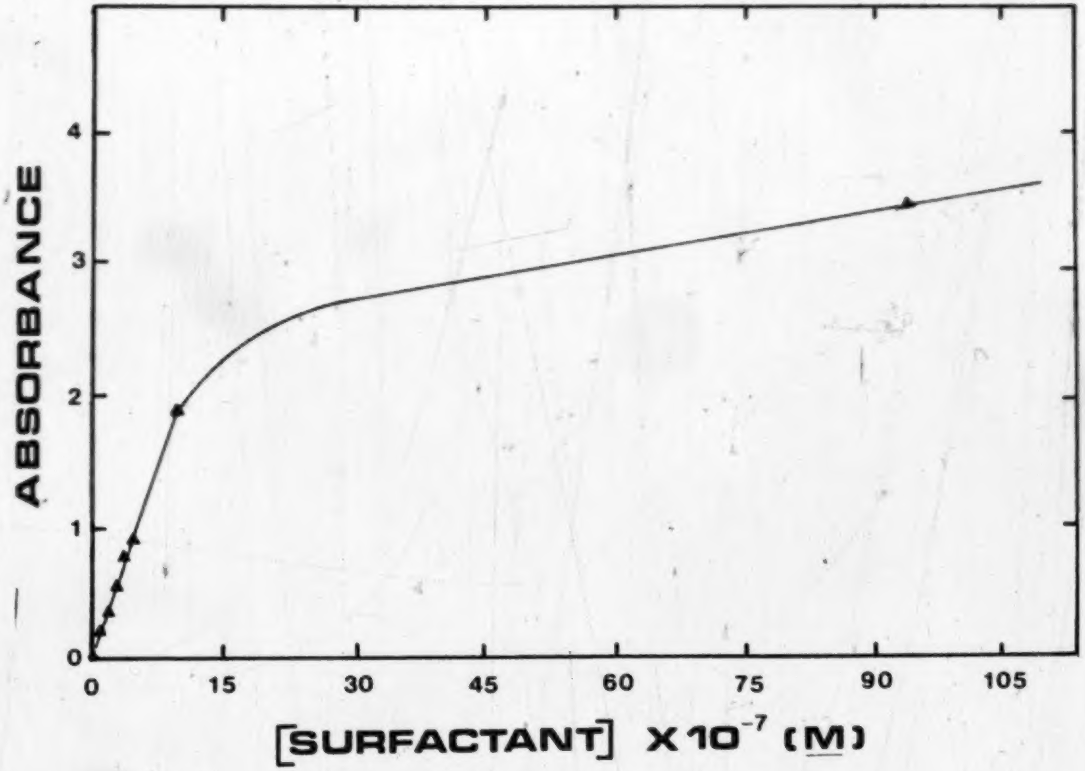

Figure 5. Calibration curve for the dodecyl sulfate-ethyl violet ion pair over a wider concentration range.

deviation (s.d.) equal to 0.03. When higher concentrations of surfactant were used, the calibration curve was observed to deviate from linearity (see figure 5). This was attributed to a combined effect of a Beer's law deviation (since the absorbance values at which this non-linearity happened were quite high and well beyond the region where Beer's law prevails), and/or the fact that the mole ratio of dye to surfactant was not sufficiently large.

Once Motomizu's method was tested and our chemicals and solvents checked, the characteristics of the SE/FIA system were studied and optimized utilizing sodium dodecyl sulfate as a model compound. Each injection of sample resulted in a peak (see figure 6). Variations in the properties of this peak (ie. area, height, and width) were observed as a function of the different parameters involved in the original manual procedure (dye, buffer, and sodium sulfate concentrations, equilibration times, etc.), as well as of new parameters arising from the use of an automated approach (injection volumes, extraction coil lengths, etc.). The result of the studies are discussed in the following sections.

2.3.2 Dye concentration

Using only ethyl violet in the "reagent" cylinder without added acetate buffer or sodium sulfate, the concentration of dye was varied while periodically injecting a constant-concentration solution of sodium dodecyl sulfate, and observing the effect on the height of the peaks obtained on the recorder. Since the sample concentration is constant throughout the experiment and only the concentration of the dye is being varied, a ratio of such concentrations, [dye]/[surf], can be computed and utilized as reference. Blanks were run by injecting distilled water, instead of the surfactant sample, into the system and observing the effect this caused on the baseline. Results are shown in table II and figure 7.

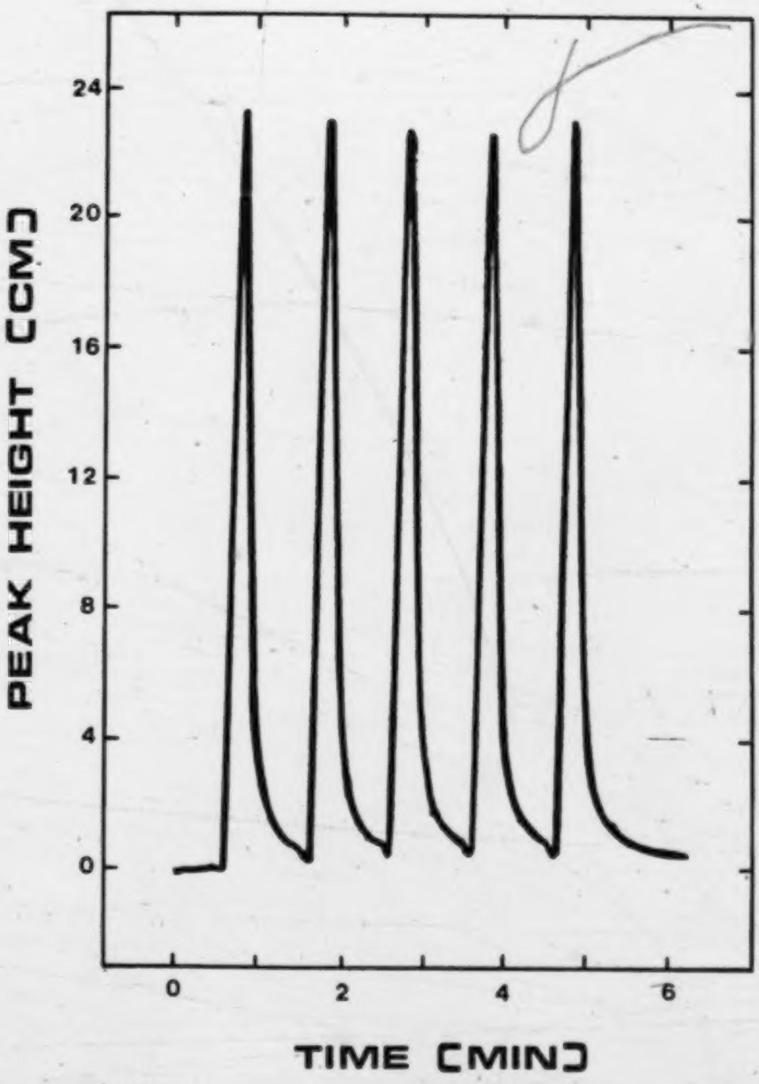

Figure 6. Replicate injections of a 5×10^{-5} M sodium dodecyl sulfate solution. Instrument parameters: Extraction coil length, 230 cm; injection volume, 50 microliters; wavelength, 546 nm; dye to surfactant ratio, 5; acetate buffer and sodium sulfate, not present; nitrogen pressure, 20 psig; $F_{o,t}$= 2.45 mL/min; $F_{a,t}$=1.82 mL/min.The average peak height was 22.8 cm with a r.s.d of 1.08%.

Table II. Peak height as a function of dye concentration in the absence of buffer and sodium sulfate. Instrument parameters: As in figure 7

[dye] (M)	[dye]/[surf]	Peak height[(a)] (cm)	r.s.d. (%)	Blank (cm)
5.00×10^{-6}	0.10	6.4	3.1	0.0
1.00×10^{-5}	0.20	16.2	2.5	0.0
6.25×10^{-5}	1.25	17.6	2.3	0.0
2.50×10^{-4}	5.00	22.8	1.8	0.0
3.75×10^{-4}	7.50	22.4	1.8	0.0
5.00×10^{-4}	10.0	23.4	0.9	0.0
6.25×10^{-4}	12.5	24.8	3.2	0.0
7.50×10^{-4}	15.0	24.4	3.3	0.0

(a) The data were normalized using equation 2.2

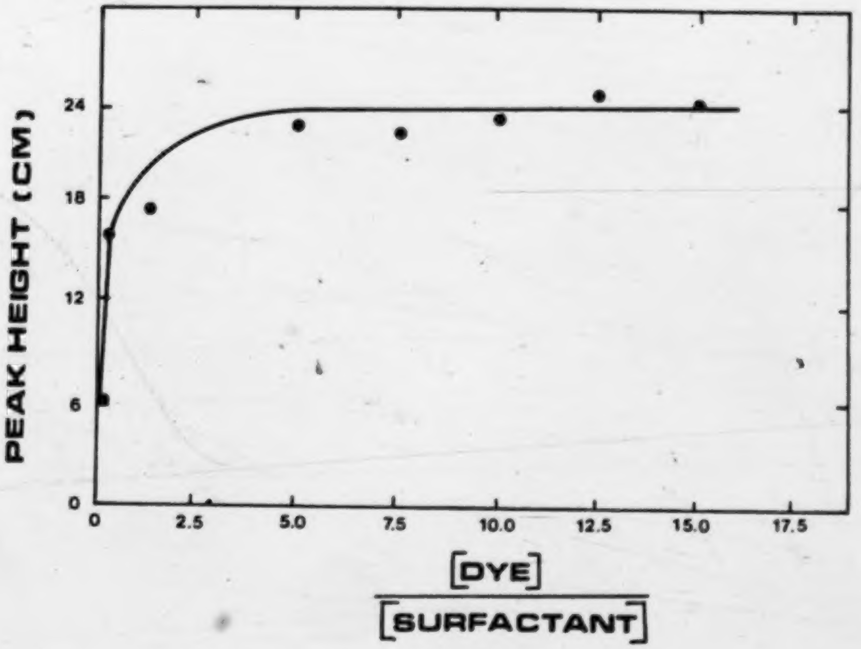

Figure 7. Peak height as a function of dye concentration in the absence of buffer and sodium sulfate. Instrument parameters: Extraction coil length, 230 cm; injection volume, 50 microliters; wavelength, 546 nm; nitrogen pressure, 20 psig; $F_{o,t}$= 2.45 mL/min; $F_{a,t}$=1.8 mL/min.

The peak height values obtained were normalized to an arbitrarily chosen detector range of 0.04 AUFS by means of the following formula:

$$\frac{\text{(Peak height observed) (Actual range)}}{0.04} = \text{normalized peak height} \qquad (2.2)$$

The purpose of this was to allow uniformity in reporting peak heights regardless of the actual range setting utilized in the detector at the time of the experiment. All the peak heights reported throughout this work will be normalized in this way, unless otherwise is specified.

The plot of peak height as a function of dye concentration (figure 7), indicated that when the dye to surfactant ratios were smaller than about 5, ion pair formation and extraction was incomplete. This was obviously due to the lack of sufficient ethyl violet to react with the number of moles of surfactant present in the system. In this plot, it could also be seen that there was no substantial gain in signal size using ratios higher than 5, since an almost constant-response plateau was obtained. The baseline, on the other hand, was observed to deteriorate progressively, by becoming erratic and noisy, upon the addition of higher amounts of dye. As indicated in table II, the blanks injected gave no response and, therefore, when plotted on figure 7 a straight line superimposed on the X axis was obtained. A dye to surfactant ratio equal to six was chosen as a compromise.

In developing his manual method, Motomizu observed a maximum and constant absorbance using ratios of dye to surfactant ranging from 20 to 50, and a value of 40 was chosen by him for the standard procedure. A direct comparison of the numerical values of [dye]/[surf] for the two methods is inappropriate because the ratios calculated in the present work are merely estimates obtained by assuming that the sample zone experiences no band broadening. This is obviously not the case, but the transient character of the SE/FIA system represents an obstacle to determine the actual concentration of surfactant due to non-uniform dilution. When the sample is injected into the carrier stream and this is in turn added to the reagent stream, dilution of the original solution takes place up to a certain (unknown) extent. In the case of the dye, the extent of dilution can be calculated via equation 2.3 since the flow rates of both the carrier (F_C) and the reagent (F_R) streams are known and the rate of mass transfer is sufficiently large.

$$[\text{dye}]_{SE/FIA} = (F_R / F_R + F_C)\ [\text{dye}]_{flask} \qquad (2.3)$$

In the case of the sample, however, the assumption has to be made that multiplying the surfactant concentration in the flask by the ratio F_C/F_C+F_R; would give the concentration of surfactant in the SE/FIA system, even though this is not actually true. Nonetheless, since the dilutions are proportional as long as the configuration, the lengths of the tubing, and the pressure applied to the system are kept constant, the arbitrary values of dye to surfactant ratios estimated under this assumption can be used to follow the behavior of the signal monitored.

2.3.3 Buffer concentration

Utilizing a ratio of dye to surfactant of six, an acetate buffer was incorporated in the ethyl violet solution in the "reagent" cylinder. The composition of the stock buffer solution was 0.28 M sodium acetate and 0.24 M acetic acid (pH= 4.8). As in the case of section 2.3.2, a ratio of the concentration of acetic acid in the buffer to that of sodium dodecyl sulfate can be calculated for reference purposes. This ratio was varied by diluting the buffer, thereby changing the concentrations of acetic acid (and hence, also of sodium acetate), while keeping the concentration of surfactant constant. The effect on peak height can be observed in table III and figure 8. Blanks were run for each buffer mixture by injecting surfactant-free water.

Figure 8, a plot of peak height as a function of acetic acid concentration, showed a gradual increase in signal size with increasing concentration of acetate buffer; but at sufficiently large ratios of acetic acid to surfactant, the response was observed to become essentially constant. The baseline, on the other hand, was seen to be stable if acetic acid to surfactant ratios were smaller than 2×10^3; and to become progressively noisy if such ratios were higher. Blanks were negligible for small ratios of acetic acid to surfactant, but a small peak that became increasingly bigger was observed for the higher ratios.

Motomizu studied the effect of pH on extraction. A maximum and constant absorbance was observed for pH values ranging from 3.5 to 6.0, and a value of pH=5 was chosen for his standard procedure. Under these conditions, the ratio of acetic acid to surfactant was equal to 2×10^4. In our case, a pH value of 4.8 was selected for our experiments, which corresponds to the midpoint in the maximum absorbance range. A ratio of acetic acid in the buffer to surfactant equal to 3.2×10^3 was chosen as the best compromise between the increasing noise level and the most stable peak height observed. As mentioned in section 2.3.2, the numerical values of the acetic acid to surfactant ratios for both methods should not be directly compared.

The fact that the absorbance decreases when the pH is outside the 3.5-6.0 range may be due to the processes depicted in reaction 2.4 for ethyl violet. Similar behavior has been observed for crystal violet, another member of the family of triphenylmethane dyes, which has the same structure of ethyl violet but bears methyl groups instead of ethyl groups [133]. The products of these

Table III. Peak height as a function of acetic acid concentration in a pH 4.8 acetate buffer. Dye to surfactant ratio, 6; sodium sulfate, absent. Instrument parameters: As in figure 7.

Buffer Mixture [SA] (M)	[AA] (M)	[AA]/[surf]	Peak height[(a)] (cm)	r.s.d. (%)	Blank (cm)
0.00	0.00	0	22.8	1.7	0.0
0.05	0.04	8.0×10^2	43.6	2.3	0.0
0.09	0.08	1.60×10^3	49.0	0.8	0.0
0.14	0.12	2.40×10^3	50.4	1.6	0.4
0.18	0.16	3.20×10^3	57.4	2.8	1.2
0.23	0.20	4.00×10^3	57.4	1.7	2.0
0.28	0.24	4.80×10^3	59.6	4.4	3.8

(a) The data were normalized using equation 2.2.

Note: SA and AA stand for sodium acetate and acetic acid, respectively.

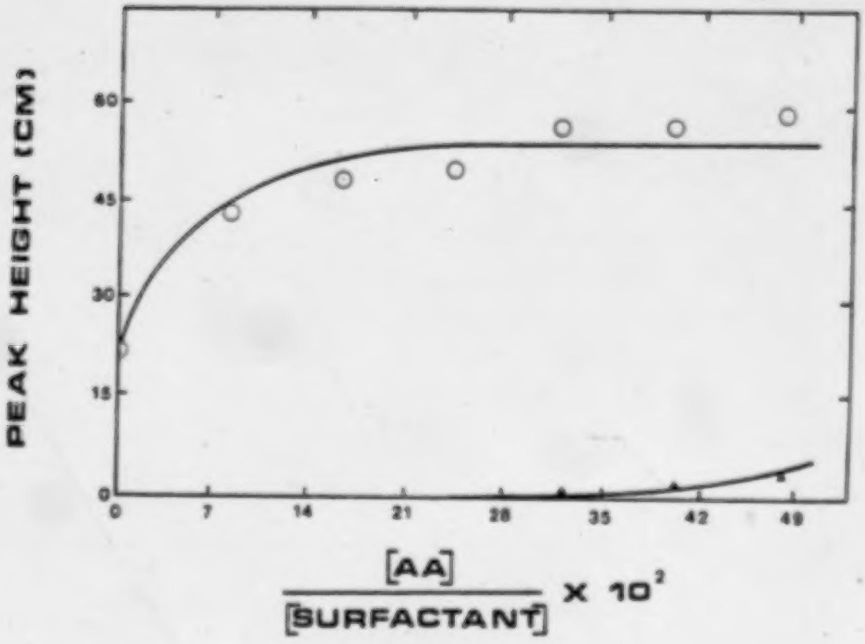

Figure 8. Peak height as a function of acetic acid concentration in an acetate buffer. Dye to surfactant ratio, 6; sodium sulfate, absent. Instrument parameters: As in figure 7. Curve (⊙) corresponds to the signal due to the samples whereas curve (▲) corresponds to that of the blanks.

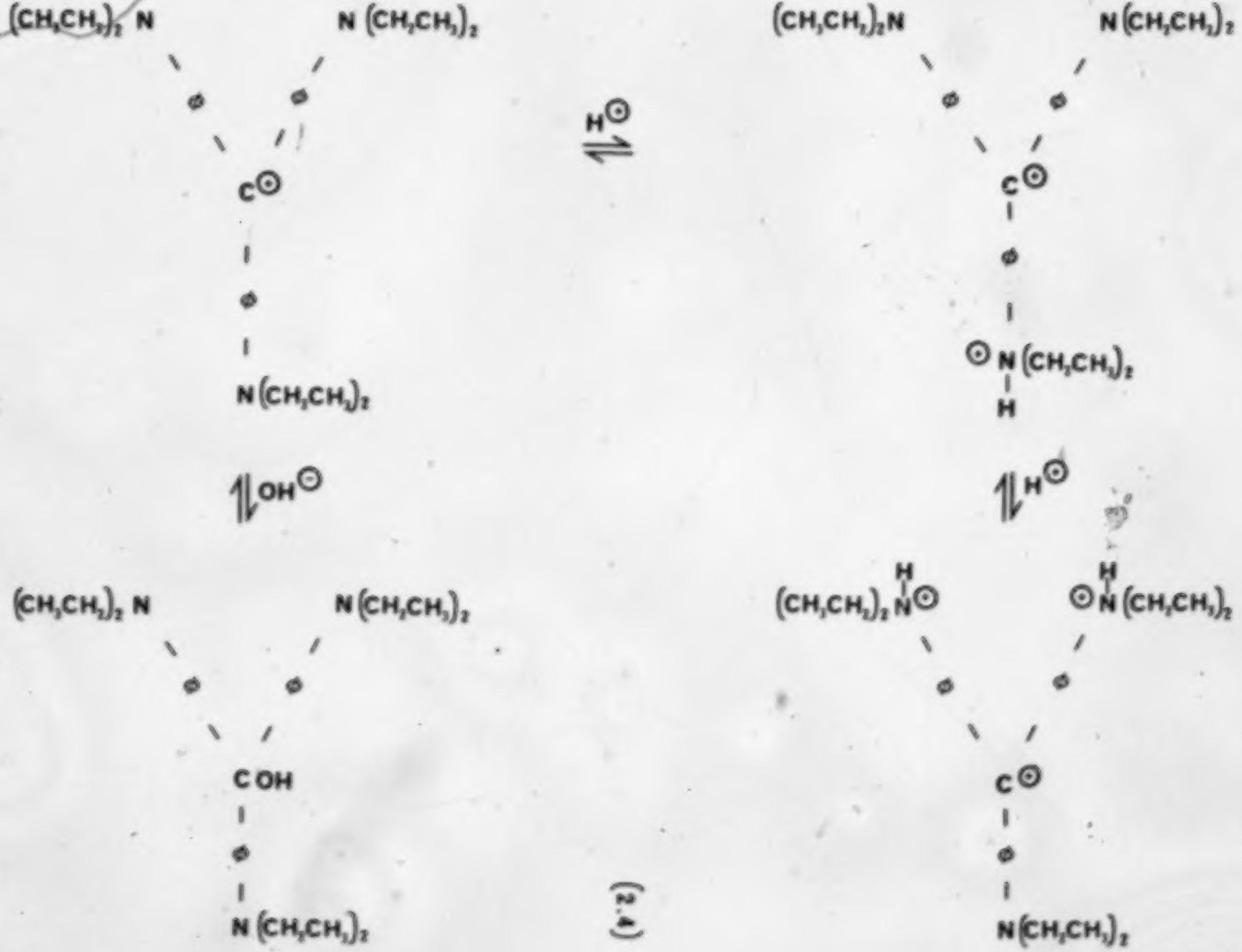

(2.4)

processes would be either unable to react with anionic surfactants, or would have a different absorption spectra due to changes in the structure of the original molecule and in the conjugation of the double bonds. In both cases, the absorbance of the surfactant-ethyl violet ion pair would be affected.

The small positive deflections obtained upon injecting water (blanks) or surfactant solutions are presumably due to the fact that when the injector is going from the "load" to the "inject" position, the concentration of the components in the combined carrier-reagent flow stream (dye, acetic acid, and sodium sulfate) goes up slightly since the flow of carrier (distilled water) is momentarily interrupted. This conclusion was confirmed by the fact that the magnitude of the deflection is increased when the concentration of buffer goes up and by the disappearance of the deflection upon achieving a continous flow of carrier via installing a by-pass around the injector.

2.3.4 Sodium sulfate concentration

Sodium sulfate was used by Motomizu as a salting-out agent. He observed that in the absence of this agent, it took about 60 minutes for complete phase separation; whereas, one minute was enough to obtain similar results when sodium sulfate was present. Consequently, using a dye to surfactant ratio of 6 and an acetic acid to surfactant ratio of 3.2×10^3, sodium sulfate was added to the reagent in varying amounts. Results are sumarized in figure 9 and table IV.

The behavior observed upon the addition of increasing amounts of sodium sulfate was a gradual increase in noise level, and a bigger peak height for the sample. A ratio of sodium sulfate to surfactant equal to 1.2×10^4 was chosen as a compromise between these two variables, since a significant amount of noise is introduced into the system after the sodium sulfate to surfactant ratio was higher than 1.5×10^4 (Motomizu used a ratio of 1.0×10^5). This gradual increase in

Table IV. Peak height as a function of sodium sulfate concentration. Dye to surfactant ratio, 6; acetic acid in buffer to surfactant ratio, 3200. Instrument parameters: As in figure 7.

[SS] (M)	[SS]/[surf]	Peak height(a) (cm)	r.s.d (%)	Blank (cm)
0.0	0	57.4	2.8	1.0
0.2	4.00×10^3	62.8	1.3	1.0
0.4	8.00×10^3	65.6	3.1	- (b)
0.6	1.20×10^4	83.8	3.8	- (b)
0.8	1.60×10^4	100.0	4.2	- (b)
1.0	2.00×10^4	108.0	5.2	- (b)

(a) The data were normalized using equation 2.2.

(b) Noise was too large to permit accurate measurement of peak height for these blanks.

Note: SS stands for sodium sulfate.

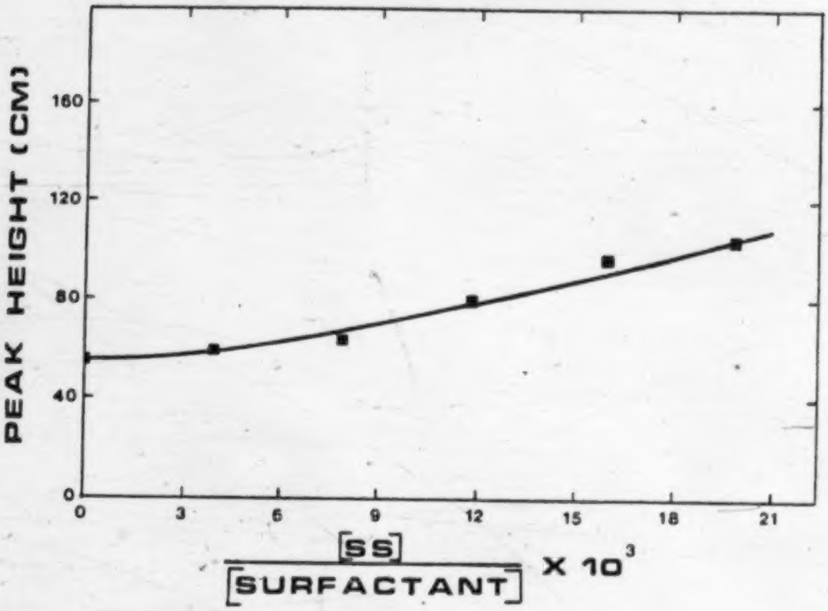

Figure 9. Peak height as a function of sodium sulfate concentration. Dye to surfactant ratio, 6; acetic acid to surfactant ratio, 3200. Instrument parameters: As in figure 7.

signal size was not easy to interpret considering that if the only effect of sodium sulfate is to accelerate the phase separation, then higher responses should not be obtained once the ion pair formation has been completed and quantitative extraction has been achieved. Reasons for the observed behavior will be considered in sections 2.3.5 and 2.3.6.

Blanks increased in magnitude with higher sodium sulfate concentrations. They were measured for low sodium sulfate to surfactant ratios. However, the noise also increased and, at higher sodium sulfate to surfactant ratios, it was so big that it literally "buried" the blank signal. In an effort to understand this behavior, several blanks were prepared manually and scanned from 750 to 400 nm. These blanks were obtained following Motomizu's procedure but were intended to reflect the effect on absorbance upon the addition of dye, buffer, and sodium sulfate in the SE/FIA system. The conditions utilized and the results obtained are shown in table V. These data suggest that the presence of sodium sulfate per se does not involve a higher magnitude in the blanks. This observation agrees with Motomizu's study on the effect of coexisting ions. In his work, using toluene, a contribution smaller than 0.005 absorbance units was found for sodium sulfate at the1 x 10^{-2} M level. In the extraction with benzene, Motomizu found that the absorbances of the blank increased markedly with the progressive increase of sodium sulfate concentrations and that, to avoid interference, the benzene extract had to be washed.

2.3.5 Extraction coil length

The influence of length of the extraction coil in the SE/FIA system was studied by varying it from 10 to 680 cm while keeping constant the rest of the variables in the system. Replicate injections of sodium dodecyl sulfate were made and their peak heights and peak widths at half-height were observed. Total

Table V. Absorbance values of blanks for various concentrations of dye, acetate buffer, and sodium sulfate. Blanks were prepared following the manual procedure [131].

[dye] (M)	Buffer (M)	[SS] (M)	Absorbance at 546 nm (absorbance units)	Absorbance at 615 nm (absorbance units)
5.0×10^{-6}	0	0.0	0.005	0.009
3.0×10^{-4}	0	0.0	0.015	0.023
7.5×10^{-4}	0	0.0	0.032	0.047
3.0×10^{-4}	0	0.0	0.015	0.023
3.0×10^{-4}	0.18 SA & 0.16 AA	0.0	0.029	0.049
3.0×10^{-4}	0.28 SA & 0.24 AA	0.0	0.040	0.057
3.0×10^{-4}	0.18 SA & 0.16 AA	0.0	0.029	0.049
3.0×10^{-4}	0.18 SA & 0.16 AA	0.6	0.030	0.052
3.0×10^{-4}	0.18 SA & 0.16 AA	1.0	0.031	0.054

Note: SS, SA, and AA stand for sodium sulfate, sodium acetate, and acetic acid, respectively.

flow rates of the aqueous ($F_{a,t}$) and organic ($F_{o,t}$) phases were also monitored, and residence times were obtained with a manual stop-watch. In an effort to understand the role of the acetate buffer and of sodium sulfate in the SE/FIA system, the variable extraction coil length experiment was performed under three differerent sets of conditions: (i) utilizing the dye, the acetate buffer, and sodium sulfate; (ii) in the absence of sodium sulfate; (iii) in the absence of both the acetate buffer and sodium sulfate. The data obtained from these experiments (presented in tables VI,VII, and VIII) were called "raw data" since no special handling was done with such data. Afterwards, and due to the fact that flow rates were allowed to change during the experiments, a correction of the "raw data" was performed. In the case of peak heights, the data was multiplied by the ratio of the total flow of organic phase to the flow of carrier, as required by a recently derived equation [147]. For peak areas, calculated from peak height and peak width at half-height, the effect of changing flow rates was compensated by multiplying the data by the total flow rate of organic phase [94]. These corrected data are presented in tables IX, X, and XI; as well as in figures 10 and 11.

The plot of corrected peak heights versus extraction coil length (figure 10) indicates that under the three sets of conditions employed, peak height increases sharply with longer extraction coils at coil lengths shorter than about 320 cm, but after this point height becomes more or less constant. Figure 11, a plot of corrected peak areas versus extraction coil length, shows essentially the same pattern.

Drawing an analogy between the extraction coil length in the SE/FIA system and the effect of shaking time in the manual separatory funnel method can be useful. At very short coil lengths the extraction of the ion pair is incomplete, but approaches an "equilibrium" value as coil length is increased. In this view a coil about 320 cm long would correspond to the attainment of "equilibrium".

Table VI. "Raw data" of peak heights and peak widths at half-heigtht as a function of variable extraction coil length. Instrument parameters: Injection volume, 50 microliters; wavelength, 546 nm; dye concentration, 3 x 10^{-4} M; buffer composition, 0.18 M sodium acetate and 0.16 M acetic acid; sodium sulfate concentration, 0.6 M; surfactant concentration, 5 x 10^{-5} M.

Extraction coil length (cm)	Peak height(a) (cm)	r.s.d. (%)	Peak width(b) (cm)	r.s.d. (%)	$F_{o,t}$ (mL/min)	$F_{a,t}$ (mL/min)	Residence time (sec)
10	8.1	4.2	0.17	4.1	2.3	1.3	11
20	14.7	4.5	0.16	3.1	2.3	1.3	11
50	29.8	1.3	0.15	2.0	2.3	1.3	15
80	38.9	0.8	0.15	2.0	2.2	1.3	17
110	47.4	0.8	0.15	0.0	2.1	1.2	20
140	54.3	1.3	0.15	0.0	2.0	1.2	23
170	60.5	1.5	0.15	2.0	2.0	1.2	26
200	64.8	0.9	0.16	0.0	1.9	1.1	30
230	71.3	1.0	0.17	1.8	1.9	1.1	33
260	71.3	0.3	0.17	1.8	1.8	1.1	36
320	74.8	2.2	0.18	1.7	1.7	1.0	43
440	70.0	2.3	0.24	0.0	1.7	0.9	65
560	67.1	0.8	0.28	1.1	1.5	0.9	90
680	71.6	0.6	0.29	1.0	1.4	0.8	115

(a) Peak height data were normalized using equation 2.2.

(b) Peak widths required no normalization.

Table VII. "Raw data" of peak heights and peak widths at half-height as a function of variable extraction coil length in the absence of sodium sulfate. Except for the sodium sulfate concentration, the instrument parameters are the same as in table VI.

Extraction coil length (cm)	Peak height[a] (cm)	r.s.d. (%)	Peak width[b] (cm)	r.s.d. (%)	$F_{o,t}$ (mL/min)	$F_{a,t}$ (mL/min)	Residence time (sec)
10	7.8	3.1	0.19	2.6	2.3	1.4	11
20	11.7	3.7	0.17	5.1	2.3	1.4	11
50	20.0	3.4	0.19	2.7	2.3	1.4	14
80	27.1	2.3	0.17	1.7	2.1	1.2	17
140	33.4	2.2	0.19	1.6	2.0	1.2	23
170	38.2	1.8	0.19	1.6	2.0	1.2	26
200	44.3	1.0	0.19	1.6	1.9	1.2	30
230	46.6	0.6	0.19	0.0	1.9	1.2	33
260	49.5	1.8	0.21	1.4	1.9	1.1	37
320	57.2	1.2	0.21	1.4	1.8	1.1	44
440	58.2	1.5	0.24	1.3	1.7	1.0	63
560	65.2	2.0	0.25	1.2	1.6	0.9	85
680	68.2	1.9	0.31	1.6	1.4	0.9	110

(a) Peak height data were normalized using equation 2.2.

(b) Peak widths required no normalization.

Note: $F_{o,t}$ and $F_{a,t}$ stand for total flow rates of organic and aqueous phases.

Table VIII. "Raw data" of peak heights and peak widths at half-height as a function of variable extraction coil length in the absence of sodium sulfate and buffer. Except for the sodium sulfate and the buffer concentrations, the instrument parameters are the same as in table VI.

Extraction coil length (cm)	Peak height[(a)] (cm)	r.s.d. (%)	Peak width[(b)] (cm)	r.s.d. (%)	$F_{o,t}$ (mL/min)	$F_{a,t}$	Residence time (sec)
10	0.9	9.3	0.39	5.5	2.4	1.4	11
20	2.4	2.1	0.34	2.9	2.3	1.3	13
50	7.2	5.8	0.26	1.9	2.2	1.3	15
80	13.3	2.9	0.20	2.5	2.2	1.3	17
110	17.9	2.6	0.18	3.3	2.1	1.2	17
170	23.7	0.8	0.19	1.6	2.0	1.2	27
200	29.3	2.0	0.19	4.3	1.9	1.1	31
230	32.5	2.0	0.19	1.6	1.9	1.1	34
320	33.2	1.5	0.23	0.0	1.7	0.9	47
440	27.6	1.5	0.24	2.1	1.5	0.9	69
560	30.5	1.7	0.28	1.1	1.5	0.8	92
680	29.9	3.6	0.36	1.4	1.3	0.8	120

(a) Peak height data were normalized using equation 2.2.

(b) Peak width required no normalization.

Note: $F_{o,t}$ and $F_{a,t}$ stand for total flow rates of organic and aqueous phases.

Table IX. Corrected peak heights and peak areas as a function of variable extraction coil length. Instrument parameters as in table VI.

Extraction coil length (cm)	$\frac{\text{Peak height} \times F_{o,t}}{F_c}$ (cm)	Peak area[a] x $F_{o,t}$ ($cm^2\ mL\ min^{-1}$)
10	28.66	3.17
20	52.01	5.41
50	105.45	10.28
80	131.66	12.84
110	165.90	14.93
140	181.00	16.29
170	201.67	18.15
200	223.85	19.70
230	246.31	23.30
260	233.34	21.82
320	254.32	22.89
440	264.44	28.56
560	223.67	28.18
680	250.60	29.07

(a) Peak areas were calculated from heights and peak widths at half-height. Note: $F_{o,t}$ and F_c stand for total flow rate of organic phase and flow rate of carrier, respectively.

Table X. Corrected peak heights and peak areas as a function of variable extraction coil length in the absence of sodium sulfate. Except for the sodium sulfate concentration, the instrument parameters were as in table VI.

Extraction coil length (cm)	$\frac{\text{Peak height} \times F_{o,t}}{F_c}$ (cm)	Peak area[a] $\times F_{o,t}$ (cm^2 mL min^{-1})
10	25.63	3.41
20	38.44	4.57
50	65.71	8.74
80	94.85	9.67
140	111.33	12.69
170	127.33	14.52
200	140.28	15.99
230	147.57	16.82
260	171.00	19.75
320	187.20	21.62
440	197.88	23.75
560	232.18	26.12
680	212.17	29.60

(a) Peak areas were calculated from heights and peak widths at half-height. Note: $F_{o,t}$ and F_c stand for total flow rate of organic phase and flow rate of carrier, respectively.

Table XI. Corrected peak heights and peak areas as a function of variable extraction coil length in the absence of sodium sulfate and buffer. Except for the sodium sulfate and the buffer concentrations, the instrument parameters are the same as in table VI.

Extraction coil length (cm)	$\frac{\text{Peak height} \times F_{o,t}}{F_c}$ (cm)	Peak area[a] x $F_{o,t}$ ($cm^2\ mL\ min^{-1}$)
10	3.08	0.84
20	8.49	1.88
50	24.37	4.12
80	45.01	5.85
110	62.65	6.77
170	79.00	9.01
200	101.22	10.58
230	112.27	11.73
320	125.42	12.98
440	92.00	9.94
560	114.37	12.81
680	97.17	13.99

(a) Peak areas were calculated from heights and peak widths at half-height. Note: $F_{o,t}$ and F_c stand for total flow rate of organic phase and flow rate of carrier, respectively.

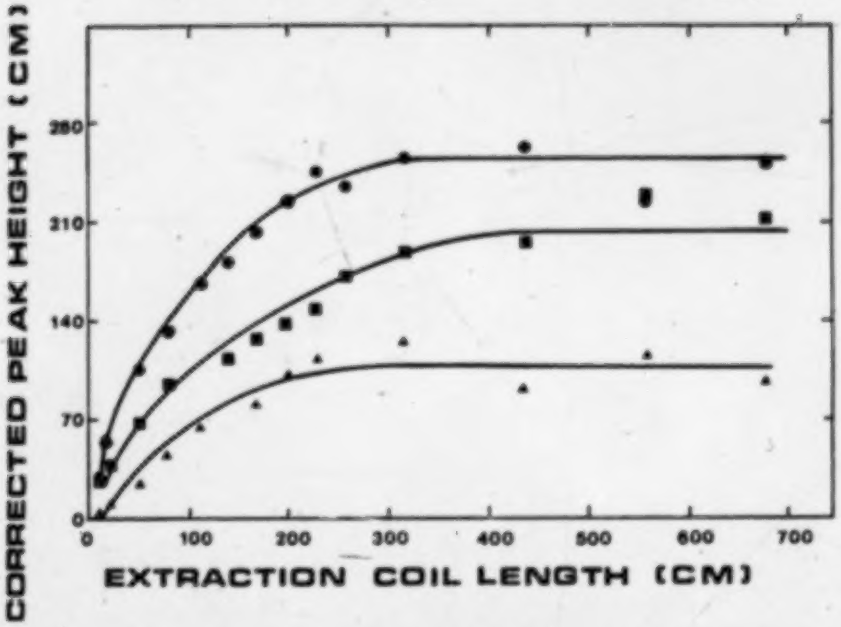

Figure 10. Corrected peak heights as a function of variable extraction coil length (●) in the presence of dye, buffer, and sodium sulfate; (■) in the absence of sodium sulfate; and (▲) in the absence of sodium sulfate and the buffer. Instrument parameters: Injection volume, 50 microliters; wavelength, 546 nm; nitrogen pressure, 20 psig; sample, sodium dodecyl sulfate.

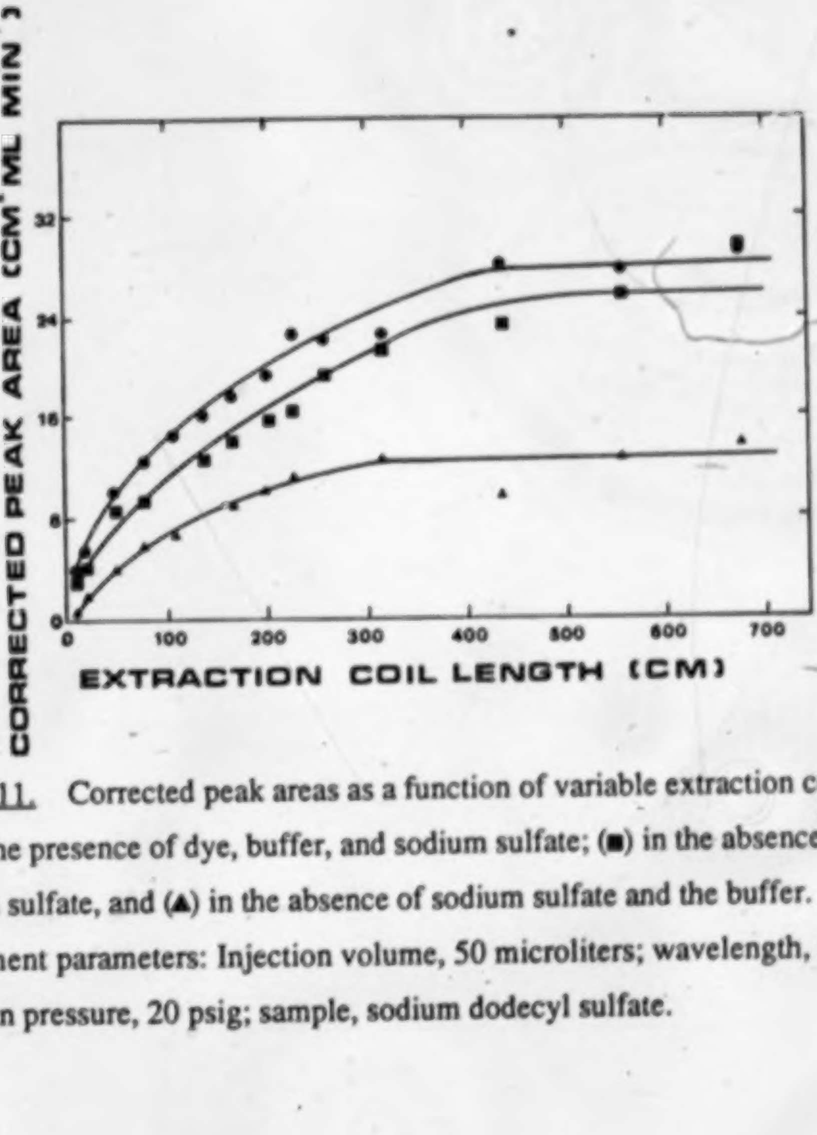

Figure 11. Corrected peak areas as a function of variable extraction coil length (●) in the presence of dye, buffer, and sodium sulfate; (■) in the absence of sodium sulfate, and (▲) in the absence of sodium sulfate and the buffer. Instrument parameters: Injection volume, 50 microliters; wavelength, 546 nm; nitrogen pressure, 20 psig; sample, sodium dodecyl sulfate.

Nonetheless, the fact that the plateau value observed on figures 10 and 11 depends on the set of conditions utilized clearly indicates that a distribution equilibrium is not being attained and that an unexpected effect is involved. Such an effect may be related to adsorption of a certain amount of surfactant and/or of ion pair onto the walls of the SE/FIA system or at the organic-aqueous interfaces; to the formation of charged aggregates such as colloids or micelles; or to other processes that may compete or interfere with the extraction of the ion pair. This interpretation is suggested by the fact that the efficiency of extraction is greatly enhanced upon increasing the ionic strength in the system via the addition of the buffer and/or sodium sulfate.

Even though an extraction coil length of 0.0 cm is physically unattainable, an extrapolation of the data plotted on figures 10 and 11 seems to indicate that a non-zero response would be obtained. This suggests that ion pair extraction occurs, to a certain extent, in the segmentor and/or the phase separator. Since in all the SE/FIA experiments described so far an extraction coil length of 230 cm has been used and this length is in the region of increasing response, a longer coil was used on all subsequent studies to ensure that the system was working on the constant response range.

2.3.6 Effect of added electrolyte

In his work, Motomizu added sodium sulfate in order to decrease the time required for phase separation. In the absence of sodium sulfate, it took about 60 minutes for complete phase separation after shaking; while in the presence of sodium sulfate, a standing time of one minute was sufficient for complete phase separation. In the present work, sodium sulfate has been observed to increase the signal size whenever it has been incorporated into the SE/FIA system. In order to understand the role of the buffer and the sodium sulfate electrolytes the following tests were performed.

The instrument used was essentially the same as the one described in section 2.2.2, except that an extraction coil length of 680 cm was utilized. Either a 5×10^{-5} M sodium dodecyl sulfate solution or distilled water was utilized in the "carrier" cylinder. The amounts of dye, buffer, and sodium sulfate employed were adjusted to give the familiar ratios of 6, dye to surfactant; 3.2×10^3, acetic acid to surfactant; and 1.2×10^4, sodium sulfate to surfactant. The extraction coil was disconnected from the phase separator. In some experiments toluene was flowing ("toluene" cylinder open) and in others there was no toluene ("toluene" cylinder closed). The system was allowed to stabilize and a sample of the one or two phase liquid was collected at the end of the extraction coil either to form a thin layer of solution to be visually examined for the presence of precipitate (when toluene was absent); or to measure the absorbance of the toluene phase at 546 nm (when toluene was present). The results obtained are summarized in table XII.

In the absence of sodium sulfate, no precipitate (absorbance = 0.007) was detected for a blank (tests 1 and 2); but in the presence of surfactant, a small amount of precipitate (absorbance = 0.282) was observed (tests 3 and 4). Similarly, when sodium sulfate was incorporated into the system, no precipitate (absorbance = 0.015) was observed for the blank (tests 5 and 6); while in the presence of surfactant, a large amount of precipitate (absorbance = 0.425) was seen (tests 7 and 8).

It may be concluded from these tests (1-8), that "salting-out" of the dye-surfactant ion pair in the presence of only the buffer does occur to some extent since a small amount of precipitate was observed in test 3; and that sodium sulfate produces a greater "salting out" effect since the amount of precipitate

Table XII. Electrolyte effect. Instrument parameters: Dye to surfactant ratio, 6; acetic acid to surfactant ratio, 3200 (pH= 4.8); sodium sulfate to surfactant ratio, 12000; wavelength 546 nm; injection volume, 50 microliters; extraction coil length, 680 cm; nitrogen pressure, 20 psig; injection frequency, one injection/10 sec; "carrier" cylinder, distilled water

Test	Surfactant	"Reagent" cylinder	Toluene cylinder	Observations
1	0	dye + buffer	closed	no ppt
2	0	dye + buffer	open	abs.= 0.007
3	5×10^{-5} M	dye + buffer	closed	small amount of ppt
4	5×10^{-5} M	dye + buffer	open	abs.= 0.282
5	0	dye + buffer + SS	closed	no ppt
6	0	dye + buffer + SS	open	abs.= 0.015
7	5×10^{-5} M	dye + buffer + SS	closed	ppt
8	5×10^{-5} M	dye + buffer + SS	open	abs.= 0.425

Note: ppt stands for precipitate.

obtained in test 7 was considerably larger than that obtained in test 3. The precipitate observed in the surfactant-containing solutions in the presence of buffer and sodium sulfate, as well as the increased absorbance of the toluene phase in these systems, could be due to either of two causes: (i) it could be a simple salting-out effect in which the solubility of a solute such as the dye-surfactant compound is reduced in the presence of electrolyte, or (ii) it could be that the dye-surfactant compound is present in the aqueous phase at low ionic strengths in the form of a charged colloid which cannot be observed by eye but which coagulates in the presence of higher electrolyte concentrations. This latter phenomenon has been observed for tetra-alkylammonium picrates [155], where it was also found that the rate of extraction of the tetra-alkylammonium ion pair into chloroform occurs much more rapidly at higher ionic strengths. This could explain the behavior observed in section 2.3.5 (extraction coil length), since charged colloid formation would compete with the extraction process. Considering that the extraction constant of the sodium dodecyl sulfate-ethyl violet ion pair in toluene is on the range of 10^7; a salting-out effect, as utilized in the usual sense, would not account for the behavior seen on section 2.3.5 because this extraction constant is so large that the raising of the ionic strength should not make the extraction any more quantitative. This subject will be discussed further in the next section.

2.3.7 Sample injection volume

Utilizing constant instrument parameters in the SE/FIA system, the volume of sample injected was varied (by changing the volume of the loop in the injection valve) under three different sets of conditions: (i) utilizing a low surfactant concentration and the dye dissolved in water, (ii) using a relatively high surfactant concentration with the dye dissolved in water, and (iii) employing a medium surfactant concentration and the dye dissolved in toluene. The volume injected by each loop was determined in a separate calibration experiment using spectrophotometry [132]. As the injection volume was varied, the effect was monitored in terms of peak area (measured via a HP-3390A integrator), peak height, and peak width at half-height. A normalization of these data was carried out for inter-comparison purposes among the three sets of conditions used. Since peak areas are independent of the absorbance range value used in the detector during the experiment, this normalization was done by dividing the data obtained by the surfactant concentration. Peak heights were normalized by multiplying the data by the range setting used, and dividing by the surfactant concentration. Peak widths at half-height are independent of the range set on the detector, and of the surfactant concentration; thus, no normalization was required. The conditions used and the results obtained are shown in tables XIII, XIV, and XV; as well as in figures 12-17.

Theoretically, a plot of peak area versus injection volume should yield a straight line with zero-intercept since peak area is directly proportional to the number of moles of sample injected. For the first set of conditions, utilizing a relatively high surfactant concentration (5×10^{-5} M) and the dye dissolved in water, such a plot (figure 12) was linear with a slope of 5.72×10^{9} (r.s.d.=1.62%) and an intercept of -2.72×10^{10} (s.d.=2.50×10^{10}). A plot of peak height and peak width versus injection volume (figure 13) shows that peak height increases with sample volume until a plateau is reached at about 300 microliters; while peak width is nearly constant for sample volumes below about 150 microliters, and later it increases with the higher sample volumes. This behavior can be rationalized as has been done in the past [94]. When injection volumes are sufficiently small (less than about 150 microliters), peak width at half-height remains essentially constant due to the fact that a mixing chamber

Table XIII. Variations of peak area, height, and width with injection volume for "high" surfactant concentrations, utilizing the dye dissolved in water. Instrument parameters: Surfactant concentration, 5 x 10^{-5} M; extraction coil length, 450 cm; nitrogen pressure, 20 psig; wavelength, 546 nm; dye concentration (dissolved in water), 4.5 x 10^{-4} M; buffer composition 0.18 M sodium acetate and 0.16 M acetic acid; sodium sulfate concentration, 0.6 M; injection volume, variable.

Injection volume (μL)	Peak area [surf] $\frac{\text{a.i.u. x } 10^{11}}{\text{M}}$	r.s.d. (%)	Peak height x range [surf] $\frac{\text{cm AUFS x } 10^{4}}{\text{M}}$	r.s.d. (%)	Peak width (cm)	r.s.d. (%)
47.7	2.67	2.0	5.8	3.7	0.25	2.0
78.5	4.35	4.7	7.2	4.2	0.27	2.7
142	7.38	3.8	13.2	3.6	0.28	1.3
369	21.0	3.0	21.6	2.9	0.57	1.2
445	25.2	2.6	20.6	0.7	0.75	0.5

Note: Peak areas were normalized by dividing them over the concentration of surfactant; whereas peak heights were normalized by multiplying them by the ratio of the range setting utilized in the detector to the surfactant concentration. Peak widths were not normalized.

Note: AUFS stands for absorbance units at full scale; whereas a.i.u. stands for arbitrary integrator units.

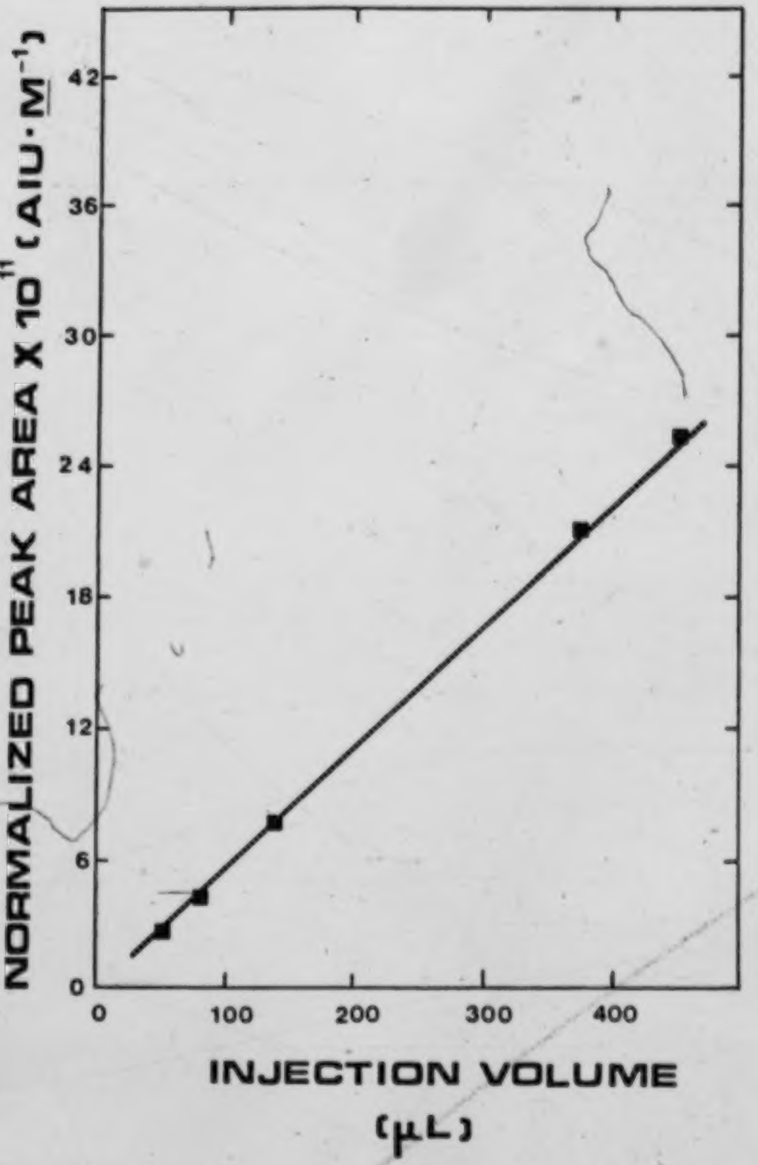

Figure 12. Normalized peak area versus injection volume for "high" surfactant concentrations and the dye dissolved in water. The concentration of surfactant was 5 x 10^{-5} M and the dye concentration 4.5 x 10^{-4} M. Instrument parameters: As in table XIII.

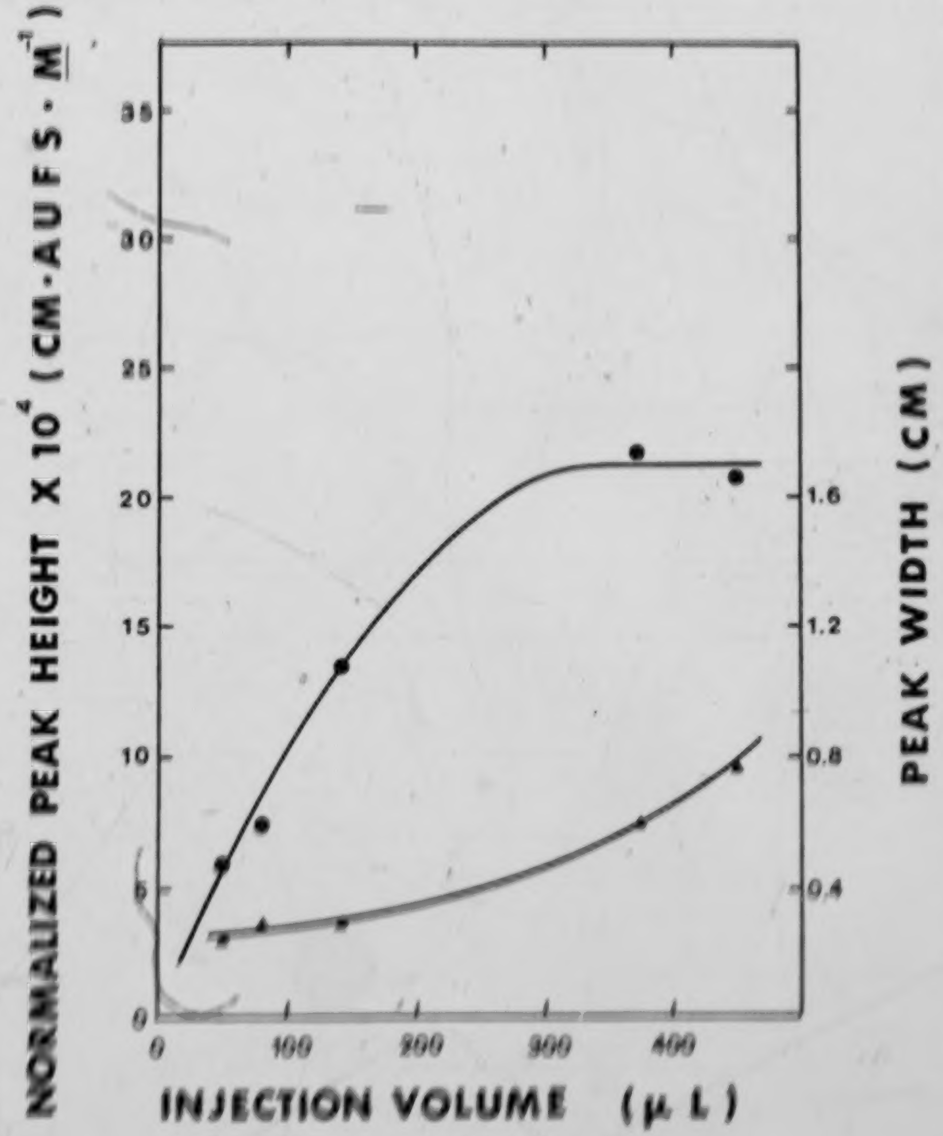

Figure 13. Peak widths (▲) and normalized peak heights (●) versus injection volume for "high" surfactant concentrations and the dye dissolved in water. Surfactant concentration was 5 x 10^{-5} M and the dye concentration 4.5 x 10^{-4} M. Instrument parameters:As in table XIII.

Table XIV. Variations of peak area, height, and width with injection volume for "low" surfactant concentrations, utilizing the dye dissolved in water. The instrument parameters were the same as those indicated in table XIII, except that the surfactant concentration was 5×10^{-6} M.

Injection volume (μL)	Peak area [surf] $\frac{\text{a.i.u.} \times 10^{11}}{\text{M}}$	r.s.d. (%)	Peak height x range [surf] $\frac{\text{cm AUFS} \times 10^{4}}{\text{M}}$	r.s.d. (%)	Peak width (cm)	r.s.d. (%)
47.7	5.68	4.9	13.2	1.8	0.23	0.0
78.5	7.88	3.9	15.6	1.8	0.25	2.5
142	13.3	2.9	21.4	2.4	0.35	4.0
369	34.3	1.2	28.8	3.9	0.71	0.0
445	42.2	1.7	27.3	2.8	0.90	2.6

Note: Peak areas were normalized by dividing them over the concentration of surfactant; whereas peak heights were normalized by multiplying them by the ratio of the range setting utilized in the detector to the surfactant concentration. Peak widths were not normalized.

Note: AUFS stands for absorbance units at full scale; whereas a.i.u. stands for arbitrary integrator units.

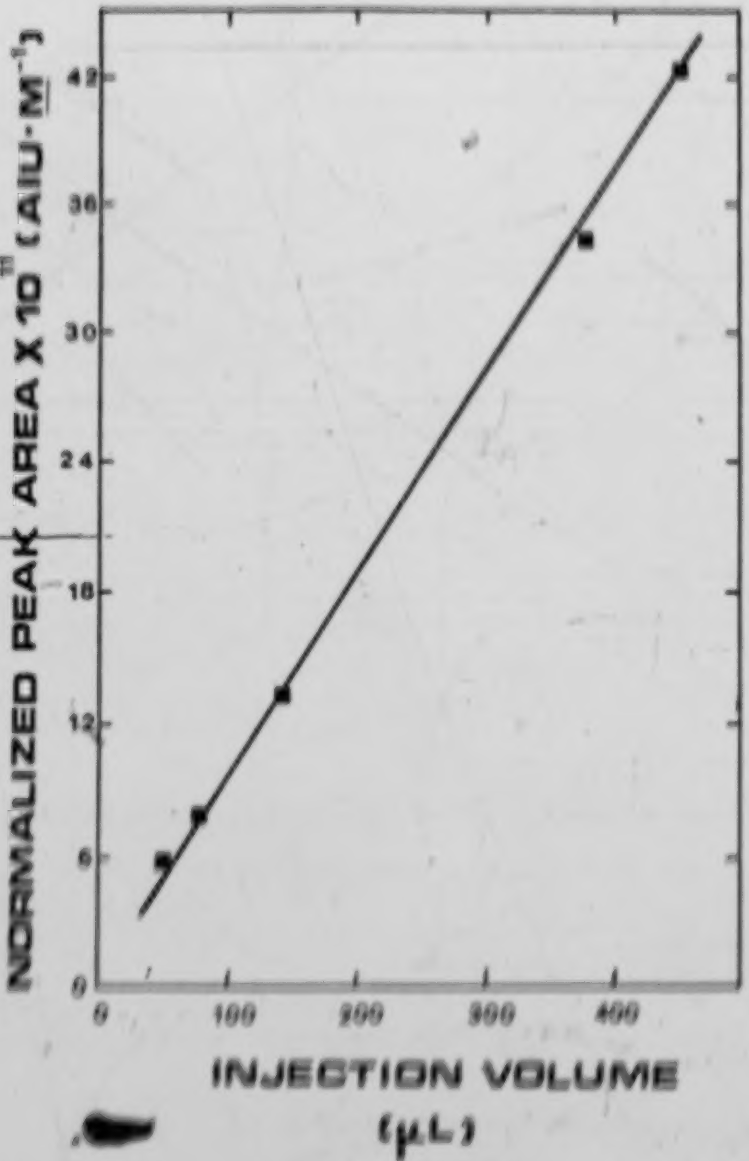

Figure 14. Normalized peak area versus injection volume for "low" surfactant concentrations and the dye dissolved in water. The concentration of surfactant was 5 x 10^{-6} M and the dye concentration 4.5 x 10^{-4} M. Instrument parameters: As in table XIII.

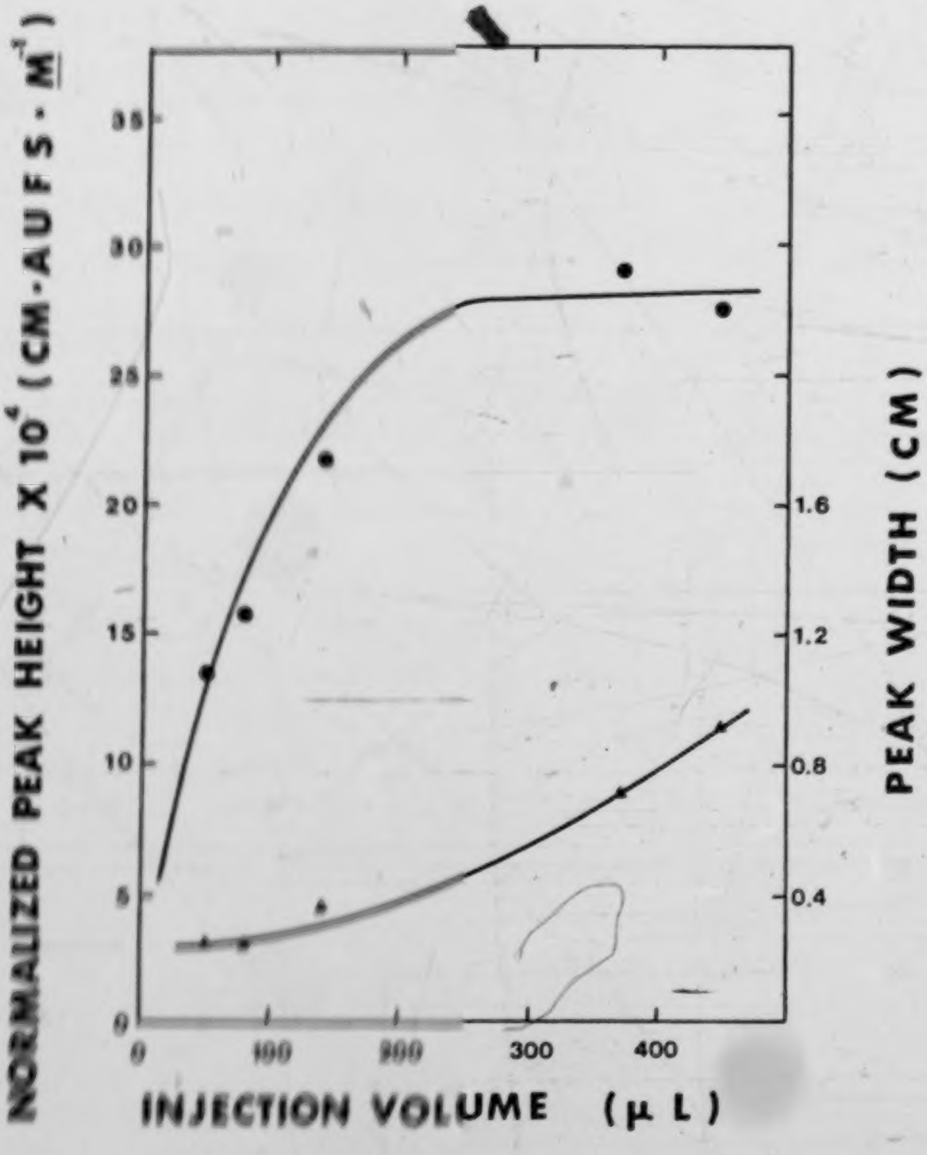

Figure 15. Peak widths (▲) and normalized peak heights (●) versus injection volume for "low" surfactant concentrations and the dye dissolved in water. Surfactant concentration was 5 x 10^{-6} M and the dye concentration 4.5 x 10^{-4} M. Instrument parameters as in table XIII.

Table XV. Variations of peak area, height, and width with injection volume for "medium" surfactant concentrations, utilizing the dye dissolved in toluene. The instrument parameters were the same as those indicated in table XIII, except that the surfactant was dissolved in toluene and its concentration was 2×10^{-5} M.

Injection volume	$\frac{\text{Peak area}}{[\text{surf}]}$	r.s.d.	$\frac{\text{Peak height x range}}{[\text{surf}]}$	r.s.d.	Peak width	r.s.d.
(μL)	$\frac{\text{a.i.u.} \times 10^{11}}{\text{M}}$	(%)	$\frac{\text{cm AUFS} \times 10^{4}}{\text{M}}$	(%)	(cm)	(%)
47.7	5.82	1.4	12.4	0.7	0.22	1.6
78.5	7.61	0.7	15.7	0.7	0.25	1.1
142	13.3	0.5	22.4	0.7	0.32	0.9
369	32.4	0.2	27.8	0.8	0.67	0.4
445	39.9	0.4	28.3	0.8	0.86	0.3

Note: Peak areas were normalized by dividing them over the concentration of surfactant; whereas peak heights were normalized by multiplying them by the ratio of the range setting utilized in the detector to the surfactant concentration. Peak widths were not normalized.

Note: AUFS stands for absorbance units at full scale; whereas a.i.u. stands for arbitrary integrator units.

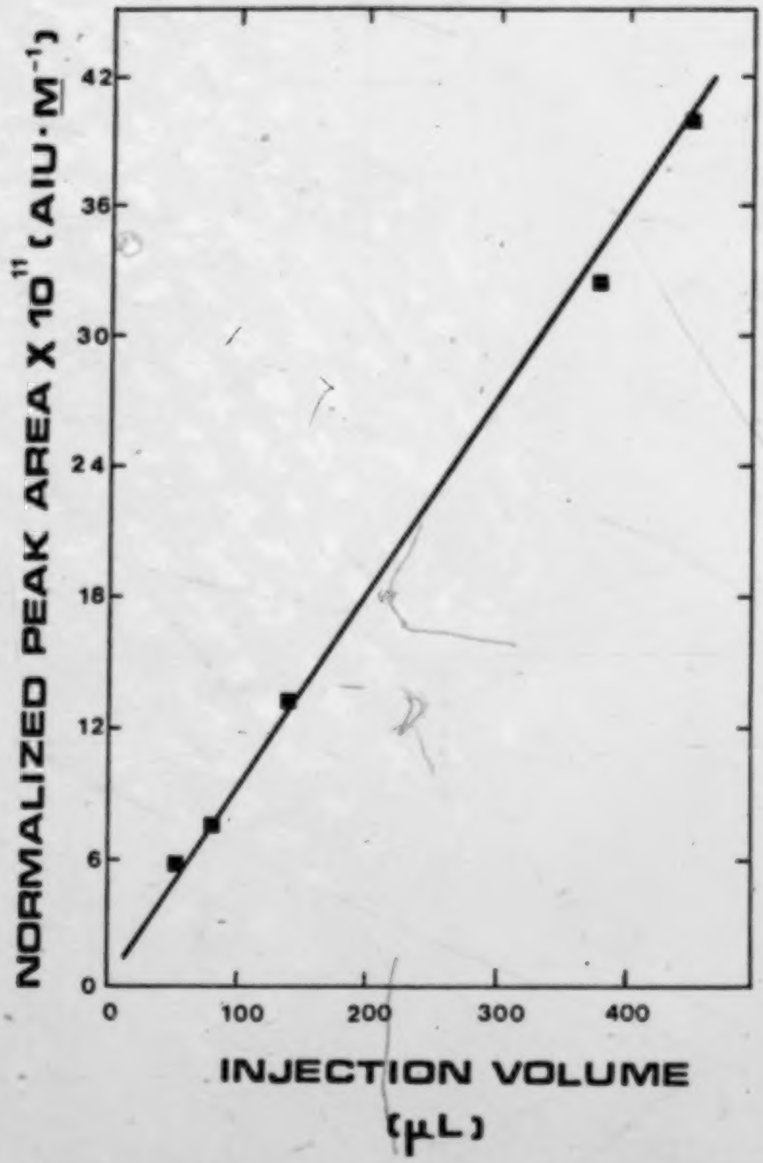

Figure 16. Normalized peak area versus injection volume for "medium" surfactant concentrations and the dye dissolved in toluene. The concentration of surfactant was 2 x 10^{-5} M and the dye concentration 9 x 10^{-5} M in toluene (equivalent to 4.5 x 10^{-4} M in water). Instrument parameters: As in table XIII.

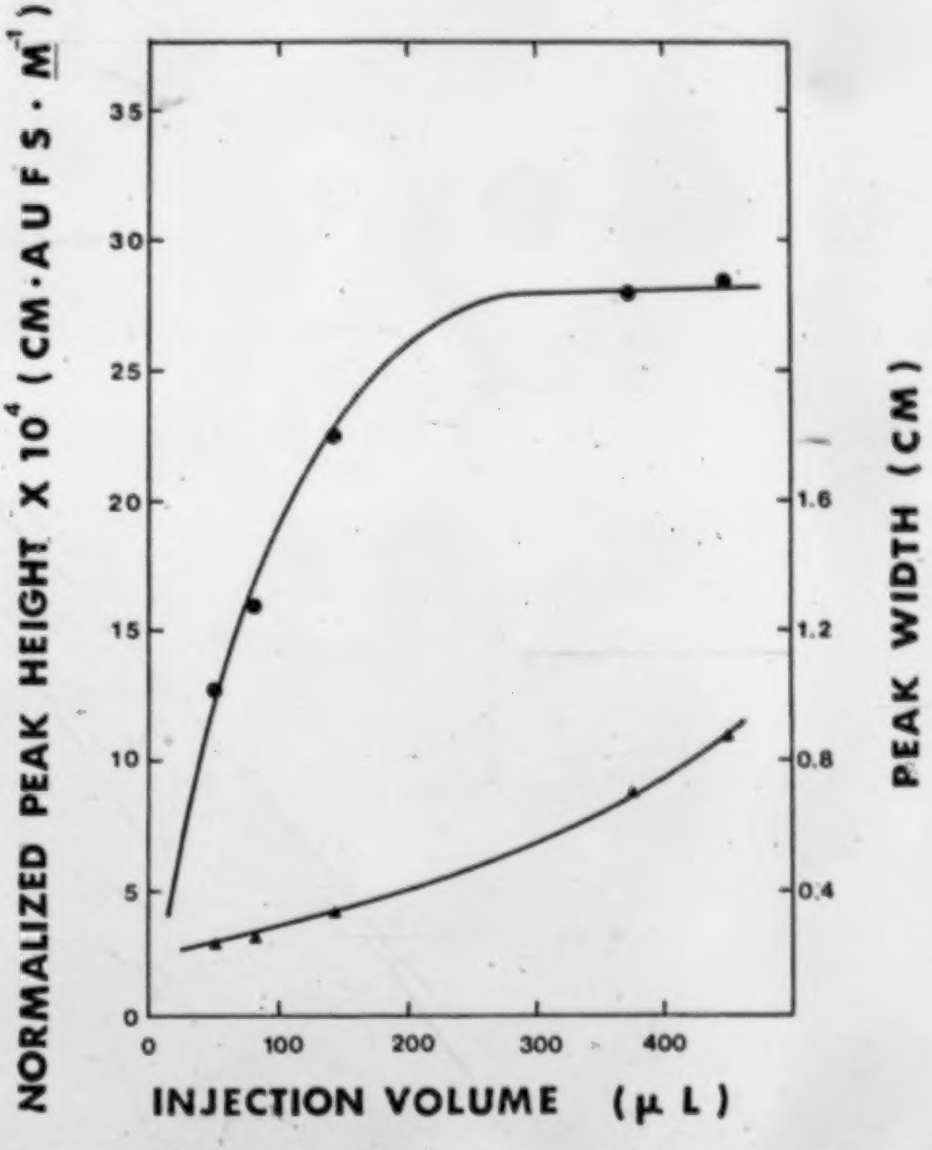

Figure 17. Peak widths (▲) and normalized peak heights (●) versus injection volume for "medium" surfactant concentrations and the dye dissolved in toluene. Surfactant concentration was 2×10^{-5} M and the dye concentration was 9×10^{-5} M in toluene (equivalent to 4.5×10^{-4} M in water). Instrument parameters: As in table XIII.

effect in the phase separator and a laminar flow effect in the unsegmented regions of the SE/FIA are sufficiently large to act upon the whole length of the sample zone. When the injection volumes are large enough (more than about 400 microliters), the two effects mentioned above affect only the leading and trailing edges of the sample zone. Since the central portion is not affected, peak height becomes independent of injection volume; whereas peak width becomes proportional to it. For injection volumes between 150 and 400 microliters, an intermediate behavior is observed.

When the concentration of surfactant was lowered by a factor of 10 while keeping the rest of parameters constant, the variable injection volume experiment yielded similar results as those obtained when the concentration of surfactant was 10 times higher. The plot of normalized peak area versus injection volume (figure 14) was again observed to be linear (slope=9.22 x 10^9, r.s.d.=1.74%; intercept=0.71 x 10^{11}, s.d.=0.43 x 10^{11}); and the plot of normalized peak height and peak width versus injection volume (figure 15), followed the same pattern of figure 13. However, as can be seen by comparing tables XIII and XIV, at the lower surfactant concentration (5 x 10^{-6} M), normalized areas were observed to be about 80% higher on average than they were for the higher surfactant concentration (5 x 10^{-5} M). Similarly, average increments of about 75% and 10% were seen for peak heights and peak widths, respectively.

It appears that when the surfactant concentration is relatively high, a substantial fraction of the dye-surfactant ion pair is "lost" resulting in an attenuated sensitivity. Conversely, when low surfactant concentrations are utilized, the fraction of dye-surfactant ion pair being formed and" loss" is smaller; thus, the sensitivity is not so severely affected. Such a "loss" of ion pair might be consistent with the view that the formation of a charged colloid competes with the extraction process and that the colloid once formed extracts only very slowly. If the attenuated sensitivity is attributed to the competitive formation of a charged colloid by the dye-surfactant compound, avoidance of this behavior can be achieved by dissolving the dye in the organic phase rather than in the aqueous phase. If the dye were dissolved in the organic phase, the following sequence would take place: (a) the dye would transfer to the aqueous phase very quickly as soon as both phases were brought together; (b) if there were no surfactant present, the dye would stay dissolved in the aqueous phase; (c) if surfactant were present, the transferred dye would react very rapidly with it to form the surfactant-dye ion pair and, subsequently, extraction of this ion pair into the organic phase would take place without the surfactant having been present together with a high dye concentration in the aqueous phase.

In an effort to find out if the use of the organic phase as solvent for the dye would reduce the concentration dependence of the sensitivity that was observed when the aqueous phase was utilized, the organic solvent stream (toluene) was replaced by a solution of the dye dissolved in toluene. The concentration of this solution is such that after taking into account the individual flow rates from the "organic" and "reagent" cylinders, the net amount of dye is still the same (see figure 2). In this experiment, the aqueous "reagent" cylinder which used to contain dye, buffer, and sodium sulfate, now contains only the buffer and the sodium sulfate. Keeping the rest of the parameters the same as those used when the dye was dissolved in water, and utilizing a surfactant concentration of 2×10^{-5} M, the variable injection volume test was performed again. This concentration value was intended to depict the behavior of the system when neither so large nor so low concentrations of surfactant were utilized. Results are sumarized in table XV and figures 16 and 17.

As in figures 12 and 14, the plot of peak area versus injection volume (figure 16) was again linear, with a slope of 8.59×10^9 (r.s.d.=1.75%) and an intercept of 1.20×10^{11} (s.d.=0.41×10^{11}); whereas the plot of peak height and peak width versus injection volume (figure 17) indicated that the same general trends are followed as in figures 13 and 15. However, a quantitative comparison of the magnitude of the signal obtained under the three sets of conditions, showed that the normalized values of peak areas, peak heights, and peak widths observed when the dye was dissolved in toluene rather than in water were comparable to the higher sensitivity obtained for the low surfactant concentration in table XIV.

As a consequence of these experiments, toluene was adopted as the solvent for the dye since it provides an enhanced sensitivity. An injection volume of 50 microliters was chosen for subsequent studies since it represents a favorable compromise between maximum sampling frequency (small peak widths) and an unnecessary sacrifice in sensitivity (large peak heights).

2.3.8 Calibration curves with SLS

Calibration curves were obtained at various stages during the development of the SE/FIA system. These curves were intended to give an evaluation of the status of the system, as the optimization steps were carried out, based on parameters such as intercept values, relative standard deviation of the slope, and dynamic range. A total of four calibration curves, presented in tables XVI-XIX and figures 18-21, were obtained under a variety of different working conditions by injecting several sodium dodecyl sulfate solutions over a wide range of concentrations. Experimental conditions are given in the figure and table captions.

After the extraction coil length study was performed (section 2.3.5), it became apparent that the coil length utilized before was inappropriate since

Table XVI. Calibration curve #1. Instrument parameters: Dye concentration, 3×10^{-4} M (aqueous); sodium sulfate concentration, 0.6 M; buffer composition, 0.18 M sodium acetate and 0.16 M acetic acid; wavelength, 546 nm; extraction coil length, 450 cm; nitrogen pressure, 20 psig; injection volume, 50 microliters; sample, sodium dodecyl sulfate.

[Surfactant] (M)	Peak height(a) (cm)	r.s.d. (%)	Peak area (a.i.u. x 10^6)	r.s.d. (%)
1.0×10^{-4}	114	2.6	18.3	5.1
7.5×10^{-5}	83.8	7.7	14.6	5.9
5.0×10^{-5}	55.9	2.2	9.34	2.4
2.5×10^{-5}	35.5	3.5	5.93	2.5
1.0×10^{-5}	20.5	3.7	3.30	2.0
5.0×10^{-6}	11.6	4.3	1.74	5.4
1.0×10^{-6}	3.5	13.4	0.71	22.2
5.0×10^{-7}	Not detectable	—	Not detectable	—

(a) The data were normalized using equation 2.2

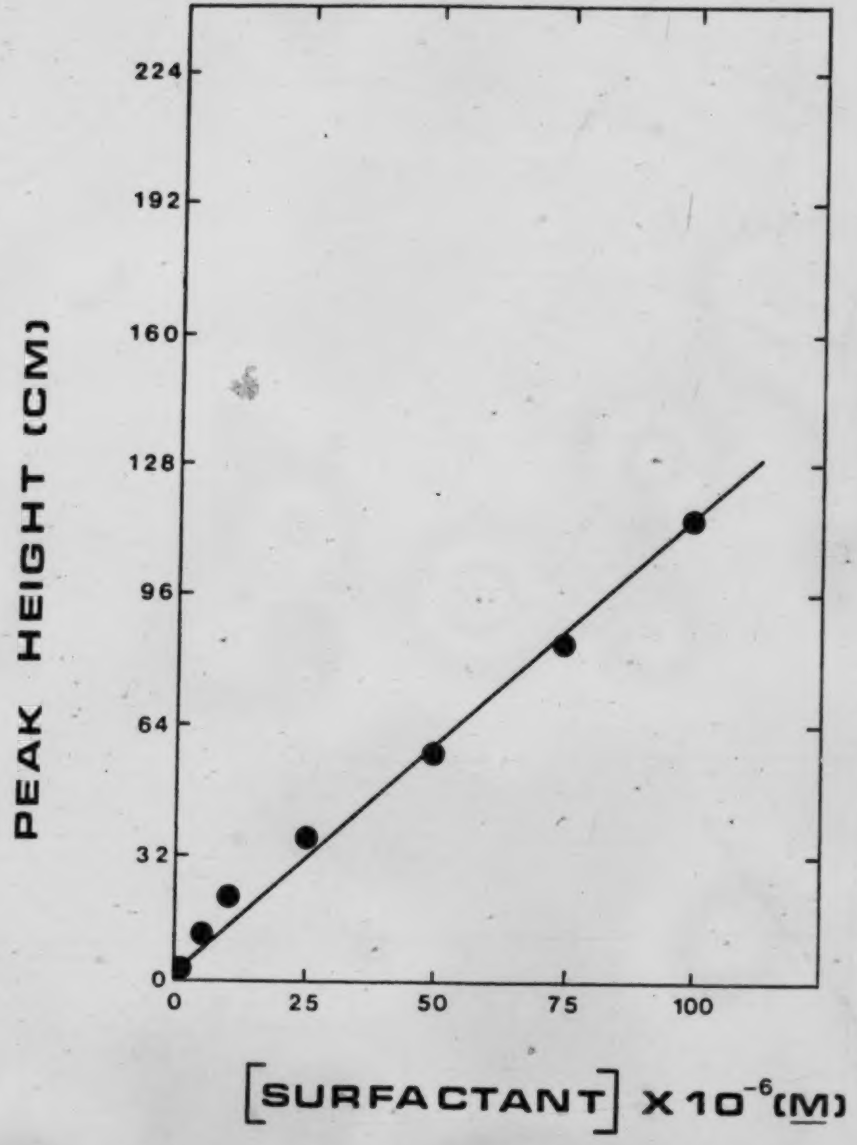

Figure 18. Calibration curve #1. Instrument parameters: Dye concentration, 3 x 10^{-4} M (aqueous); sodium sulfate concentration, 0.6 M; buffer composition, 0.18 M sodium acetate and 0.16 M acetic acid; wavelength, 546 nm; extraction coil length, 450 cm; nitrogen pressure, 20 psig; injection volume, 50 microliters; sample, sodium dodecyl sulfate.

Table XVII. Calibration curve #2. Instrument parameters: As in table XVI, except that the dye concentration was 4.5×10^{-5} M (aqueous).

[Surfactant] (M)	Peak height$^{(a)}$ (cm)	r.s.d. (%)	Peak area (a.i.u. x 10^6)	r.s.d. (%)
1.0×10^{-4}	125	8.3	20.6	5.9
7.5×10^{-5}	92.9	5.4	16.9	4.5
5.0×10^{-5}	60.0	5.6	11.8	17.5
2.5×10^{-5}	36.5	2.9	6.15	4.0
1.0×10^{-5}	21.5	2.4	3.13	2.8

(a) The data were normalized using equation 2.2

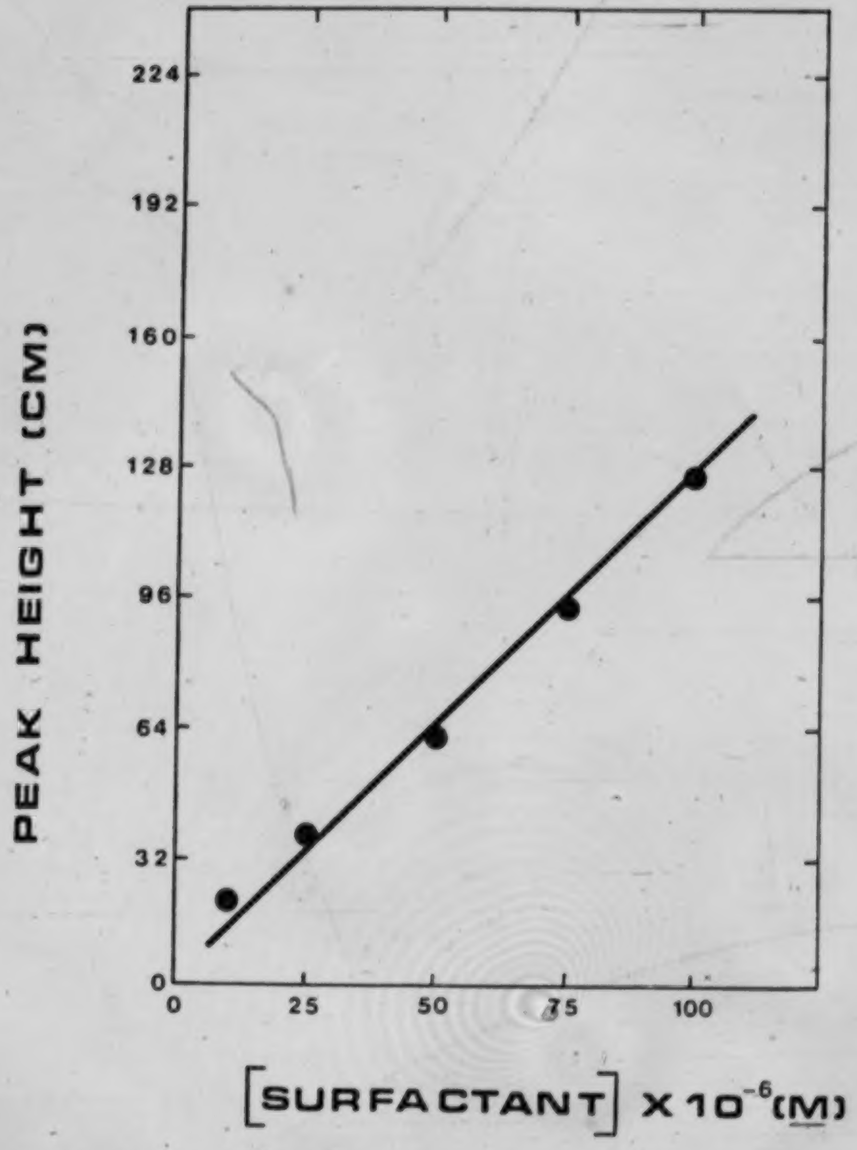

Figure 19. Calibration curve #2. Instrument parameters: As in calibration curve #1, except that the dye concentration was 4.5 x 10^{-4} M (aqueous).

Table XVIII. Calibration curve #3. Instrument parameters: As in table XVI, except that the dye concentration was 6×10^{-5} M dissolved in toluene (equivalent to a 3×10^{-4} M aqueous dye solution).

[Surfactant] (M)	Peak height (cm)	(r.s.d.) (%)	Peak area (a.i.u. x 10^6)	r.s.d. (%)
1.0×10^{-4}	140	0.7	27.9	1.1
7.5×10^{-5}	126	1.2	23.5	0.4
5.0×10^{-5}	114	1.4	18.9	1.1
2.5×10^{-5}	57.6	1.0	9.78	0.7
1.0×10^{-5}	23.9	1.1	3.94	0.8
5.0×10^{-6}	11.6	1.7	1.97	1.7
2.5×10^{-6}	5.7	1.9	0.97	2.4
1.0×10^{-6}	2.3	4.8	0.43	2.4
7.5×10^{-7}	Not detectable	—	Not detectable	—

(a) The data were normalized using equation 2.2

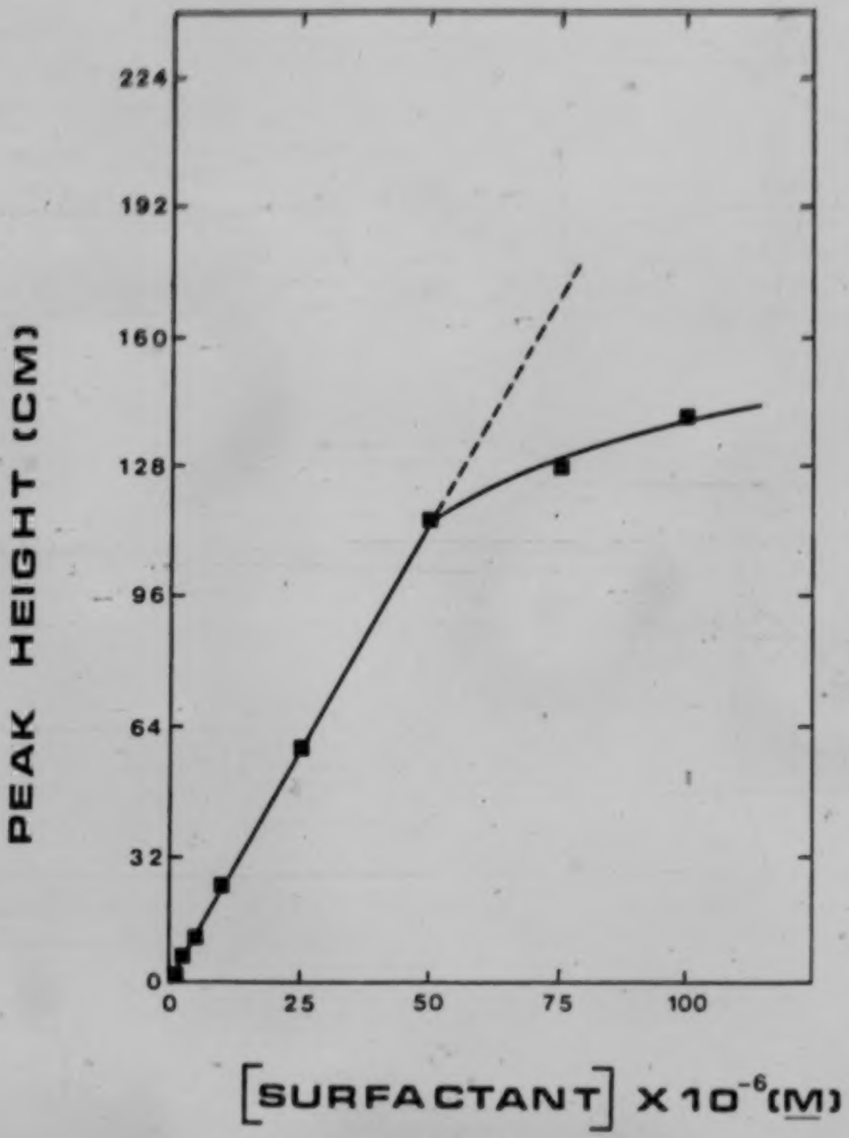

Figure 20. Calibration curve #3. Instrument parameters: As in calibration curve #1, except that the dye concentration was 6 x 10^{-5} M dissolved in toluene (equivalent to 3 x 10^{-4} M in water).

Table XIX. Calibration curve #4. Instrument parameters: As in table XVI, except that the dye concentration was 9×10^{-5} M dissolved in toluene (equivalent to a 4.5×10^{-4} M aqueous dye solution).

[Surfactant] (M)	Peak height[a] (cm)	r.s.d. (%)	Peak area (a.i.u. x 10^6)	r.s.d. (%)
1.0×10^{-4}	224	0.7	34.9	1.6
7.5×10^{-5}	199	0.7	29.0	1.0
5.0×10^{-5}	138	0.7	21.2	0.9
2.5×10^{-5}	60.6	1.0	9.40	0.9
1.0×10^{-5}	23.2	1.0	4.06	0.5
5.0×10^{-6}	11.8	1.7	2.31	2.4
1.0×10^{-7}	2.96	5.1	0.72	4.1
7.5×10^{-7}	Not detectable	—	Not detectable	—

(a) The data were normalized using equation 2.2

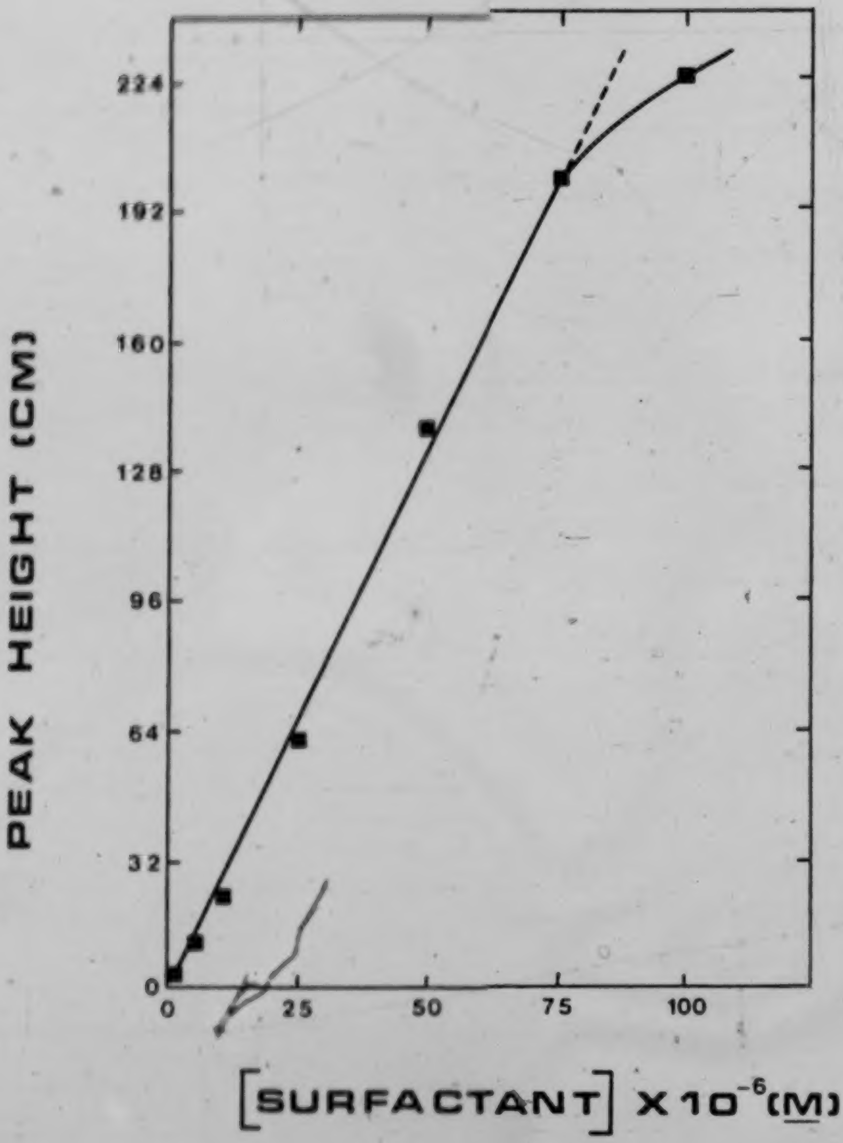

Figure 21. Calibration curve #4. Instrument parameters: As in calibration curve #1, except that the dye concentration was 9×10^{-5} M dissolved in toluene (equivalent to 4.5×10^{-4} M in water).

distribution equlibrium had not been attained at the short coil lengths used. A calibration curve was obtained using a solution of dye in water and employing an extraction coil of 450 cm. The results are presented in table XVI and figure 18. In addition to peak heights, measured manually from a strip chart recorder, peak areas were also obtained by means of an integrator. Peak heights were normalized using equation 2.2. Since peak areas are independent of the range setting in the detector and of the attenuation value used in the integrator, no normalization was required. The range of concentrations studied was from 1×10^{-7} M to 1×10^{-4} M and the results obtained were as follows: Between 1×10^{-6} M and 1×10^{-4} M, a linear relationship was observed for both peak heights and areas. Concentrations at and below 5×10^{-7} M were undetectable. For heights, the slope was 1×10^{6} (r.s.d.=3.30%) and the intercept was 6.15 (s.d.=1.79); whereas for areas, the slope was 1.75×10^{11} with a relative standard deviation of 3.04% and the intercept was 1.06×10^{6} with a standard deviation equal to 0.28×10^{6}.

A second calibration curve was obtained under conditions similar to the first except that the concentration of dye in the aqueous phase was raised from 3×10^{-4} M to 4.5×10^{-4} M (table XVII and figure 19). The behavior of the system was monitored in terms of peak heights and peak areas, and it was found that the dynamic range was narrower than that which had been seen in figure 18. This was due to a substantial increase in the noise level, which also caused the precision of this curve (estimated as the relative standard deviation of the slope) to deteriorate. Surfactant concentrations smaller than 1×10^{-5} M were not detectable, and linearity was obtained for peak heights (slope= 1.15×10^{6}, r.s.d. of the slope= 4.28%, intercept= 7.35, s.d. of the intercept=3.02) and for peak areas (slope= 1.99×10^{11}, r.s.d. of the slope= 4.08%, intercept= 1.40×10^{6}, s.d.

of the intercept= 0.50 x 10^6) when working at surfactant concentrations ranging between 1 x 10^{-5} and 1 x 10^{-4} M.

After realizing that the formation of a charged colloid of the ion pair is likely when the dye is present in the aqueous phase (see sections 2.3.5 - 2.3.7), a calibration curve was obtained starting with the dye in the toluene phase. The dye concentration in toluene was 6 x 10^{-5} M which is equivalent to a 3 x 10^{-4} M aqueous dye solution. The equivalence arises from a difference in flow rates. The results are presented in table XVIII and figure 20. Peak heights and peak areas were used to monitor the experiment. The detection limit was found to be 1 x 10^{-6} M and linearity in the calibration curve was observed in the concentration range between 1 x 10^{-6} and 5 x 10^{-5} M surfactant. This represented a narrower dynamic range than in previous calibration curves but, in contrast, the precision of the curve was extremely good. For peak heights, the relative standard deviation of the slope was 0.60% (slope= 2.27 x 10^6, intercept= 0.40, standard deviation of the intercept= 0.32); whereas for peak areas, a value of 0.85% was found (slope= 3.78 x 10^{11}, intercept= 0.11 x 10^6, s.d. of intercept= 0.07 x 10^6).

In an effort to expand the limited dynamic range obtained on calibration curve #3 while keeping the excellent linearity, a new calibration curve (table XIX and figure 21) was obtained utilizing a more concentrated solution of the dye dissolved in toluene. The concentration used was 9 x 10^{-5} M in toluene, which would be equivalent to 4.5 x 10^{-4} M in water, and the rest of the instrument variables were kept as in calibration curve #3. As a result, a limit of detection equal to 1 x 10^{-6} M was found, and a linear relationship was observed for both peak heights and areas in the concentration range from 1.0 x 10^{-6} to 7.5 x 10^{-5} M surfactant. Even though an expanded dynamic range was obtained, the precision of the curve deteriorated to 2.14% for peak heights (slope=

2.70×10^6, intercept= 2.20, s.d. of the intercept= 2.23), and 3.20% for peak areas (slope= 3.92×10^{11}, intercept= 0.28×10^6, s.d. of the intercept= 0.48×10^6).

A comparison of the calibration curves shown above indicated that, based on relative standard deviation of the slope, intercept, and standard deviation of the intercept, the best calibration curve would be curve #3 (see figure 20). However, the dynamic range of this curve was not very broad, thereby imposing a restriction on the analytical method. For the purpose of discovering the reasons for this limited dynamic range, several hypotheses were postulated and examined. The results obtained are presented thoughout the following sub-sections (2.3.8.1 - 2.3.8.5).

2.3.8.1 Non-linearity of the detector

To test this hypothesis, a stock solution of dye in toluene was prepared in a separatory funnel taking care to pre-saturate the toluene with an aqueous solution of sodium sulfate and buffer, so as to duplicate the SE/FIA conditions. Afterwards, serial dilution was employed to prepare a series of dye solutions of decreasing concentration in pre-saturated toluene. The absorbance values of these solutions were measured using both the flow-through FIA detector (Spectra-Physics 8200; at 546 nm) and a spectrophotometer (Cary 118; scanning from 750 to 400 nm). The observed values are presented in table XX and on figures 22 and 23, where it can be seen that the absorbance measurements obtained with the SE/FIA detector and with the spectrophotometer were found to agree reasonably well. Linear response and close agreement was observed for both detectors when measuring absorbance values ranging from 0.1 to 1.1. For higher absorbance values, it could not be established if the same resemblance existed because the maximum absorbance setting in the SE/FIA detector was 1.28 AUFS thereby making the maximum absorbance value that could be

Table XX. Calibration curve data for ethyl violet. The absorbance values were obtained at 546 nm using both a flow-through FIA detector (Spectra-Physics 8200) and a spectrophotometer (Cary 118,Varian Inc.). A manual method was followed to prepare the samples (see text for details).

[dye] (M)	Carry 118 (Abs. units)	SP-8200 (Abs. units)
4.0×10^{-5}	2.063	—[(a)]
3.6×10^{-5}	1.691	—[(a)]
2.4×10^{-5}	1.094	1.091
1.2×10^{-5}	0.570	0.622
0.6×10^{-5}	0.287	0.300
0.3×10^{-5}	0.108	0.107

(a) The fact that the maximum range setting in the detector is 1.28 AUFS restricted the absorbance measurements in the SP-8200 to 1.28 absorbance units.

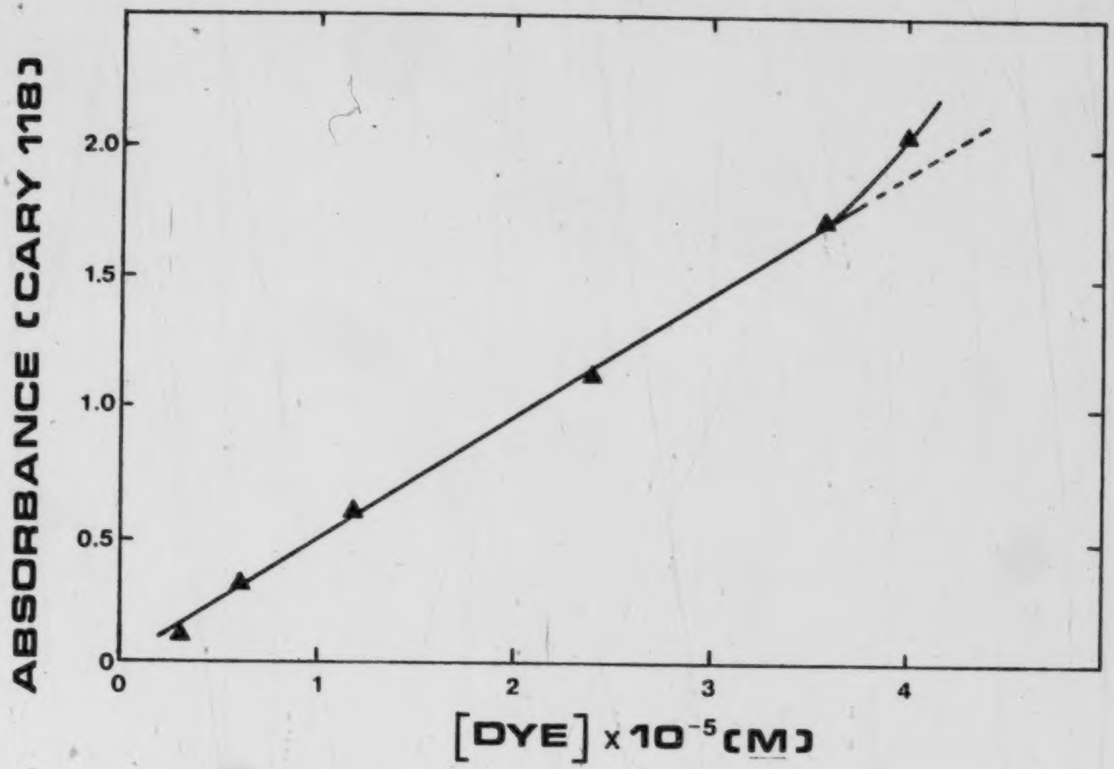

Figure 22. Calibration curve for ethyl violet. Solutions were prepared manually in toluene and their absorbances at 546 nm were measured in a spectrophotometer (Cary 118. Varian Inc.)

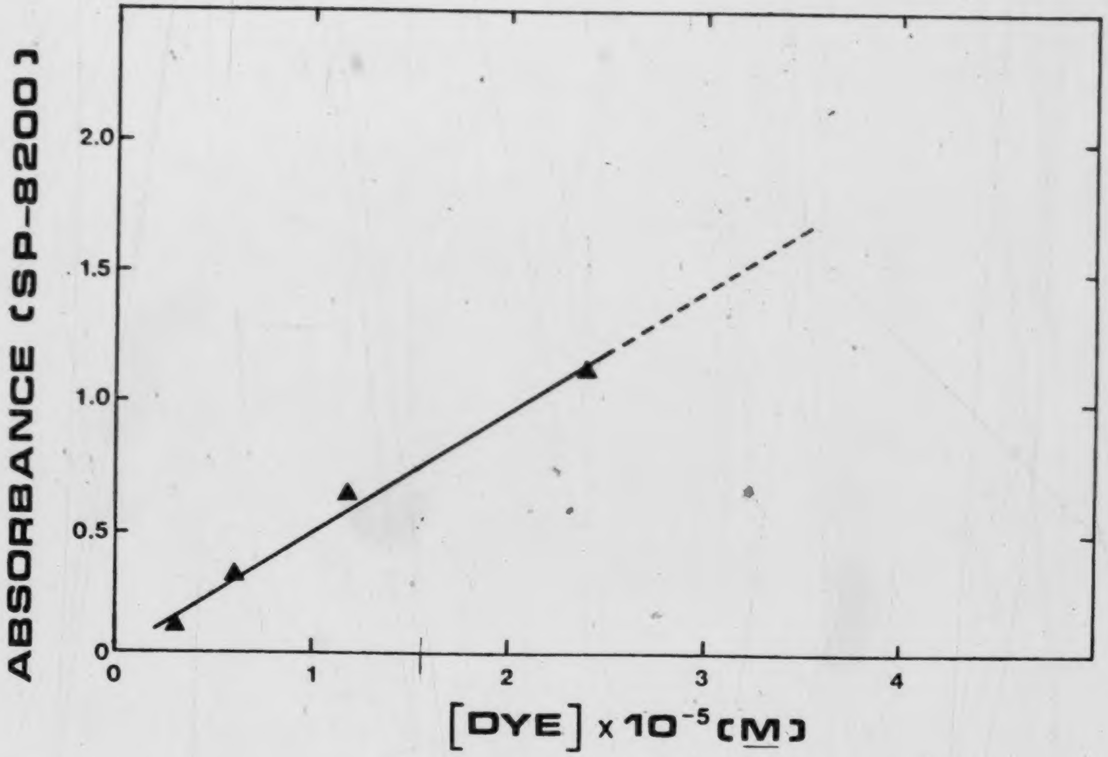

Figure 23. Calibration curve for ethyl violet obtained by measuring the absorbance values in the FIA flow-through detector (Spectra- Physics 8200). Sample solutions were prepared as in figure 22.

measured 1.28 absorbance units. However, since calibration curve #3 (see figure 20) was observed to flatten out at an absorbance value of about 0.3, while the SE/FIA detector was able to handle values of up to 1.1, it was concluded that the hypothesis of detector non-linearity is not true.

It was observed during this experiment that if a dye solution is left exposed to light, slight decomposition seems to occur. The spectrum of a freshly made dye solution or of a solution that has been protected from the light shows only two maxima at around 613 and 543 nm; whereas the spectrum of a dye solution exposed to light for about 24 hours or more shows an additional small peak between 575 and 425 nm. Fortunately, for experimental purposes in the SE/FIA system, a freshly made solution of dye is prepared and introduced into a cylinder where it is protected from light.

2.3.8.2 Chemical deviation from Beer's law

To find out if the calibration curves were flattening out as a consequence of a chemical deviation from Beer's law, two experiments were done. In the first experiment, a dye-surfactant ion pair stock solution was prepared in a separatory funnel emulating the FIA conditions; namely, the organic to aqueous phase ratio, the dye to surfactant molar ratio, and the buffer and sodium sulfate concentrations. A shaking time of 5 min was used after a test showed that there was no difference in the absorbance of the stock solution when shaking times ranging from 3 to 30 min were utilized. The stock solution was then diluted to obtain several dye-surfactant ion pair solutions, and their spectra recorded in a spectrophotometer. The absorbance values of these solutions at 546 nm are presented in table XXI and figure 24, where it can be seen that a linear relationship between absorbance and concentration exists (slope= 6.11×10^4, r.s.d. of the slope= 1.57%, intercept= -0.01, s.d. of the intercept= 0.01).

Table XXI. Data for Beer's law plot for the dye-surfactant ion pair. A stock sample solution was prepared manually (see text for details) and diluted to obtain several dye-surfactant ion pair solutions. Their absorbances were measured in a spectrophotometer at 546 nm.

[Ion pair] (M)	Absorbance at 546 nm (Abs. units)
10.0×10^{-6}	0.602
8.00×10^{-6}	0.475
6.00×10^{-6}	0.359
5.00×10^{-6}	0.277
3.00×10^{-6}	0.172
2.00×10^{-6}	0.112
1.00×10^{-6}	0.051

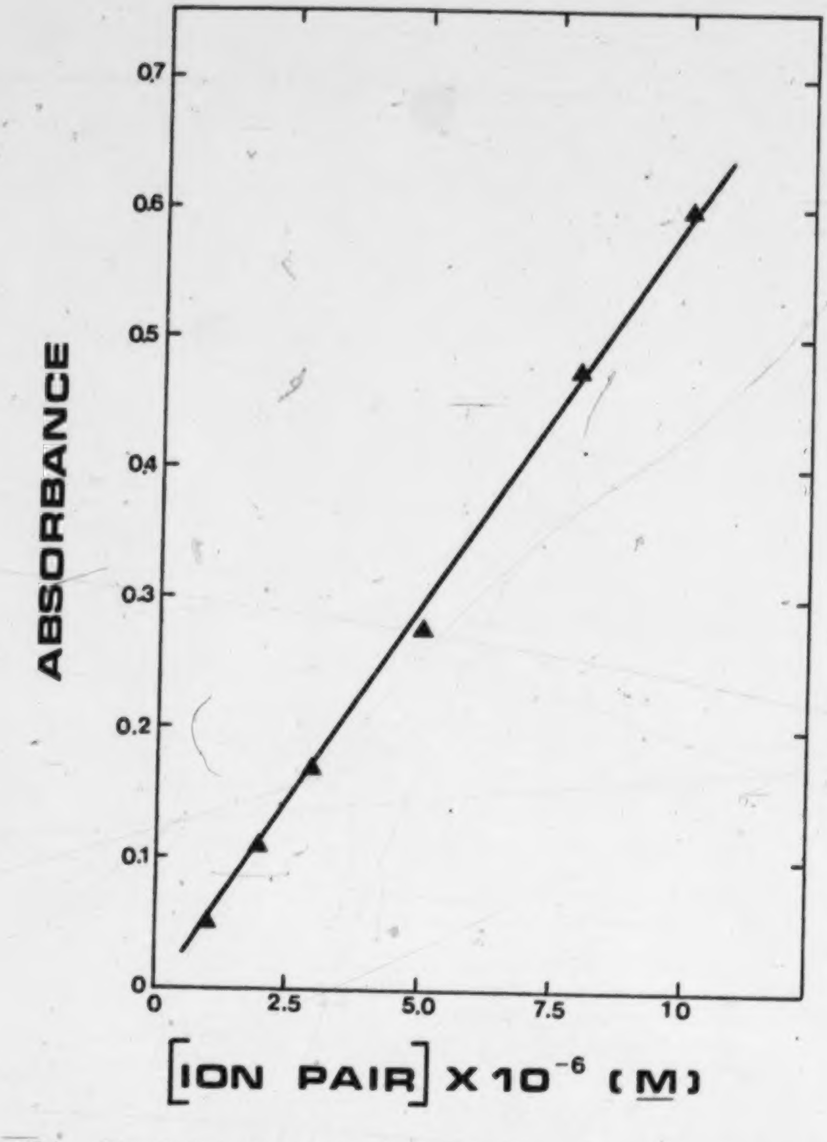

Figure 24. Beer's law plot for the dye-surfactant ion pair. A stock sample solution was prepared manually (see text for details) and diluted to obtain several dye-surfactant ion pair solutions.Their absorbances were measured in a spectrophotometer at 546 nm.

In the second experiment, the ion pair formation and extraction was done individually for a series of surfactant concentrations, in contrast with the previous experiment where only one such operation was done and the resulting solution subsequently diluted. A shaking time of one min was utilized in the present experiment to mimic more closely the SE/FIA system, where the whole process from injection to detection takes 64 sec. The results obtained are shown in table XXII and figure 25. Linearity between absorbance and concentration was also observed in this case (slope= 4.91 x 10^4, r.s.d. of the slope= 1.34%, intercept= -0.001, s.d. of the intercept= 0.004).

Despite the apparent similarity between conditions in the present experiments and those in the SE/FIA system, the absorbance-concentration behavior was not similar. In the former, no deviation from linearity was observed in absorbances ranging from 0.01 to about 0.6; whereas in the latter, non-linearity was present at an absorbance value of about 0.3. As a consequence, the hypothesis of non-linearity being caused by a chemical deviation from Beer's law was discarded.

2.3.8.3 Dimerization or formation of higher aggregates

The possibility was investigated that formation of dimers or higher aggregates might be taking place in the organic phase at high concentrations of ion pairs. If this were occurring it might reduce absorbance values and, therefore, cause the non-linear behavior observed in our SE/FIA calibration curve. The presence of aggregates can often be inferred when changes occur in the spectra of solutions with increasingly higher concentrations. Therefore, the spectra obtained in sub-sections 2.3.8.1 and 2.3.8.2 for dye and dye-surfactant solutions were examined (see figures 26 and 27). This was done by calculating the ratio of "absorbance of peak to absorbance of valley" for the two maxima at 613 nm and 543 nm and the valley at 580 nm for all the different concentrations utilized in each set of solutions. The calculated ratios were found to be

Table XXII. Data for Beer's law plot for several dye-surfactant ion pair solutions. Sample solutions were prepared manually (see text for details) and their absorbances obtained via a spectrophotometer at 546 nm.

[Ion pair] (M)	Absorbance at 546 nm (Abs. units)
10.0×10^{-6}	0.486
8.00×10^{-6}	0.395
4.00×10^{-6}	0.195
2.00×10^{-6}	0.096

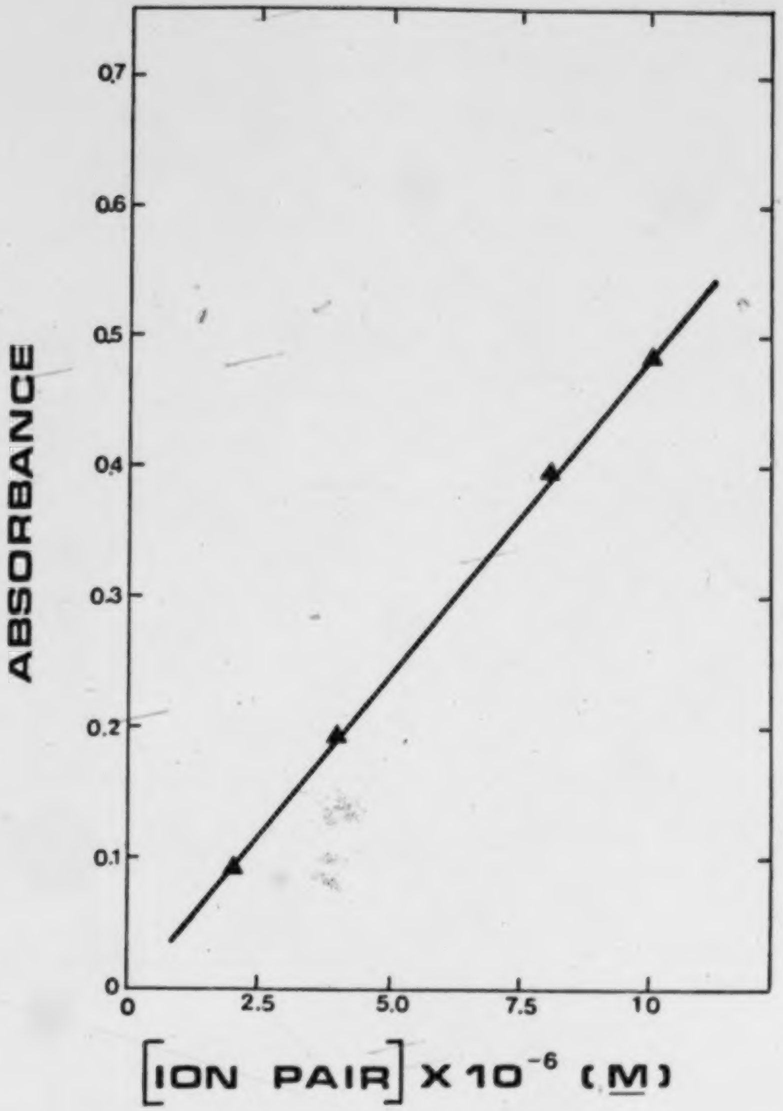

Figure 25. Beer's law plot for several dye-surfactant ion pair solutions. Sample solutions were prepared manually (see text for details) and their absorbances obtained via a spectrophotometer at 546 nm.

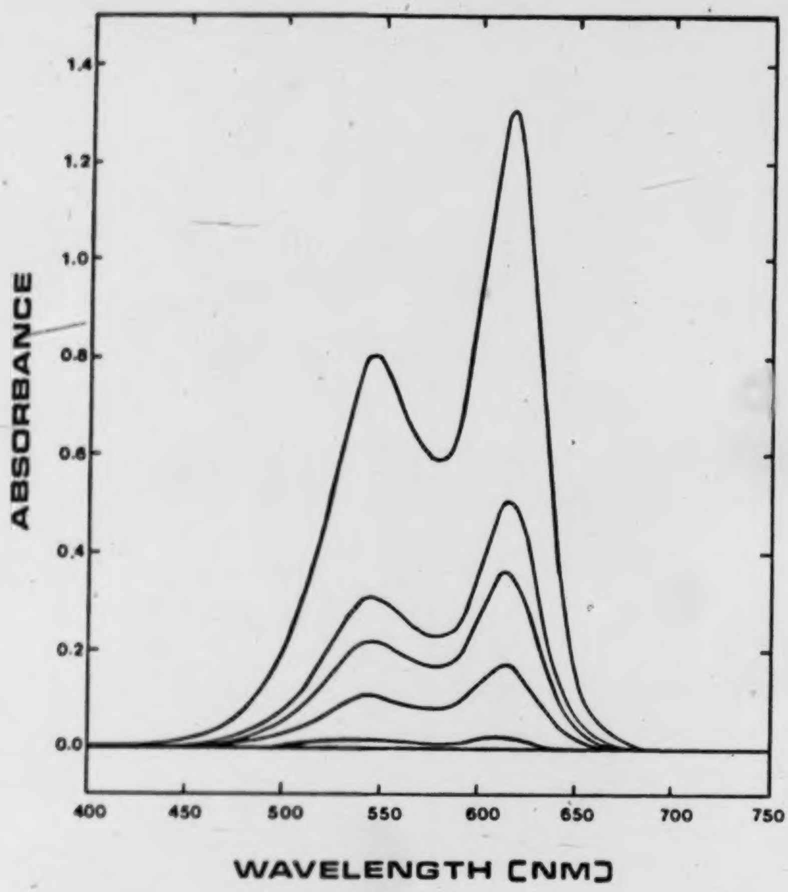

Figure 26. Spectra of ethyl violet solutions. The samples were prepared manually as described in section 2.3.8.1 and scanned in a spectrophotometer (Cary 118. Varian Inc.) from 750 to 400 nm at a speed of 2 nm/sec.

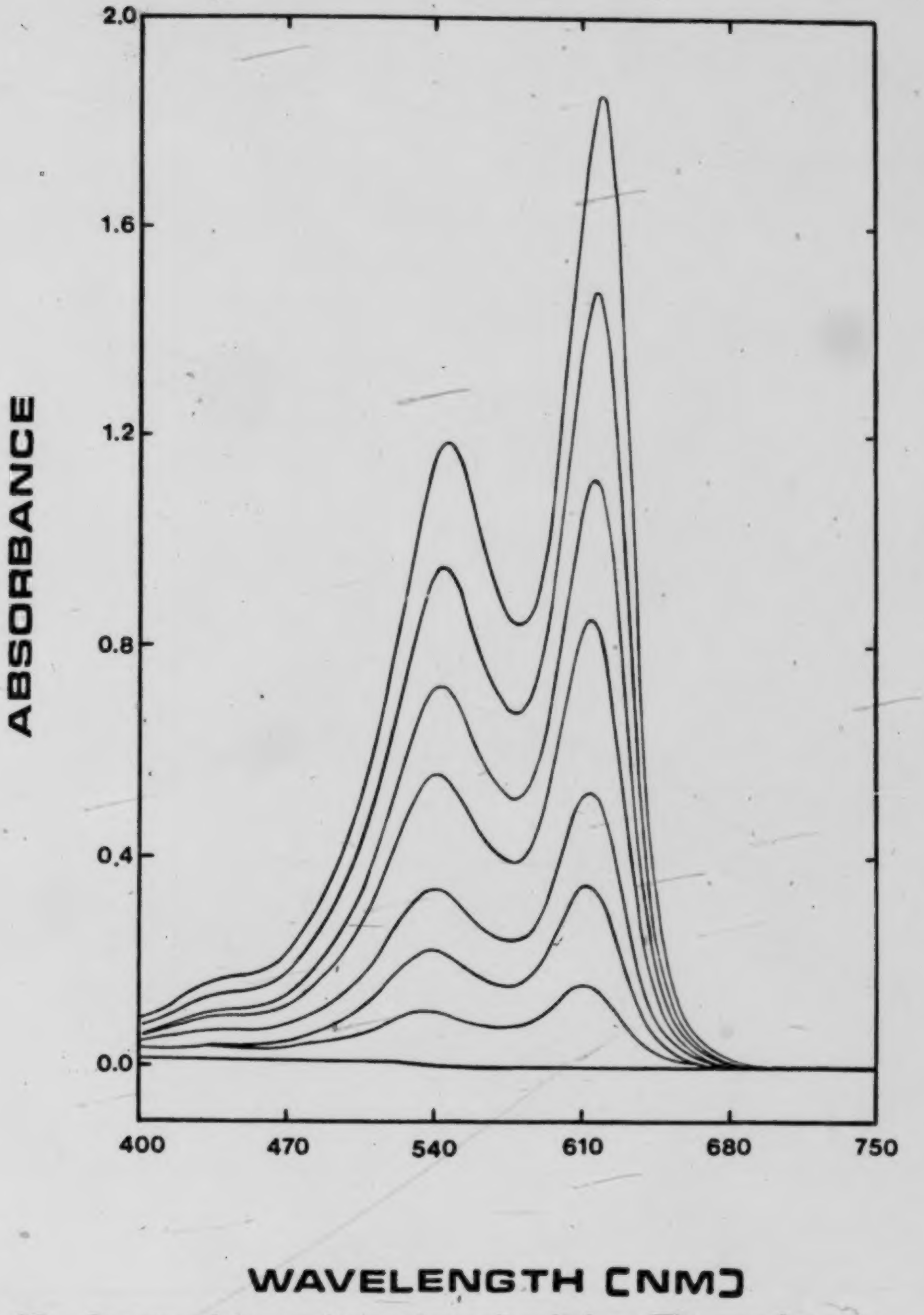

Figure 27. Spectra of dye-surfactant ion pair solutions. The samples were prepared manually as described in section 2.3.8.2 and scanned in a spectrophotometer (Cary 118. Varian Inc.) from 750 to 400 nm at a speed of 2 nm/sec.

essentially constant for both the dye and the ion-pair solutions, and this was interpreted as an indication that dimers or higher aggregates were not forming. However, these tests do not represent conclusive proof because it is possible, though unlikely, that an aggregate might exhibit the same absorption spectrum as the original species.

2.3.8.4 Insufficiently long extraction coil

The study of the effect of extraction coil length performed in section 2.3.5 showed that the use of a 450-cm coil length allowed the attainment of a distribution equilibrium. However, this experiment was performed using the dye dissolved in water. Therefore, it was hypothesized that utilizing the dye dissolved in toluene, there might not be enough time for the attainment of equilibrium since an extra step (extraction of the dye into water) is involved in the process. In order to find out, a variable extraction coil length study was performed under the same conditions as those used in calibration curve #3. The results obtained are shown in tables XXIII and XXIV as well as on figures 28 and 29. As in section 2.3.5, the data obtained directly from the experiment was called "raw data" (see table XXIII). The "corrected" data were obtained in the same manner as in section 2.3.5; that is, peak heights were corrected for flow rate variations by multiplying them times the ratio of total flow rate of organic phase to the flow rate of the carrier (see figure 28), while peak areas were calculated from peak heights and peak widths at half-height and subsequently corrected by multiplying the values obtained times the total flow rate of organic phase (see figure 29).

A comparison of figures 28 and 29 with figures 10 and 11 indicates that the distribution equilibrium attainment occurs at approximately the same coil length regardless of whether the dye is dissolved in toluene or in water. This suggests

Table XXIII. "Raw data" of peak heights and peak widths at half-height as a function of variable extraction coil length. Instrument parameters: Injection volume, 50 microliters; wavelength 546 nm; nitrogen pressure, 20 psig; dye concentration, 6×10^{-5} M in toluene (equivalent to 3×10^{-4} M aqueous solution); buffer composition, 0.18 M sodium acetate and 0.16 M acetic acid; sodium sulfate concentration, 0.6 M; extraction coil length, variable.

Extraction coil length (cm)	Peak height(a) (cm)	r.s.d. (%)	Peak width(b) (cm)	r.s.d. (%)	$F_{o,t}$ (mL/min)	$F_{a,t}$ (mL/min)	Residence time (sec)
10	33.2	2.2	0.17	4.6	2.2	1.2	12
20	44.7	1.5	0.17	2.6	2.1	1.2	12
50	71.0	0.8	0.16	1.8	2.0	1.1	18
110	91.8	1.4	0.17	1.7	2.0	1.1	21
200	113	1.6	0.16	0.0	1.9	1.1	30
320	124	1.9	0.18	0.0	1.8	1.0	45
440	131	0.9	0.19	1.5	1.8	0.9	64
560	128	1.6	0.84	2.6	1.6	0.9	86
680	119	0.7	0.27	1.9	1.5	0.8	111

(a) Peak height data were normalized using equation 2.2.

(b) Peak widths required no normalization.

Note: $F_{o,t}$ and $F_{a,t}$ stand for total flow rates of organic and aqueous phases.

Table XXIV. Corrected peak heights and peak areas as a function of variable extraction coil length. Instrument parameters as in table XXIII.

Extraction coil length (cm)	$\frac{\text{Peak height} \times F_{o,t}}{F_c}$ (cm)	Peak area[a] $\times F_{o,t}$ (cm^2 mL min^{-1})
10	121.7	12.4
20	156.5	16.0
50	270.9	23.8
80	276.7	24.3
110	334.0	31.2
200	391.0	34.4
320	447.8	40.3
440	522.4	44.7
560	454.5	45.0
680	447.6	48.3

(a) Peak areas were calculated from peak heights and peak widths at half-height.

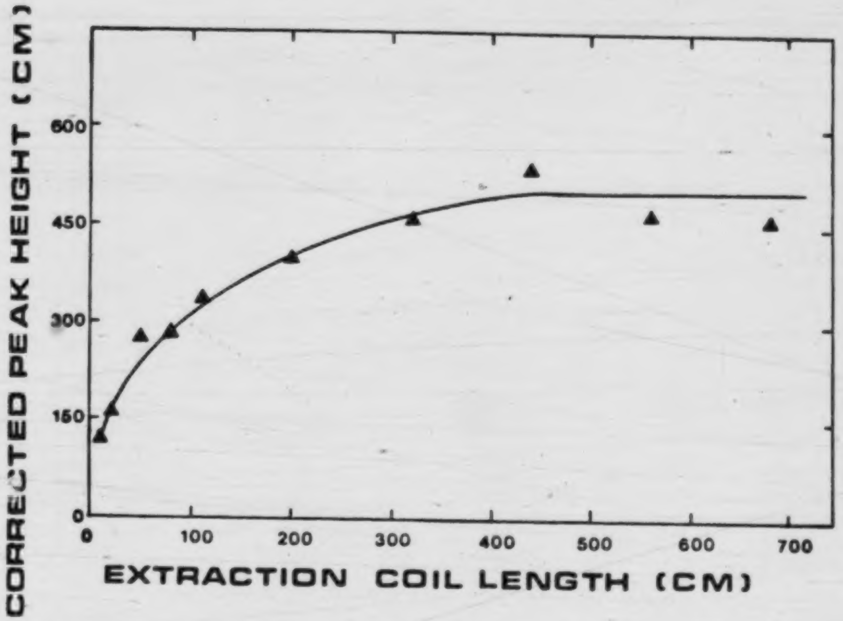

Figure 28. Corrected peak heights as a function of variable extraction coil length. Instrument parameters: Injection volume, 50 microliters; wavelength, 546 nm; nitrogen pressure, 20 psig; dye concentration, 6 x 10^{-5} M in toluene (equivalent to 3 x 10^{-4} M aqueous solution); buffer composition, 0.18 M sodium acetate and 0.16 M acetic acid; sodium sulfate concentration, 0.6 M; extraction coil length, variable.

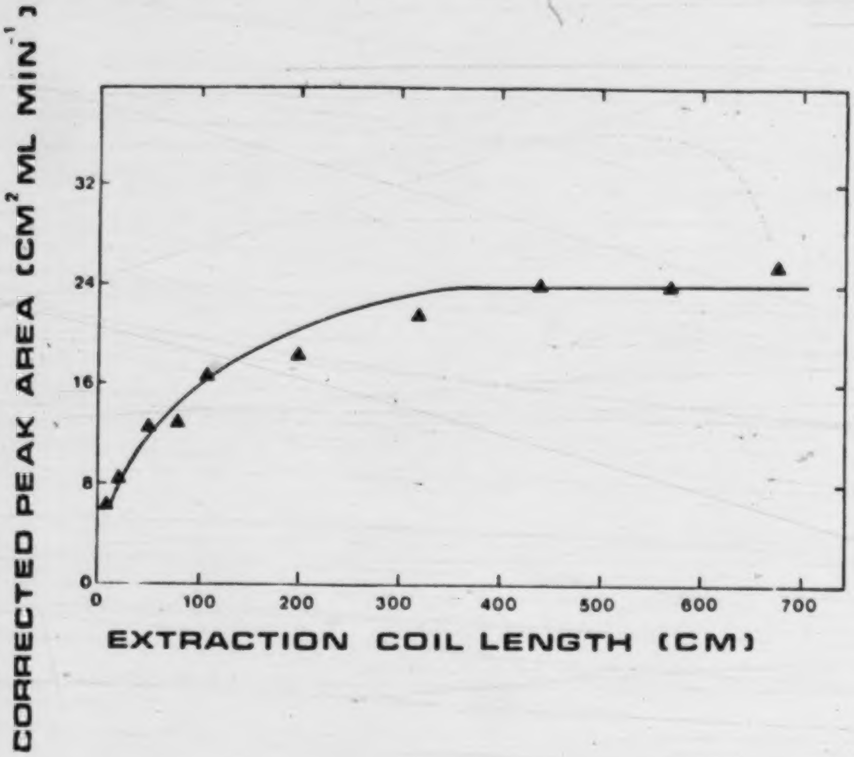

Figure 29. Corrected peak areas as a function of variable extraction coil length. Instrument parameters: As in figure 28.

that the rate of extraction of the dye into the aqueous phase is quite large, and that a longer coil length is not required.

Incidentally, it was noted that when extraction coil lengths smaller than 20 cm were used, the organic phase was observed to remain strongly colored instead of becoming colorless. This was obviously caused by the fact that at such short coil lengths, the dye is not quantitatively transfered into the aqueous phase.

In conclusion, after examining several possibilities, there was no immediately obvious reason for the rather small dynamic range on calibration curve #3 and no obvious mean to improve this situation. Nevertheless, taking calibration curve #3 as it was obtained, it can be said that a set of conditions was available for the analysis of sodium dodecyl sulfate and, hopefully, other anionic surfactants with a precision of 1%.

The factors which have been investigated so far do not shed light on the reasons why a higher dye concentration gives either a smaller dynamic range or greater noise, or both. The subject will again be addressed in chapter 3.

2.3.9 Ethyl violet

After completing the work described up to this point, the batch of ethyl violet with which all the experiments had been performed ran out. This batch was manufactured by Allied chemical but the product was no longer being produced by this company. Therefore, two new batches from different companies (Anachemia and BDH) were purchased. Unfortunately, it was immediately noticed that while the old batch had a solubility in toluene of at least 9 x 10^{-5} M, the two new batches were much less soluble. Naturally, in order to continue working on the present project it was necessary to elucidate the reason for this solubility difference.

Ethyl violet, methyl violet, malachite green, and a number of other dyes are members of the triphenylmethane group of dyes, which are acid-base indicators. These compounds act like very weak bases and consequently they are sometimes used as indicators in non-aqueous titrations of weak bases. In aqueous solutions, their use is very limited because the color change is not sharp [133]. The Color Index Numbers ranging from 42000 to 44900 belong to the triphenylmethane dyes. Number 42600 corresponds to ethyl violet, also known as basic violet 4 [134]. Its molecular formula is $C_{31}H_{42}N_3Cl$ and its synthesis is usually via the reaction depicted in equation 2.5 [135].

Since the reason for the different solubility observed for the different batches could be chemical in nature (different compounds or isomers, decomposition products, etcetera) or it could be physical, as in the case of different crystalline forms, several physico-chemical tests were performed with the "old" material (from Allied chemical) and one of the "new" batches (from BDH). The former was identified as batch 0-1 and the latter as batch N-2.

UV-VIS spectra. These spectra were obtained by preparing solutions of both batches in water and scanning them from 200 to 800 nm in a Cary 118 spectrophotometer (Varian Inc.) at a speed of 1 nm/sec. The maxima observed and their absorbances were the same for both samples. For the visible region, it has been reported [136] that ethyl violet should have two maxima at 597 and 547 nm. In the present experiment, the maxima observed were 596 and 547 nm for the visible region; and 307, 253, and 207 nm, for the UV region (see figure 30). When methanol was utilized instead of water, the observed maxima were shifted slightly but their wavelengths and intensities were again the same for both batches.

Thin layer chromatography. Four different solvent systems, chosen from the literature [137-140], were used on silica gel plates (0.25 x 5 x 20 mm, Silica gel

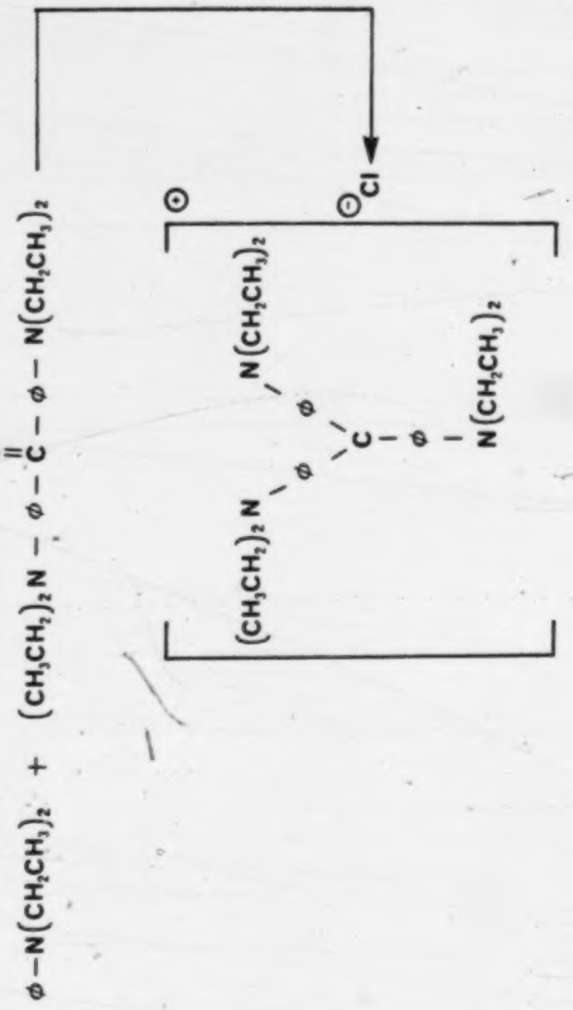
ϕ−N(CH₂CH₃)₂
+
(CH₃CH₂)₂N − ϕ − C(=O) − ϕ − N(CH₂CH₃)₂
(CH₃CH₂)₂N − ϕ
ϕ − N(CH₂CH₃)₂
C − ϕ − N(CH₂CH₃)₂
⊕
⊖Cl

(2.5)

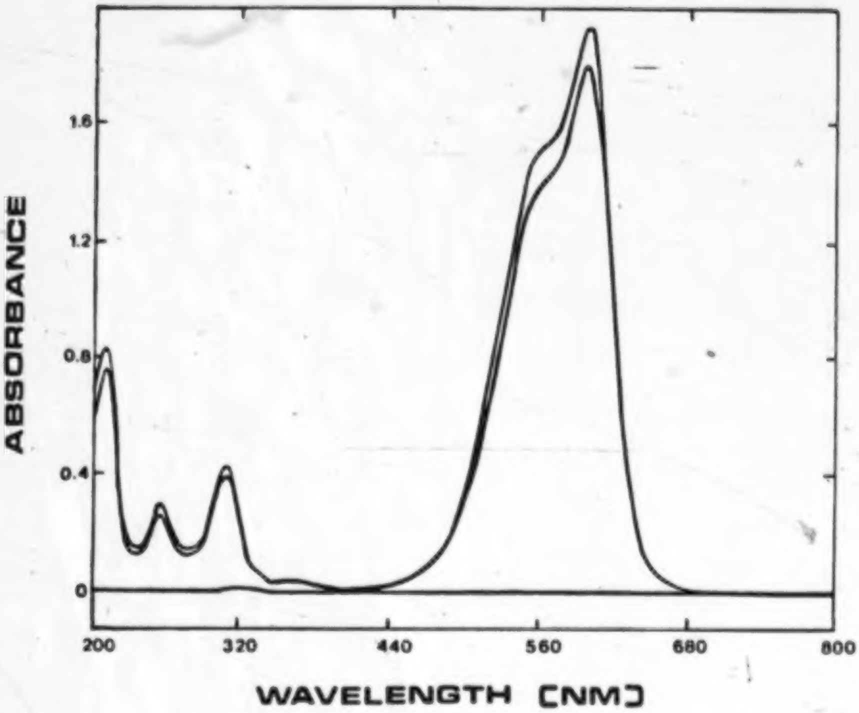

Figure 30. UV-VIS absorption spectra of ethyl violet. Scannings were done on a Cary 118 spectrophotometer (Varian Inc.) from 800 to 200 nm at a speed of 1 nm/sec. Sample solutions were prepared in water; the outer spectrum corresponds to batch 0-1 (concentration= 10.3 mg/L) and the inner spectrum to batch N-2 (concentration=9.7 mg/L).

60, incorporated fluorescent dye, catalog number 7410, E. Merck Co.) to analyze the two batches of ethyl violet by TLC. The plates were developed inside a pre-equilibrated rectangular glass chamber equipped with a solvent saturation pad and afterwards were visually examined under ordinary light, short and long wave UV light, iodine vapors, and finally, after spraying with phosphomolybdic acid. The results were the same regardless of the visualization method and are presented in table XXV. An impurity (R_F= 0.08) was detected in batch N-2 with the n-butanol-ethanol-water solvent system, but it was estimated to constitute only a small percentage of the mixture.

Melting point. This determination was performed in a melting point apparatus equipped with a microscope (Dynamic Optics AHT, catalog number 702043). Both batches were observed as dark green crystals that melted into a blue liquid which, if kept hot, eventually became brown. The melting range was taken as being from the temperature where crystals first started to melt to the temperature where all crystals disappeared. For batch 0-1 this range was 179-180 °C whereas that for batch N-2 it was 219-221 °C.

IR spectra. Two different types of spectra were obtained on an FT-IR spectrophotometer (Nicolet model 7199). In the first one the samples were dissolved in methanol, whereas in the second case a suspension of the samples was prepared in Nujol. The spectra of the two batches in methanol were found to be virtually identical to one another (see figures 31 and 32). On the other hand, the Nujol mull spectra showed small differences in the fingerprint region of the spectrum (see figures 33 and 34). Examples of these disimilarities are: The presence of doublets in the spectrum of batch O-1 at 1577, 1410, and 1180 cm^{-1} where singlets were found in the spectrum of batch N-2 (the opposite was true at 820 cm^{-1}); and the presence of an absorption band at 1300 and 850 cm^{-1} for

Table XXV. Thin layer chromatography retention factors of ethyl violet batches 0-1 and N-2 (See text for details on the analysis).

Solvent System	# of times developed	Batch 0-1	Batch N-2
		Retention factor	
4:1= Carbon tetrachloride: methanol	3	0.13	0.13
9:1:1= n-Butanol: ethanol: water	1	0.42	0.42
4:1:5= n-Butanol: acetic acid: water	1	0.57	0.57
2:2:1= Methyl ethyl ketone: acetic acid: isopropanol	1	0.50	0.50

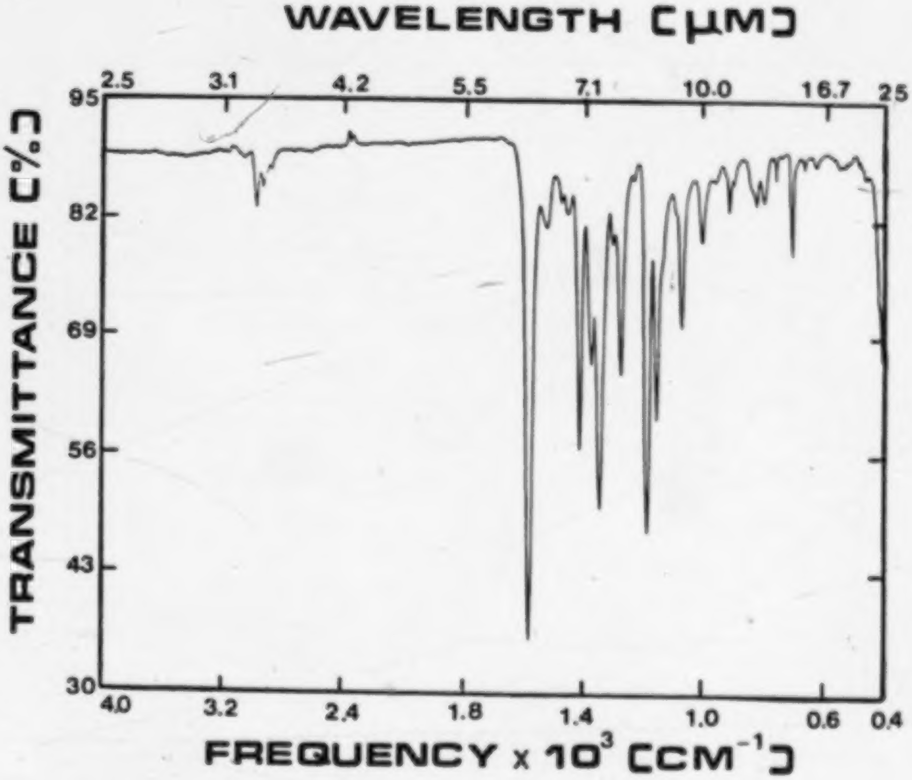

Figure 31. IR absorption spectrum of ethyl violet batch 0-1 in methanol The spectrum was obtained on a Nicolet model 7199 FT-IR spectrophotometer. The sample solution was prepared on a qualitative basis.

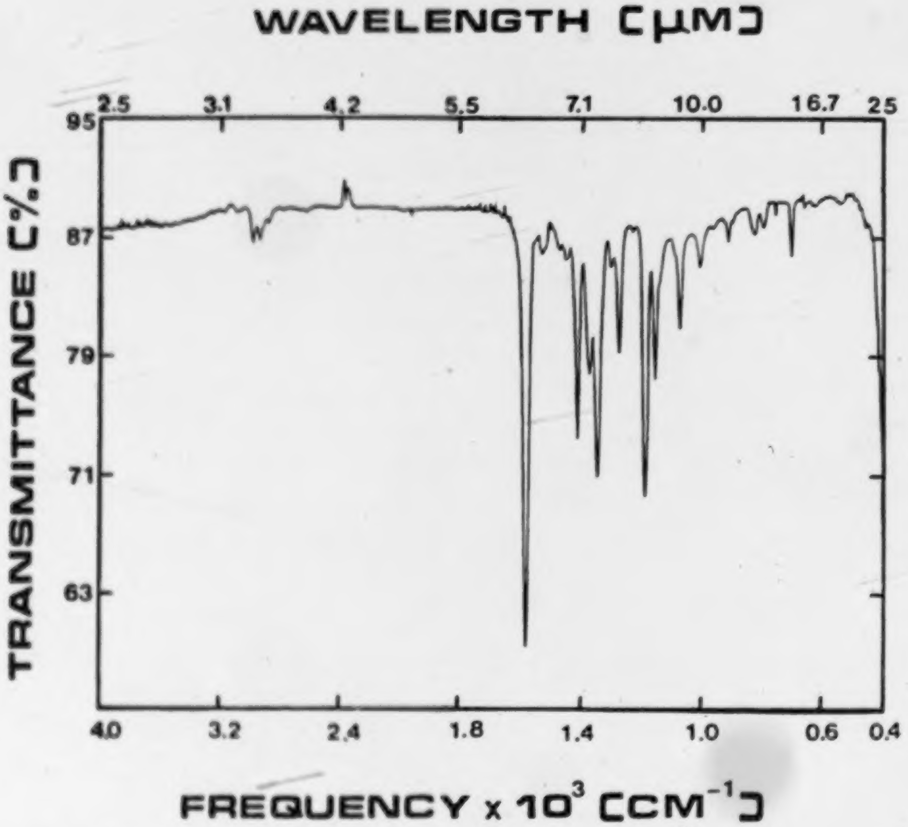

Figure 32. IR absorption spectrum of ethyl violet batch N-2 in methanol. The spectrum was obtained on a Nicolet model 7199 FT-IR spectrophotometer. The sample solution was prepared on a qualitative basis.

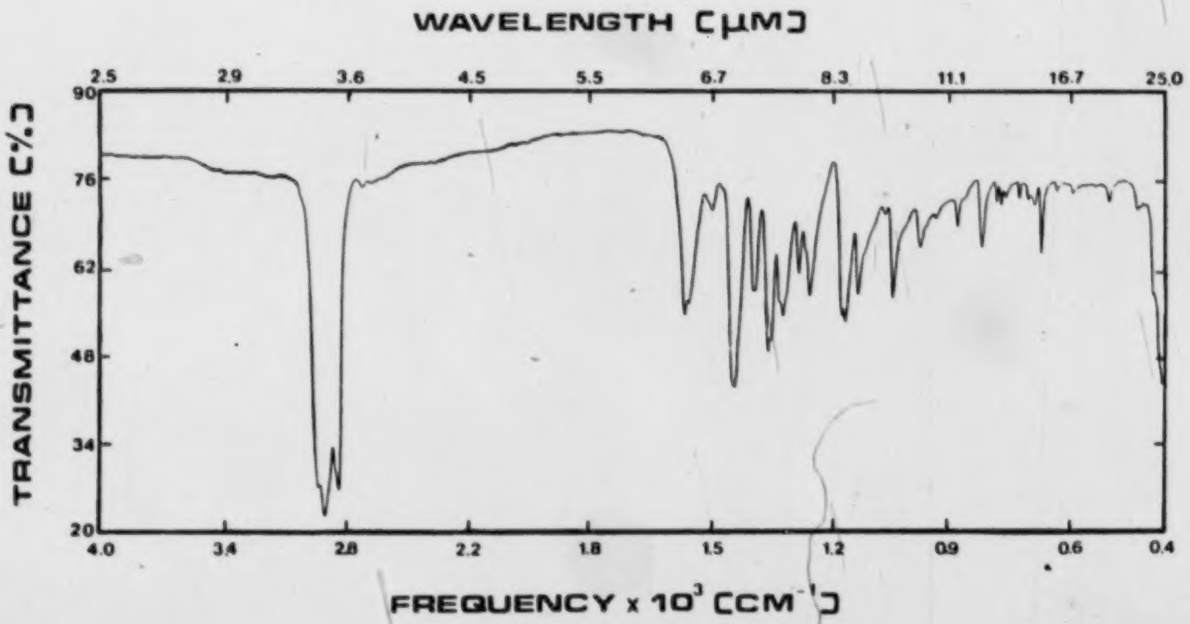

Figure 33. IR absorption spectrum of ethyl violet batch 0-1 in nujol. The sample was prepared by suspending a small amount of the solid in nujol. The spectrum was obtained on a Nicolet 7199 FT-IR spectrophotometer.

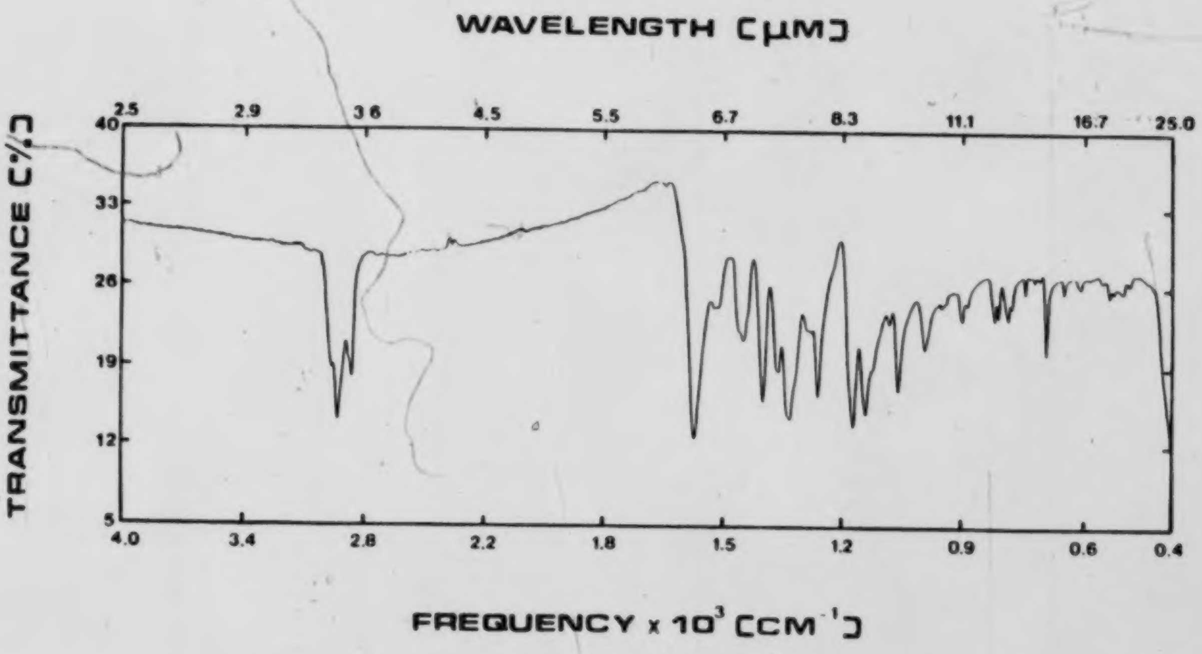

Figure 34. IR absorption spectrum of ethyl violet batch N-2 in nujol. The sample was prepared by suspending a small amount of the solid in nujol. The spectrum was obtained on a Nicolet 7199 FT-IR spectrophotometer.

batch O-1 where no band was observed for batch N-2 (the opposite was true at 550, 515, and 500 cm^{-1}).

Mass spectra. Two types of spectra were obtained. In the first one, the samples were volatilized from the solid and the spectra obtained on a MS-50 spectrometer (Associated Electrical Industries LTD) utilizing electron impact ionization. In the second case, the spectra were obtained from a solution of the samples in glycerol on a MS-9 spectrometer (Associated Electrical Industries LTD) utilizing fast atom bombardment. In the electron impact experiment, using a source temperature of 150 ^{o}C, batch 0-1 produced a parent peak at 457 amu, corresponding to the ethyl violet cation obtained via the loss of chlorine. However, batch N-2 produced a spectrum with intensities much lower, in comparison with batch 0-1, even when the source temperature was raised to 170 ^{o}C (see figures 35 and 36). On the other hand, in the fast atom bombardment experiment the spectra obtained for both batches had similar fragmentation patterns but it was observed that the relative intensities of batch N-2 were still different from those of batch 0-1 (see figures 37 and 38). Furthermore, the spectrum of batch N-2 showed prominently peaks at 93,185, and 277 amu corresponding to (glycerol), $(glycerol)_2$, and $(glycerol)_3$ whereas in the spectrum of batch O-1 these peaks were not immediately noticeable. The fragmentation pattern observed included the parent peak for the cation of ethyl violet (457 amu), a peak at 429 amu produced by the loss of the $-C_2H_4$ ion from the parent ion, and a couple of peaks at 427 and 399 amu produced by the successive loss of $-C_2H_6$ and $-C_2H_4$ from the parent ion. When these peaks and their intensities were normalized, a similar response was obtained for both batches. The differences observed in the spectra were attributed to a different solubility of each batch in glycerol.

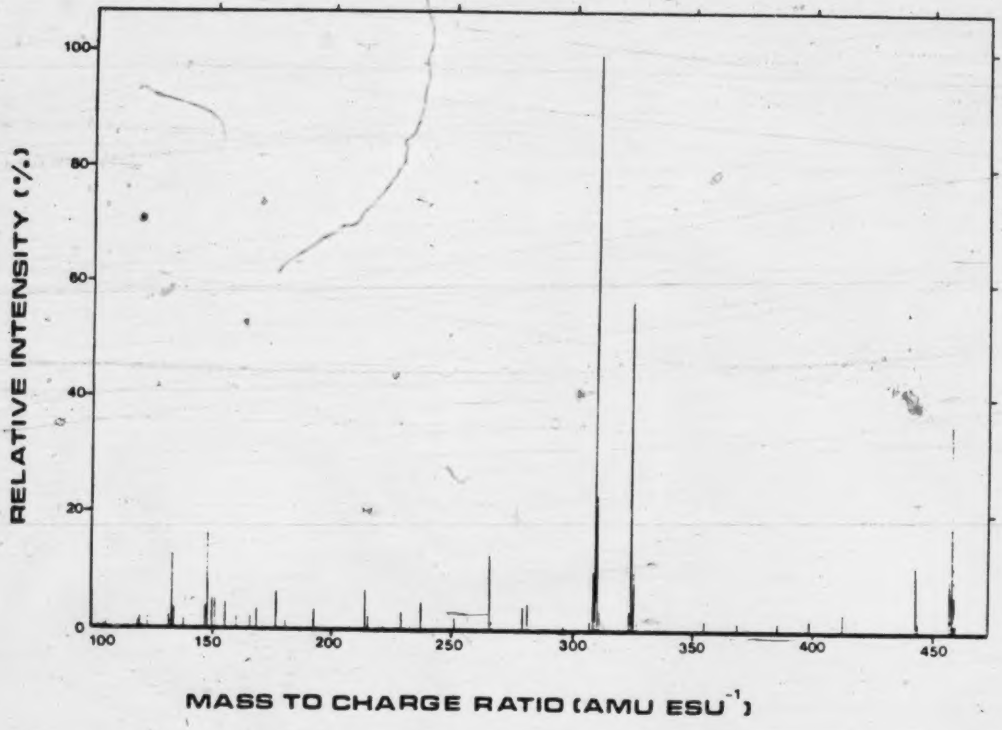

Figure 35. Electron impact mass spectrum of ethyl violet batch 0-1. The spectrum was obtained on a MS-50 (Associated Electrical Industries LTD) spectrometer by volatilizing the sample from the solid at a source temperature of 150 °C.

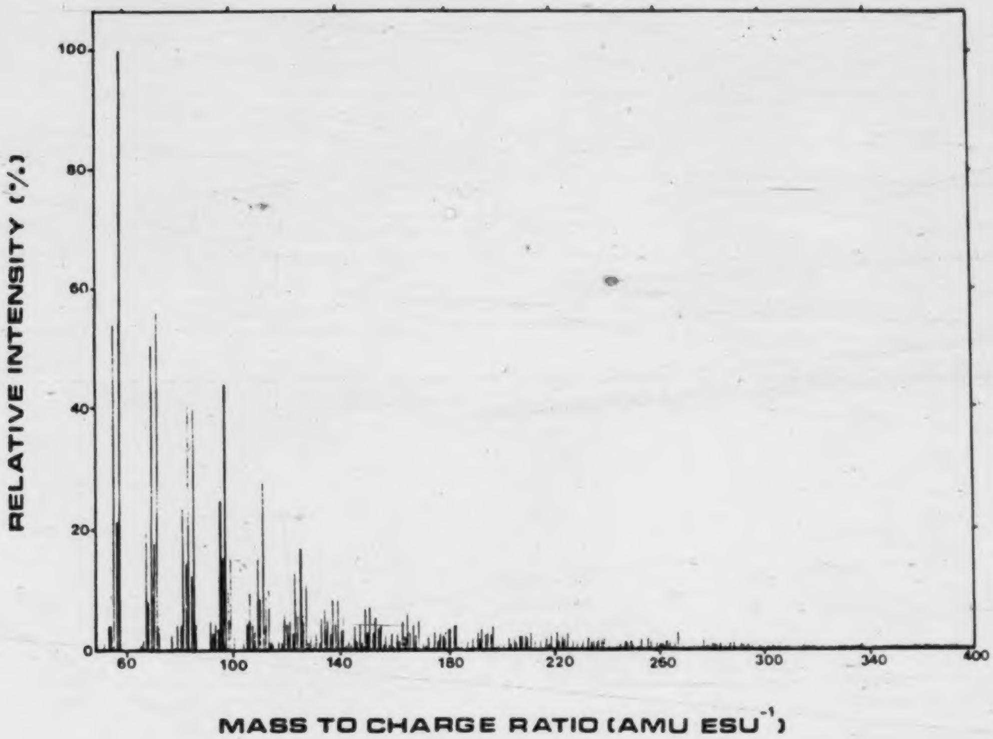

Figure 36. Electron impact mass spectrum of ethyl violet batch N-2. The spectrum was obtained on a MS-50 (Associated Electrical Industries LTD) spectrometer by volatilizing the sample from the solid at a source temperature of 170 °C.

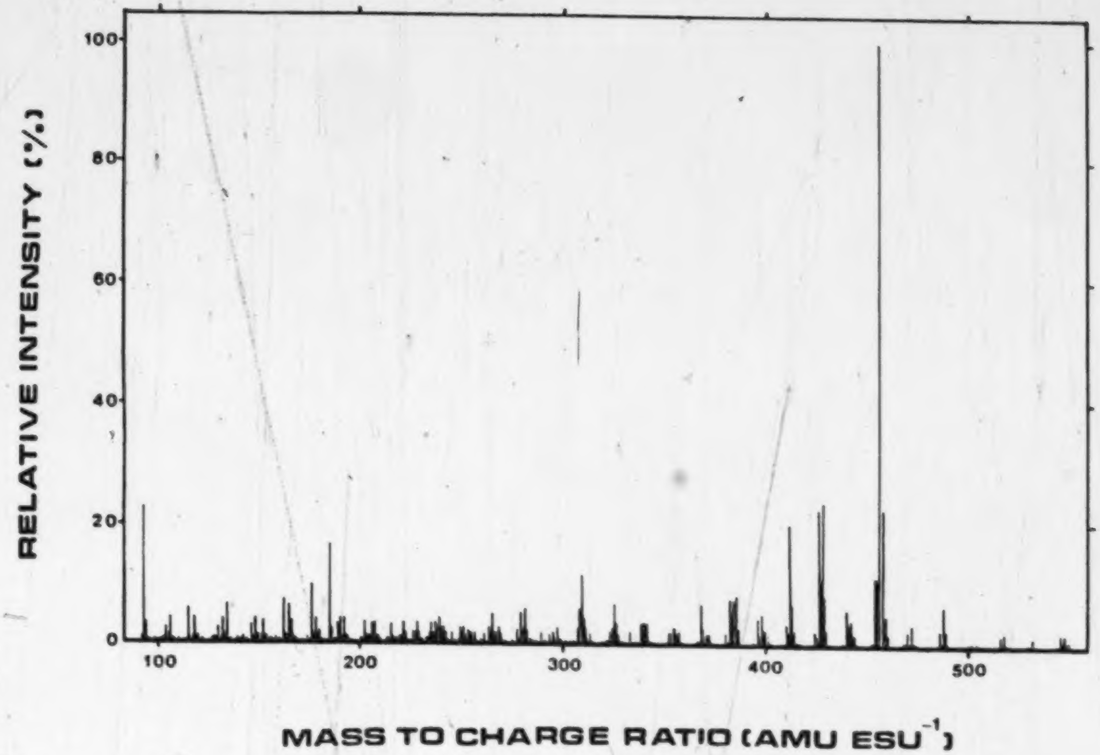

Figure 37. Fast atom bombardment mass spectrum of ethyl violet batch 0-1. The spectrum was obtained on a MS-9 (Associated Electrical Industries LTD) utilizing a solution of the sample in glycerol.

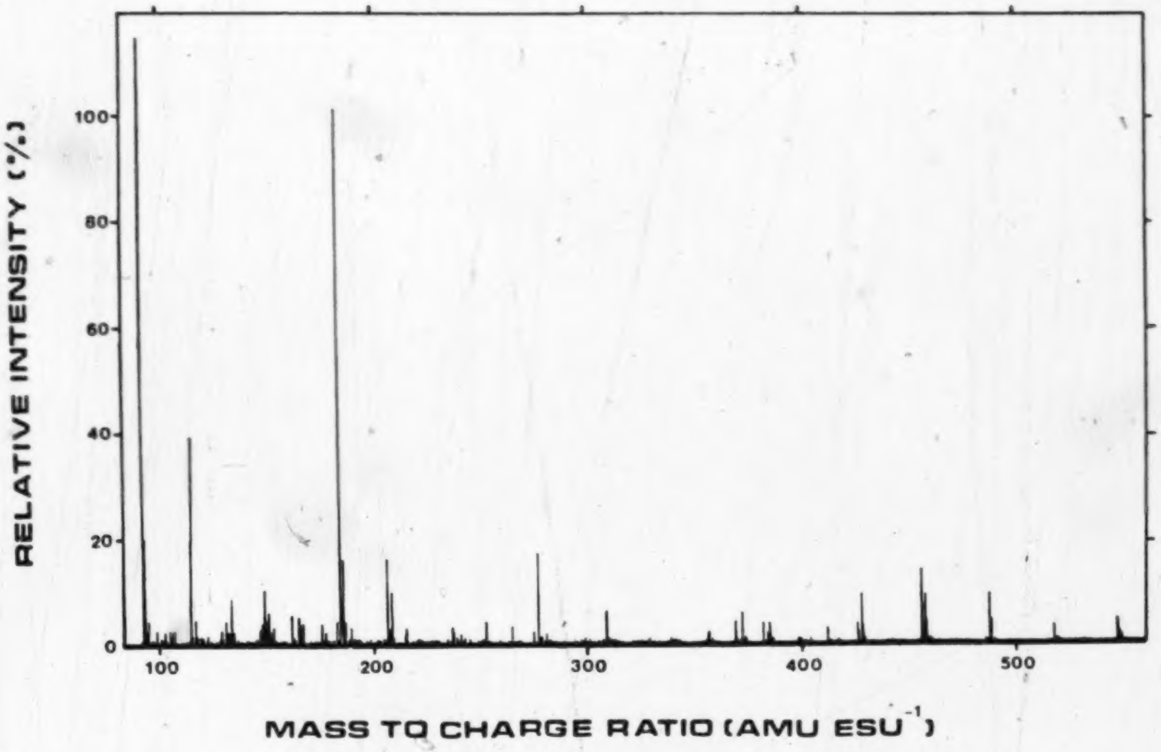

Figure 38. Fast atom bombardment mass spectrum of ethyl violet batch N-2. The spectrum was obtained on a MS-9 (Associated Electrical Industries LTD) utilizing a solution of the sample in glycerol.

Nuclear magnetic resonance. High field proton NMR spectra of the samples were obtained in a 400 MHz instrument (Bruker model WH-400) after preparing solutions of the two batches in deuterated acetone. Deuterochloroform was not used because it contains about 0.2% of chloroform which would give a signal that may have interfered with the signal of the benzylic protons of ethyl violet. No significant difference was observed in the spectra of the two batches (see figures 39 and 40). The chemical shifts, multiplicity, coupling constants, and number of hydrogens integrated were the same for the two samples, indicating that from a chemical viewpoint the two batches were identical and making it unlikely that the batches represented two different isomers. The chemical shifts obtained were: 1.27 (triplet, J=7.0 Hz, 18 H), 3.72 (quartet, J=7.0 Hz, 12 H), 7.08 (doublet, J=9.0 Hz, 6 H), and 7.43 (doublet, J=9.0 Hz, 6 H). A series of very small peaks seemed to indicate the presence of low levels of impurities in both batches. These impurities appear to be different for each batch. The group of peaks with a chemical shift of about 2.1 ppm is due to the presence of hydrogen atoms at different positions in the deuterated acetone molecule. The peak obtained around 3.0 ppm is probably due to the presence of a small amount of water.

Based on the above tests, it is likely that from a chemical viewpoint the two samples are identical. This conclusion is based on the facts that the UV-VIS spectra were identical in two different solvents (even though this test does not distinguish small structural differences); on the TLC results in four different solvent systems (despite the fact that retention factors do not provide conclusive proof on the identity of two compounds); on the identical IR spectra obtained in methanol; and on the similarity of the NMR spectra. It is considered likely that the difference between the two batches was of crystallographic origin. This was suggested by the different melting points obtained for the two batches, by the

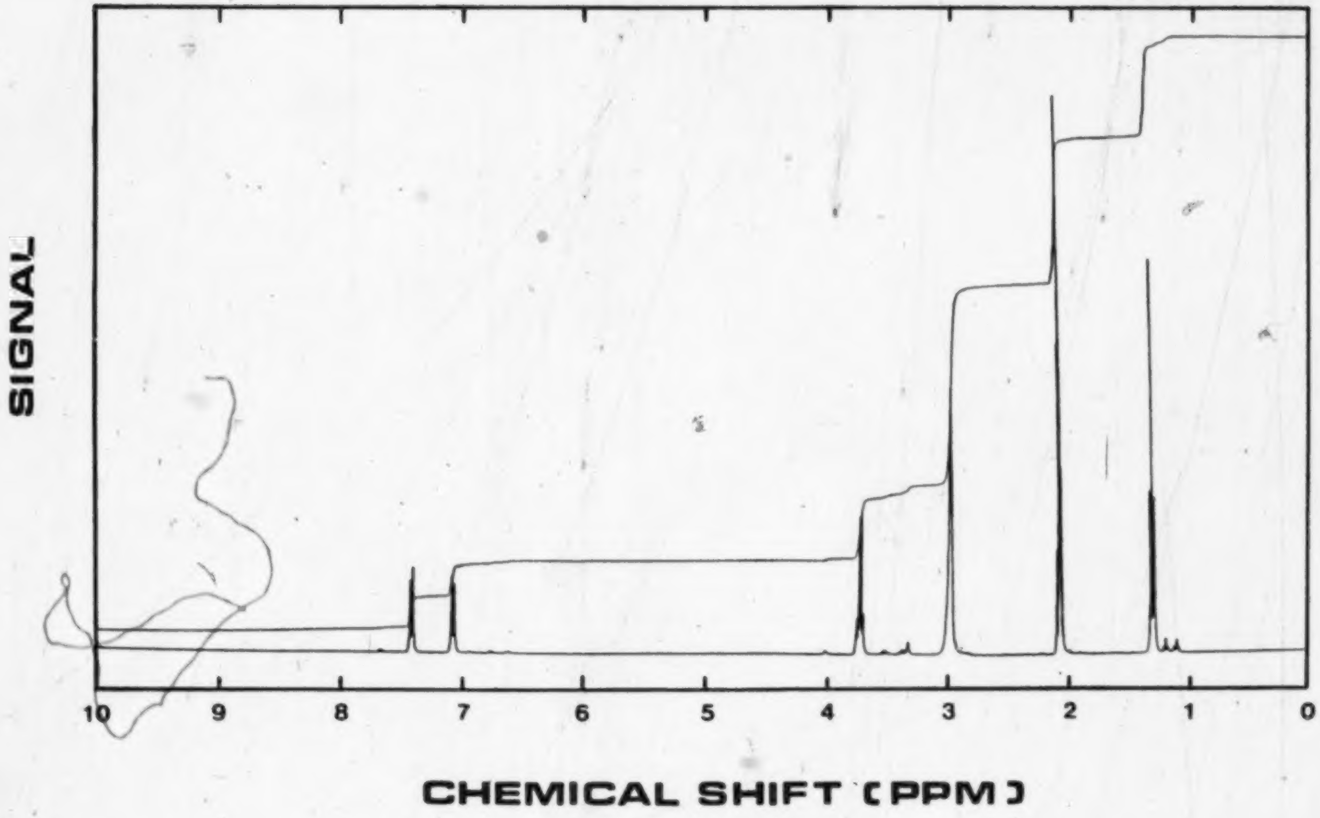

Figure 39. Proton NMR spectrum of ethyl violet batch 0-1.The spectrum was obtained on a high field instrument (Bruker model WH-400) utilizing a deuterated acetone solution of the dye.

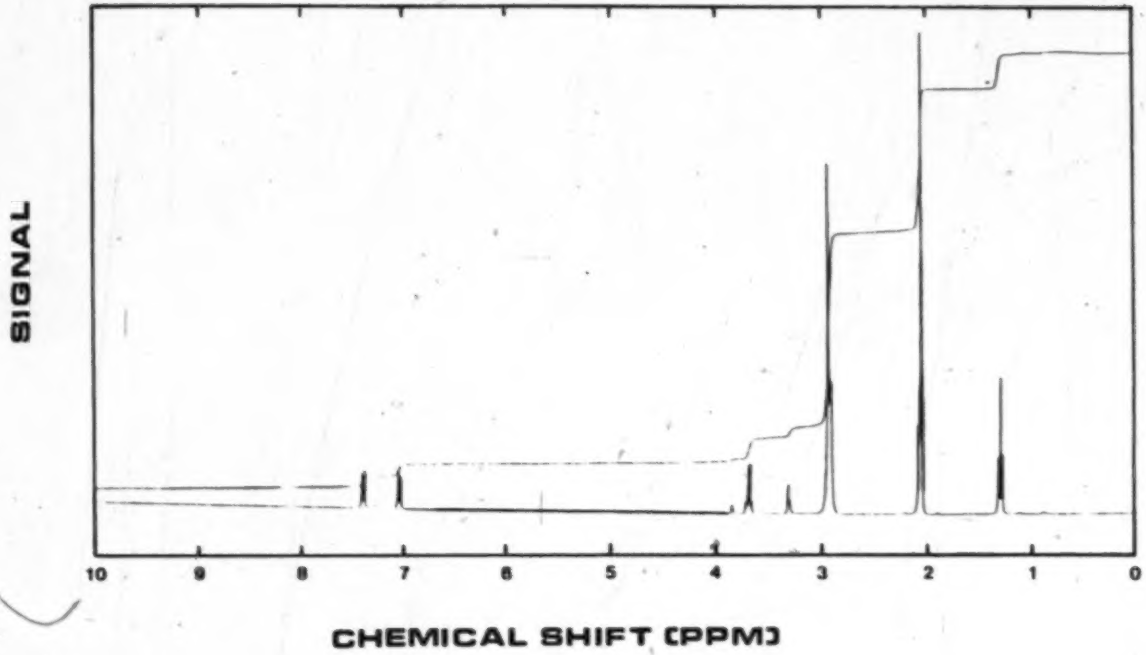

Figure 40. Proton NMR spectrum of ethyl violet batch N-2. The spectrum was obtained on a high field instrument (Bruker model WH- 400) utilizing a deuterated acetone solution of the dye.

small differences observed in the Nujol mull IR spectra, and by the fact that a different response was seen in the mass spectra when volatilized as a powder (differences in the crystalline form result in different vapor pressures and hence different volatilities) or as a solution (the two samples dissolve up to a different extent in glycerol). Since batch N-2 has a high melting point with a small range and a reduced solubility in certain solvents such as toluene and glycerol, it is postulated that this compound has a highly ordered crystalline structure with a lower free energy. On the other hand, batch 0-1 with a lower melting point, a very wide melting range, and an increased solubility, has a less ordered structure (perhaps a metastable polymorphic form) with a higher free energy.

Since the "old" form of the dye seemed to be unavailable commercially and the "new" form exhibited a solubility in toluene too low to prepare the desired concentration for use in SE/FIA system, some attempts were made to transform the "new" dye into the "old" dye. One attempt to do this involved preparing a saturated solution of the former and "seeding" it with crystals of the latter to induce recrystallization. The choice of the solvent to prepare this saturated solution is critical as it should dissolve a large amount of dye when hot and a small amount when cold, and also have a moderate volatility to prevent thermal decomposition of the product during drying. In order to choose the most appropriate solvent, the solubility of ethyl violet batch N-2 was tested in several solvents at room temperature on a semi-quantitative basis (the results obtained are shown on table XXVI). This was done by attempting to prepare a solution containing about 2 mg of the dye per mL of the solvent under careful visual observation. If a homogeneous solution was easily obtained under these conditions, the solubility was termed "good"; if the solid was only partially dissolved, the solubility was designated "medium"; and if the dye did not dissolved, the solubility was called "negligible". Based on the solubility data

Table XXVI. Solubility of ethyl violet batch N-2. Tests were performed at room temperature on a semi-quantitative basis.

Solvent	Boiling point (°C)	Dielectric constant (Debye units)	Solubility
Toluene	111	2.4	Negligible
Methanol	65	33.6	Good
Water	100	80.4	Good
Acetone	56	20.7	Good
Ethanol	78	24.3	Good
Diethyl ether	35	4.3	Negligible
Chloroform	61	4.8	Good
THF	66	7.6	Medium
Carbon tetrachloride	76	2.2	Negligible
Ethyl acetate	77	6.0	Medium
Benzene	80	2.3	Negligible
Cyclohexane	81	2.0	Negligible
Isopropanol	82	18.1	Good
Dioxane	102	2.2	Medium

Note: The solubility was evaluated by preparing a solution containing about 2 mg of dye per mL of solvent under scrutiny. If a homogeneous solution was obtained, the solubility was termed "good"; if the solid was only partially dissolved, the solubility was designated "medium"; and if the dye did not dissolved, the solubility was called "negligible".

obtained, a supersaturated solution of ethyl violet batch N-2 in ethyl acetate was prepared, filtered, cooled, and seeded with old dye crystals. Then it was kept in the freezer for 12 h and the resulting solid isolated and dried for 3 h under vacuum. Afterwards, its solubility in toluene was tested and found to have increased from "negligible" to "medium", but could not be made "good". Following exactly the same procedure but using THF instead of ethyl acetate, a material with a "negligible" solubility in toluene was obtained.

Another potential way of transforming the new batch of dye into a form more like the old batch might be possible through a very rapid precipitation, in an effort to obtain an amorphous precipitate. Therefore, a supersaturated and hot solution of the new dye in dioxane was added to a beaker containing cold cyclohexane in an ice bath. The resulting precipitate was isolated and dried for 3 h under vacuum. The solubility of this material in toluene was found to be "medium", and its melting range was intermediate between that of the new and the old material. The dark green solid melted into a blue liquid in the range from 205-209 ^{o}C, and it decomposed at 213 ^{o}C (brown liquid). This melting range does not correspond to the value observed for either batch 0-1 (179-190 ^{o}C) or for batch N-2 (219-221 ^{o}C).

Since none of the above approaches yielded a sufficiently soluble product from the new dye material, it was decided to add a strong solvent to toluene in order to achieve adequate dye solubility. It was found that a binary system containing 99.5% v/v toluene and 0.5% v/v methanol produced a solution of new dye in the concentration range required to operate the SE/FIA system. This solution was prepared by dissolving 29.5 mg of dye in 5 mL of methanol and diluting to 1 L with toluene.

Once it was known that the two batches of ethyl violet (0-1 and N-2) were the same from a chemical viewpoint, that their different solubility in toluene was probably due to a difference in crystal structure, and that this obstacle could be surmounted by using a co-solvent, the question of how the presence of methanol affects the functioning of the SE/FIA system had to be addressed. To do this, a calibration curve was obtained under the same conditions utilized in calibration curve #3 (see figure 20) except that instead of having a solution of the old dye in toluene, a solution of the new dye in 99.5% v/v toluene and 0.5% v/v methanol was utilized. The conditions used and the results obtained are shown in table XXVII and in figures 41 and 42. Manually measured peak heights and peak areas obtained from an integrator were utilized to monitor and evaluate the effect of introducing methanol into the system by comparing the results obtained versus those obtained in figure 20. The dynamic range was found to be from 1 x 10^{-6} M (detection limit) to 1 x 10^{-4} M, since higher concentrations produced a non-linear response. The linear regression analysis for peak heights was: Intercept= 4.25, s.d. of the intercept= 1.22, slope= 1.25 x 10^6, and the r.s.d. of the slope = 1.71%. For peak areas the following was obtained: Intercept= 0.52 x 10^6, s.d.of the intercept= 0.16 x 10^6, slope= 2.00 x 10^{11}, and the r.s.d. of the slope= 1.43%. In comparison with calibration curve #3, chosen as the best fitting curve from section 2.3.8, the present calibration curve has a dynamic range twice as big but the precision of the determination (expressed as the r.s.d. of the slope of this curve) has deteriorated by a factor of about 2. On a more general basis, it can be said that the amount of methanol added as a co-solvent to solubilize the dye has no significant negative effect on the functioning of the SE/FIA system.

After the above conclusion was reached, calibration curves for two different anionic surfactant samples were obtained under these conditions of analysis. The first sample was sodium alkyl aryl sulfonate, sold by Fisher Scientific as a white flaky powder. Alkyl aryl sulfonates can be divided into linear or branched, depending upon the characteristics of the alkyl chain. The linear family is widely

Table XXVII. Sodium lauryl sulfate calibration curve data. The instrument parameters were the same as those described on figure 41.

[SLS] (M)	Peak height(a) (cm)	r.s.d. (%)	Peak area (a.i.u. x 10^6)	r.s.d. (%)
1.00×10^{-6}	3.20	2.9	0.46	3.4
5.00×10^{-6}	12.6	1.6	1.37	1.5
10.0×10^{-6}	17.5	1.3	2.17	1.2
20.0×10^{-6}	31.3	1.0	5.20	1.0
30.0×10^{-6}	28.5	1.0	6.78	0.92
40.0×10^{-6}	55.6	1.1	8.74	0.85
50.0×10^{-6}	66.6	0.6	10.4	0.68
60.0×10^{-6}	78.3	1.0	12.5	0.93
70.0×10^{-6}	95.1	1.1	14.6	0.89
80.0×10^{-6}	109	1.0	16.3	1.0
90.0×10^{-6}	116	1.1	18.2	1.3
100×10^{-6}	129	1.3	20.8	1.4

(a) The data were normalized using equation 2.2.

Note: "SLS" stands for sodium lauryl sulfate and "a.i.u." for arbitrary integrator units.

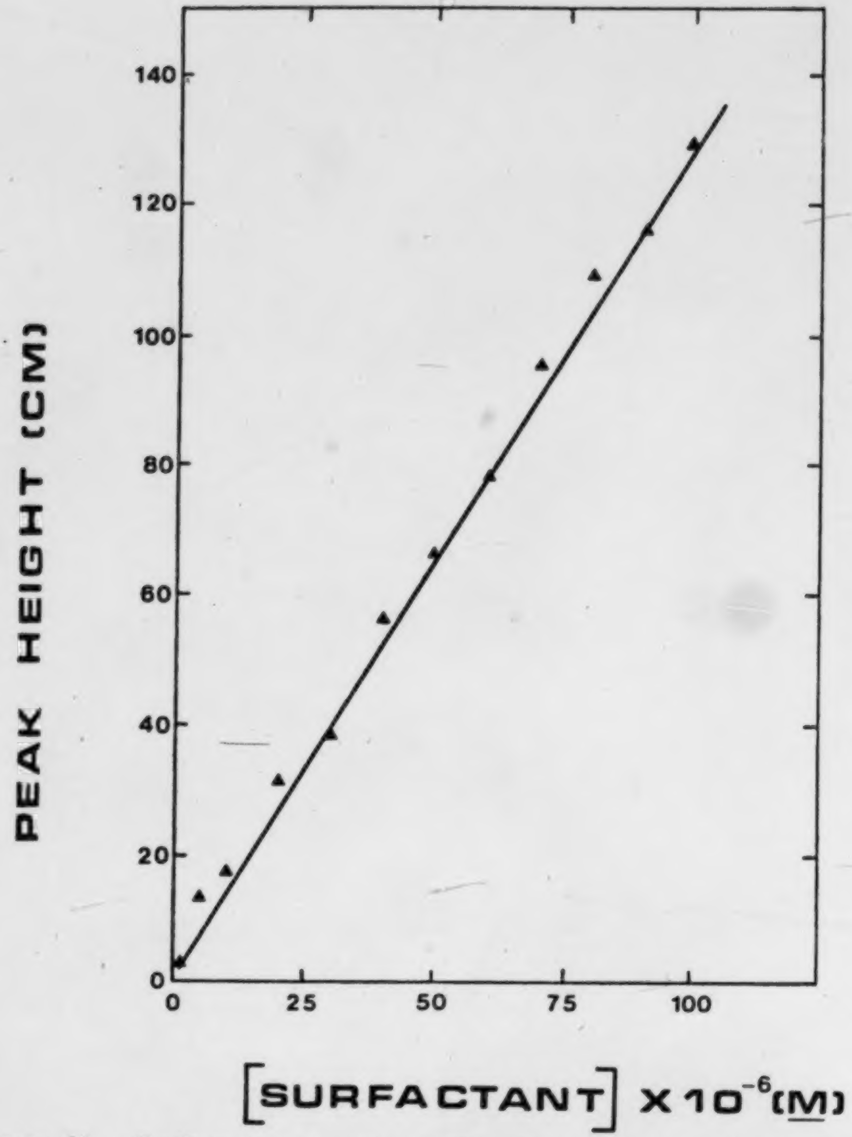

Figure 41. Sodium lauryl sulfate calibration curve (peak heights). Instrument parameters: Dye concentration, 6 x 10^{-5} M in 99.5% toluene and 0.5% methanol (equivalent to 3 x 10^{-4} M in water); buffer composition, 0.16 M acetic acid and 0.18 M sodium acetate; sodium sulfate concentration, 0.6 M; extraction coil length, 450 cm; injection volume, 50 microliters; nitrogen pressure, 20 psig; wavelength, 546 nm.

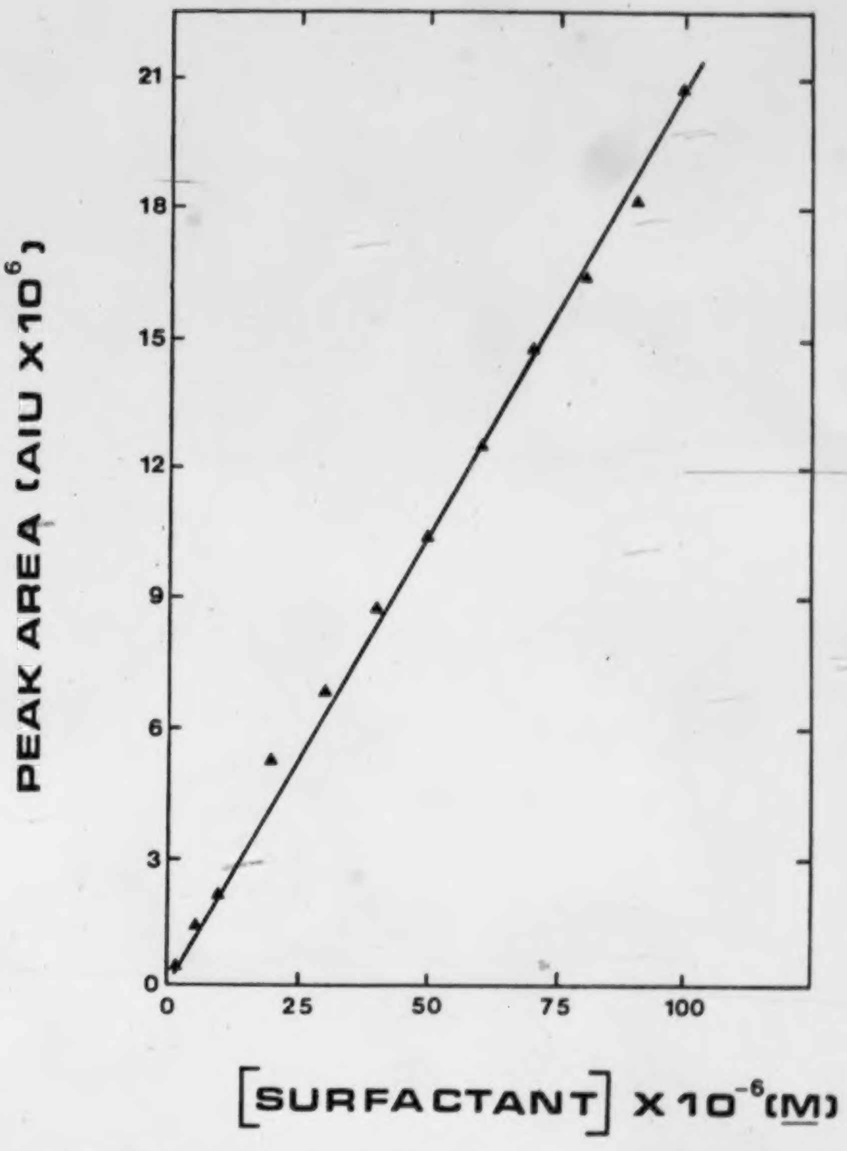

Figure 42. Sodium lauryl sulfate calibration curve (peak areas). Instrument parameters: As in figure 41.

used in detergent formulations, usually as a mixture of a homologous series of alkyl chain lengths of 10-13 carbon atoms with the aryl group attached to any methylene group of the alkyl chain [81]. Since its molecular weight was obviously not known, molar solutions could not be prepared and, consequently, a stock solution containing 5000 ppm was made instead. By successive dilution, several solutions were prepared and injected into the SE/FIA system, thereby obtaining the results shown in table XXVIII and figure 43. Since the linear alkyl aryl sulfonate family may comprise any or all of 26 related compounds with various chain lengths and isomers, an average molecular weight of 318 has been suggested to report uniformly the surfactant content in samples containing these compounds [130]. Therefore, an estimate of the molarity values utilized in the present experiment was obtained (see table XXVIII) for comparison purposes. The results obtained indicated that the detection limit was 1 ppm and that linearity was lost after the 200 ppm level. The linear regression analysis for peak areas gave the following: Intercept= -0.21 x 10^6, s.d. of the intercept= 0.36 x 10^6, slope= 2.41 x 10^5, r.s.d. of the slope= 1.45%.

Another calibration curve was obtained for sodium dodecyl benzene sulfonate, a member of the linear alkyl aryl sulfonate family, sold as a syrup by ICN Pharmaceuticals. This compound has the molecular formula $C_{18}H_{29}SO_3Na$ and a molecular weight of 348.5, when pure. However, the sample available was an inhomogeneous syrup from which a stock solution containing 3483 ppm was prepared by pre-heating the syrup in a bath at 40 °C, taking a portion of the material with a glass rod after thorough mixing, transfering this to an air-tight container, allowing the sample to cool off, weighing of the sample, and dissolving it in one liter of distilled water. When doing so, it was noticed that some insoluble material was present even after considerable shaking in an ultrasonic bath. After preparing several solutions by

Table XXVIII. Sodium alkyl aryl sulfonate calibration curve data. Instrument parameters as in figure 41.

Sodium alkyl aryl sulfonate (ppm)	(M)[a]	Peak area (a.i.u. x 10^6)	r.s.d. (%)
1.0	3.15×10^{-6}	0.51	4.5
2.5	7.86×10^{-6}	1.03	2.1
5.0	15.7×10^{-6}	1.71	1.3
10.0	31.4×10^{-6}	2.58	1.4
25.0	78.6×10^{-6}	4.86	0.39
50.0	157×10^{-6}	10.2	0.91
75.0	236×10^{-6}	17.0	0.74
100	314×10^{-6}	24.0	0.60
125	393×10^{-6}	30.6	0.41
150	472×10^{-6}	36.8	1.7
175	550×10^{-6}	42.2	1.6
200	629×10^{-6}	47.7	1.2

(a) These values were estimated assuming a molecular weight of 318 [130].

Note: "a.i.u." stands for arbitrary integrator units.

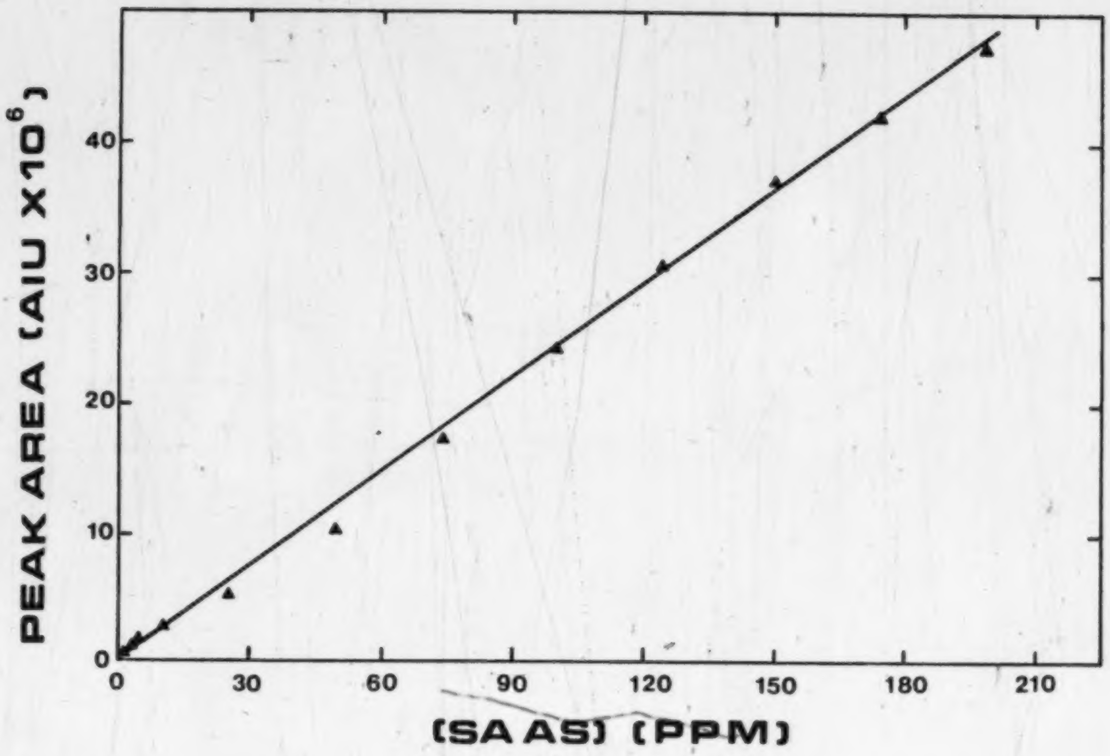

Figure 43. Sodium alkyl aryl sulfonate calibration curve. Instrument parameters: As in figure 41.

successive dilution and injecting them into the SE/FIA system, the results presented in table XXIX and figure 44 were obtained. The dynamic range was found to be from 0.5 ppm (detection limit) to 125 ppm, after which deviation from linearity was observed. The peak area regression analysis gave: Intercept= 3.53×10^4, s.d. of intercept= 5.35×10^5, slope= 3.41×10^5, and the r.s.d. of the slope= 2.66%. If the sample is assumed to be 100% pure, an estimate of the concentration range expressed in terms of molarity can be calculated (see table XXIX).

Table XXIX. Sodium dodecyl benzene sulfonate calibration curve data. Instrument parameters as in figure 41.

Sodium dodecyl benzene sulfonate (ppm)	(M)$^{(a)}$	Peak area (a.i.u. x 10^6)	r.s.d. (%)
0.5	1.43 x 10^{-6}	0.67	10
1.0	2.87 x 10^{-6}	1.03	4.5
5.0	14.4 x 10^{-6}	2.84	2.2
10.0	28.7 x 10^{-6}	3.97	0.9
15.0	43.0 x 10^{-6}	4.98	1.8
25.0	71.7 x 10^{-6}	7.61	1.6
50.0	143 x 10^{-6}	14.8	2.1
75.0	215 x 10^{-6}	24.4	1.8
100	287 x 10^{-6}	35.0	1.2
125	359 x 10^{-6}	43.8	1.7

(a) These values were estimated assuming a molecular weight of 348.5 and a purity of 100%.

Note: "a.i.u." stands for arbitrary integrator units.

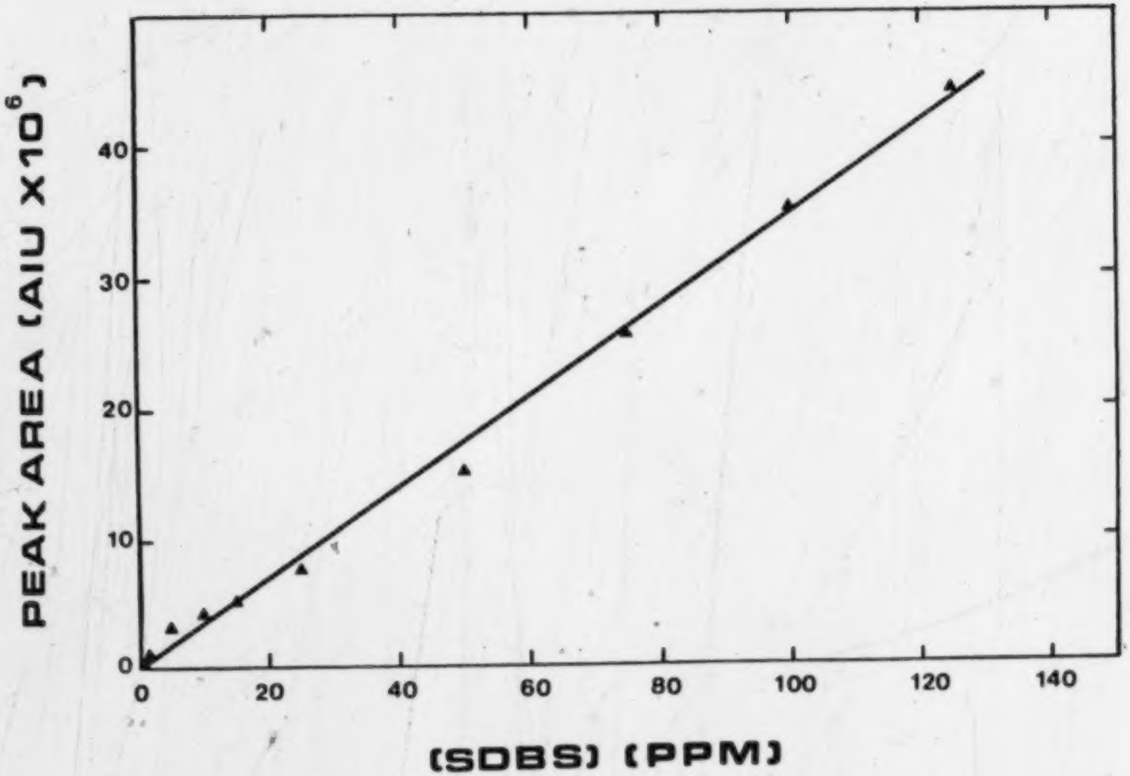

Figure 44. Sodium dodecyl benzene sulfonate calibration curve. Instrument parameters: As in figure 41.

CHAPTER 3

DETERMINATION OF SURFACTANTS

3.1 Introduction

The optimized SE/FIA conditions for the analysis of anionic surfactants described in the last chapter are applied in the present chapter to determine three different samples of surface active agents which are utilized in the enhanced recovery of oil. These samples were commercial formulations containing petroleum sulfonates, which are intended to reduce the interfacial tension at the oil-water interface and produce a microemulsion for the augmented thermal recovery of heavy oils [1]. The samples were obtained from the Alberta Research Council, where the method used to quantify them is a two-phase ion pair titration utilizing as indicator a mixture of dimidium bromide and disulphine blue, and as titrant p-tert octylphenoxyethoxyethyldimethylbenzyl ammonium chloride [148]. The precision of this mixed indicator method is reported to be 1-2%. There are many variations of the two-phase titration technique utilizing different indicators, titrants, and methods of standardization [2,15-21, 149-154].

3.2 Experimental

3.2.1 Chemicals and solvents

The following samples and standards were supplied by E. Isaacs and C. McCarthy from the Oil Sands Research department in the Alberta Research

Council, and were used as received: Suntech IV, Sun Refining and Marketing Co.; Enordet AOS, Shell International Chemical Co.; TRS 10-80 sample material; TRS 10-80 standard material; and 1-Dodecansulfonic acid sodium salt, Serva Feinbiochemica Heidelberg. These commercial formulations contain a mixture of anionic surfactants (such as linear alpha olefin sulfonates, natural petroleum sulfonates, disulfonates, synthetic sulfonates, etc.), some unsulfonated organic material, a small amount of sodium sulfate, and water. The identity of the surfactant mixture or its composition is never fully revealed by the manufacturers.

In addition to these samples, the following chemicals and solvents were also utilized as received from the suppliers:

Ethyl violet C.I. 42600, BDH Chemicals LTD. Cat. number 34114 (batch N-2).
Sodium dodecyl sulfate, Aldrich Chemical Co. Cat. number 536.
Sodium acetate tri-hydrate, ACS grade, Amachem.
Acetic acid, ACS grade, Fisher Scientific Co.
Sodium sulfate, ACS grade, Fisher Scientific Co.
Toluene, ACS grade, BDH Chemicals LTD.
Methanol, ACS grade, BDH Chemicals LTD.
Water was distilled from alkaline permanganate in an all-glass still.

3.2.2 Apparatus

The SE/FIA system utilized for the determination of the surfactant samples is depicted in figure 45. This system is quite similar to the one described in section 2.2.2 (figure 2) except that the dye, which formerly was present in the "reagent" cylinder as an aqueous solution, is now contained in the "organic" cylinder in a mixture of toluene-methanol; the cylinder that was called "reagent" now contains only the buffer and sodium sulfate; and the injector has a by-pass loop.

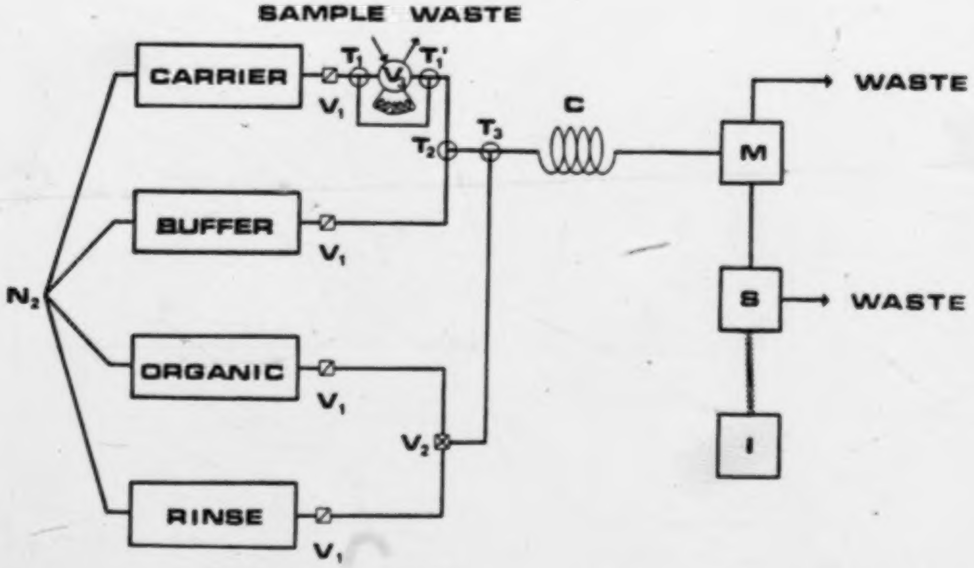
SAMPLE WASTE
CARRIER
BUFFER
ORGANIC
RINSE
N_2
V_1
V_2
V_3
T_1
T_1'
T_2
T_3
C
M
S
I
WASTE
WASTE

Figure 45. Block diagram of the SE/FIA apparatus utilized for the analysis of surfactant samples. The contents of the cylinders are: Methanol in the "Rinse" cylinder; acetate buffer and sodium sulfate in the "Buffer" cylinder; distilled water in the "Carrier"; and an ethyl violet solution prepared with a mixture of 99.5% v/v toluene and 0.5% v/v methanol in the "Organic" cylinder. "C" is the extraction coil; "M" the membrane phase separator; "S" a spectrophotometric detector; and "I" is an integrator.

All of these changes were discussed in chapter 2 during the optimization of the system.

Another apparatus (shown in figure 46) was used to determine interfacial adsorption. This instrument is similar to the one previously used in this laboratory to perform two-phase titrations [19,141]. The two-phase chamber was a beaker made of glass with a Teflon lid held in place with two screws and wing nuts. Several holes in this lid provided access into the chamber for the filter probe, the return-line, and of a non-rotating spoiler which was used to minimize vortex formation and facilitate efficient dispersion of one phase into the other. A mixture of toluene, methanol, water, and the constituents present in the SE/FIA system (dye, buffer, sodium sulfate, and sample) were placed inside the two-phase chamber together with a 1.5-inch Teflon covered stirring bar. A magnetic stirrer equipped with a powerful magnet (model 4815, Cole-Parmer Instrument Co.) controlled the stirring bar either at very high speed to achieve distribution equilibrium rapidly and produce a large amount of interfacial area where adsorption can occur, or at very low speed to study desorption which occurs upon the disappearance of the interface by coalescence. The end of the filter probe was covered with a porous membrane consisting of three layers of Teflon cloth (Zitex, pore size 10-20 microns, catalog number E249-122, Chemplast Inc.). This probe was immersed in the upper (toluene-methanol) layer of the two phase system, and connected to a peristatic pump (Polystaltic pump. Buchler Instruments). Preferential wetting of the teflon membrane by the organic phase allowed successful filtering of water out of the organic phase. The peristaltic pump moved organic phase from the two-phase chamber, via the filter probe, and passed it through the flowcell of the detector (Spectra-Physics 8200, set at 546 nm) which produced a signal fed to a recorder (Recordall series 5000. Fisher Scientific). The organic phase returned from the detector into the

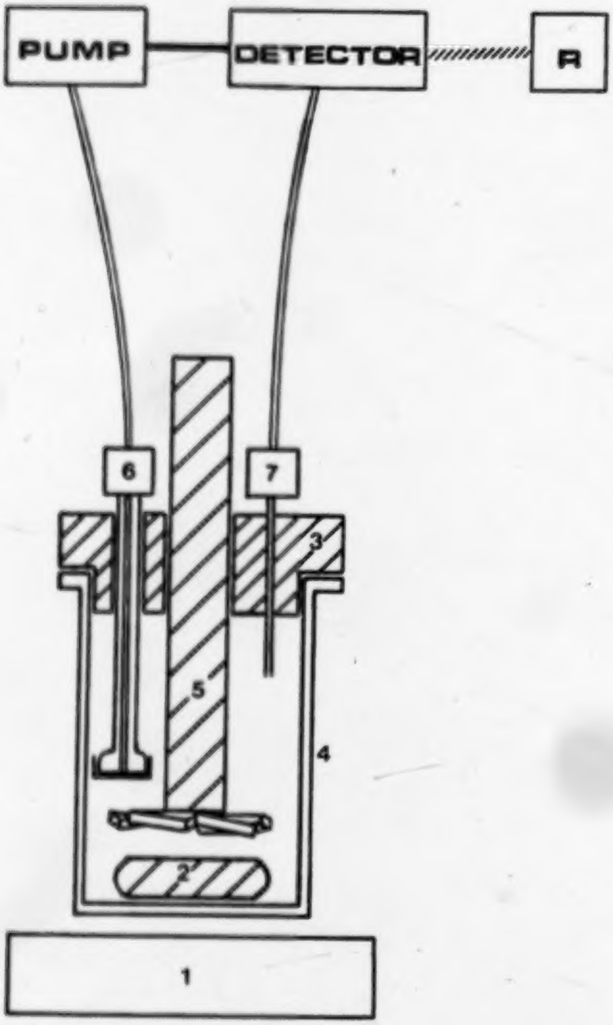

Figure 46. Diagram of the apparatus used to determine interfacial adsorption. The components of this instrument are: (1) Magnetic stirrer, (2) stirring bar, (3) lid, (4) two-phase chamber, (5) spoiler, (6) filter-probe, (7) return line, and (R) recorder.

two-phase chamber via a return line. All the tubing interconnecting the pump, detector, and chamber was made of Teflon (0.8 mm i.d.) but the pump itself had an 18-cm long, 1.14 mm i.d. tube made of Viton rubber.

3.2.3 Procedure

Prior to the SE/FIA determination, three sample solutions were prepared to contain around 1000-2000 ppm, by weighing appropriate amounts of the sample supplied by the Alberta Research Council and diluting with distilled water. From each of these three sample solutions, two sub-samples (around100-200 ppm) were prepared by further dilution. The procedure utilized in the SE/FIA determination involved injecting repeatedly standard and sample solutions into the system (one standard for every two samples) with a frequency such as to allow a particular peak to elute completely before injecting the next one. The response (peak area) obtained from these injections was used to calculate the assay value of the sample via the following relationship:

$$\frac{\text{Peak area of sample / [sample]}}{\text{Average area of standards / [standard]}} \quad \text{X} \quad \text{purity of standard} \tag{3.1}$$

where concentrations are expressed as molarities, peak areas as arbitrary integrator units, and purity values as percentages. Finally, an average value for the assay was computed along with the r.s.d. among samples. As previously, the results of seven replicate injections were averaged when reporting peak parameters.

To carry out the determination of interfacial adsorption, the parameters and conditions utilized in the SE/FIA system were mimicked whenever possible. The procedure involved placing in the two-phase chamber a 6×10^{-5} M dye solution (the solvent used was 99.5% toluene and 0.5% methanol), an aqueous buffer solution containing 0.18 M sodium acetate and 0.16 M acetic acid, a 0.6 M solution of sodium sulfate in water, and an aqueous solution of the sample. This was done in such a way as to simulate the conditions used in the SE/FIA system in terms of order of addition, the volume ratio of organic to aqueous phase, the molar ratio of reagent to sample, and the amounts of buffer and salting-out agent. Once all the components were inside the two-phase chamber, the stirrer was set at a high load mode causing a very vigorous agitation which in turn brought about the transfer of the dye from the organic into the aqueous phase, the reaction between the dye and the sample, and the extraction of the ion pair into the organic phase. At this high stirring speed, the distribution equilibrium was rapidly achieved and a large amount of interfacial area was created in the two-phase system. The peristaltic pump was then turned on, thereby circulating the organic phase through the detector for the continuous monitoring of its absorbance. The detector/recorder had previously been set to zero using a mixture of 99.5% toluene and 0.5% methanol in the reference and sample cells of the detector. After attainment of extraction equilibrium with rapid stirring, the stirrer was then set at a stirring speed so low that the two phases coalesced and the amount of organic-aqueous interface dropped to a minimum. The high/low stirring cycle was repeated a few times while monitoring the absorbance via the recorder.

3.3 Results and discussion

3.3.1 TRS 10-80

This material is composed of a mixture of petroleum sulfonates with an average molecular weight of 418. Since a standard and a sample material of TRS 10-80 were both available, the latter was compared to the former during the determination. The standard material was a creamy powder with a purity reported to be 100%, whereas the sample was a very viscous syrup with an 80.8% content of active matter estimated by the Oil Sands Research department via two-phase titration. Before the actual determination of the sample took place, a calibration curve of the standard material was obtained on the SE/FIA system shown in figure 45. The conditions used (refered to as "initial conditions") and the curve obtained are shown in table XXX and in figure 47, where it can be seen that the detection limit was 1 ppm and that linearity was lost after the 250 ppm level. Linear regression analysis showed that the intercept was -1.10×10^5 with a standard deviation of 4.26×10^5, and that the slope was equal to 1.86×10^5 with a relative standard deviation of 1.88%.

The TRS 10-80 sample was determined by first preparing three concentrated stock solutions (of about 1000 ppm). Three were prepared to determine if the viscous sample syrup was homogeneous. From each of these stock solutions, two sample solutions of about 200 ppm were prepared by dilution. The assay values were: 75.30 and 75.93% for samples 1A and 1B; 76.74 and 78.73% for 2A and 2B; and 74.55 and 76.44% for3A and 3B. From these data, an average assay value of 76.3 ± 1.4% was computed, which was comparable to the result obtained by the two phase titration method (80.8%). Sample inhomogeneity was not a problem since no significant difference was found among the diluted solutions (the relative standard deviation among samples was 1.9%).

3.3.2 Enordet

Enordet, a mixture of linear alpha olefin sulfonates with an average molecular weight of 356, is physically a yellow liquid with a large amount of white precipitate suspended in it. In order to avoid sampling problems from this inhomogeneity, the whole sample was heated to about 35 ^{o}C to dissolve the

Table XXX. TRS 10-80 calibration curve data. Instrument parameters: Injection volume, 50 microliters; wavelength, 546 nm; nitrogen pressure, 20 psig; sodium sulfate concentration, 0.6 M; buffer composition, 0.16 M acetic acid and 0.18 M sodium acetate; dye concentration 6 x 10^{-5} M (batch N-2 dissolved in 99.5% toluene and 0.5% methanol); extraction coil length, 450 cm (see figure 45).

TRS 10-80 (ppm)	TRS 10-80 (M)(a)	Peak area (a.i.u. x 10^6)	r.s.d. (%)
1.00	2.39 x 10^{-6}	0.65	4.4
5.03	12.0 x 10^{-6}	1.67	2.4
10.1	24.1 x 10^{-6}	2.52	2.0
25.2	60.2 x 10^{-6}	4.95	1.8
50.3	120 x 10^{-6}	7.99	1.8
75.5	181 x 10^{-6}	12.6	1.9
100	241 x 10^{-6}	17.7	1.9
126	301 x 10^{-6}	23.4	1.5
151	361 x 10^{-6}	27.7	0.78
201	482 x 10^{-6}	38.7	0.78
252	602 x 10^{-6}	47.0	1.9

(a) Calculated assuming a molecular weight of 418.

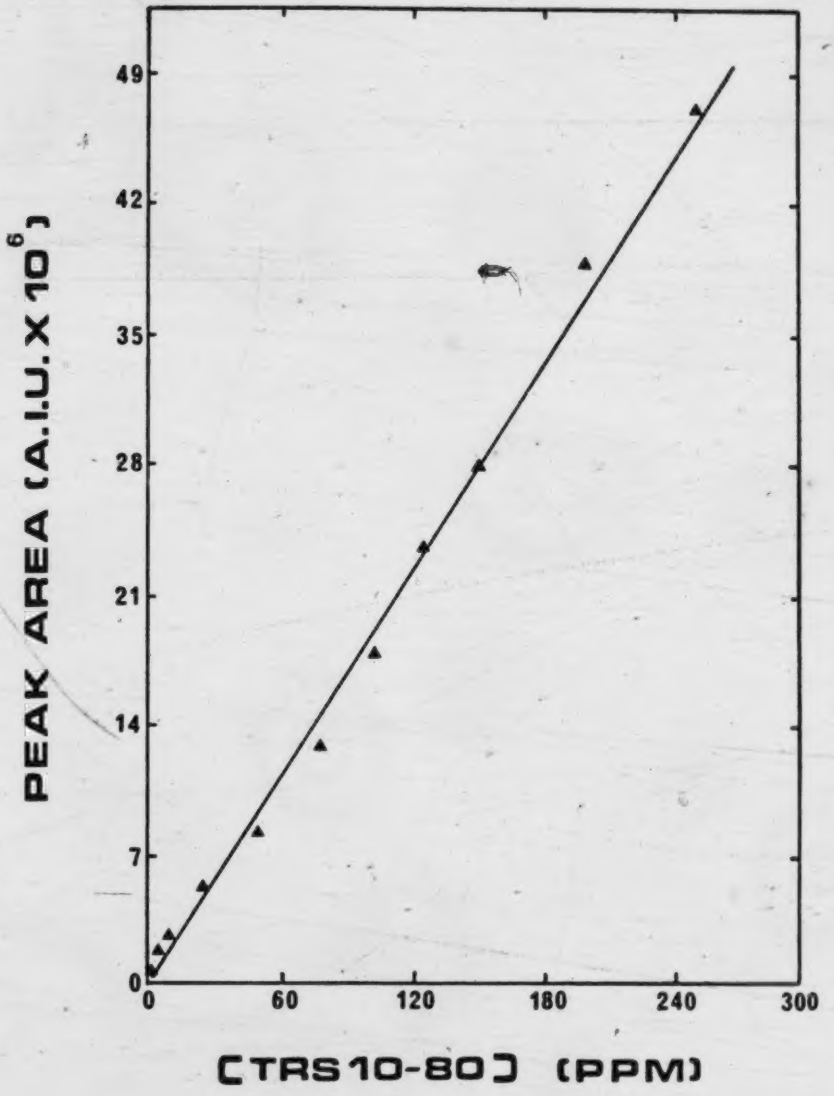

Figure 47. TRS 10-80 Calibration curve. Instrument parameters: As in table XXX.

suspended material. Once a homogeneous liquid was obtained, two solutions of about 1000 ppm were prepared, and from each of these two further dilutions were made at about 500 ppm. Since a standard of the surfactants in Enordet was not available, SLSN was utilized as a reference material in the SE/FIA determination of Enordet samples. In the two phase titration method, dodecansulfonic acid sodium salt (also referred to as sodium lauryl sulfonate, SLSN) is often used for calibration purposes in the analysis of petroleum sulfonates. This compound is utilized as a reference material due to its chemical similarity with the samples and its availability in a state of high purity. Using the same conditions as in section 3.3.1, a SLSN calibration curve was obtained first, with the results shown in table XXXI and figure 48. The response signal was found to be linear from 0.5 ppm to about the 50 ppm level, with a slope equal to 2.09×10^6 (r.s.d. of slope= 0.98%) and an intercept equal to 9.72×10^5 (s.d. of intercept= 5.95×10^5). The determination of Enordet versus SLSN standards (in the concentration range from 25 to 40 ppm) was carried out in the SE/FIA system depicted in figure 45 under the initial conditions utilized in section 3.3.1. The following values were obtained: 6.55, 6.61, 6.49, and 6.68% for samples 1A, 1B, 2A, and 2B, respectively; from which a final average purity value of 6.58 ± 0.08% and a relative standard deviation among samples of 1.2% were computed.

When this value was compared to the value obtained at the Alberta Research Council via the two-phase titration method (29.5%), an obvious disagreement was observed. It was suspected that this discrepancy might be related to the fact that Enordet is more surface active than the reference material SLSN. Therefore, Enordet was re-determined under the same conditions in the SE/FIA system but this time using the TRS 10-80 standard material as a reference. The values obtained were: 30.86, 30.11, 29.36, 28.73, 30.54, and 31.56% for

Table XXXI. Sodium lauryl sulfonate calibration curve data. Instrument parameters: As in table XXX.

Sodium lauryl sulfonate		Peak area	r.s.d.
(ppm)	(M)(a)	(a.i.u. x 10^6)	(%)
0.51	1.87 x 10^{-6}	1.19	4.1
1.03	3.79 x 10^{-6}	2.19	1.7
5.13	18.9 x 10^{-6}	11.1	1.1
10.3	37.7 x 10^{-6}	22.9	2.2
15.4	56.7 x 10^{-6}	34.0	1.2
20.5	75.5 x 10^{-6}	44.0	1.3
25.7	94.3 x 10^{-6}	54.9	1.2
30.8	113 x 10^{-6}	67.9	0.72
35.9	132 x 10^{-6}	76.0	0.86
41.1	151 x 10^{-6}	87.4	0.87
46.2	170 x 10^{-6}	97.2	1.4
51.3	189 x 10^{-6}	106	0.81

(a) Calculated using a molecular weight of 272.

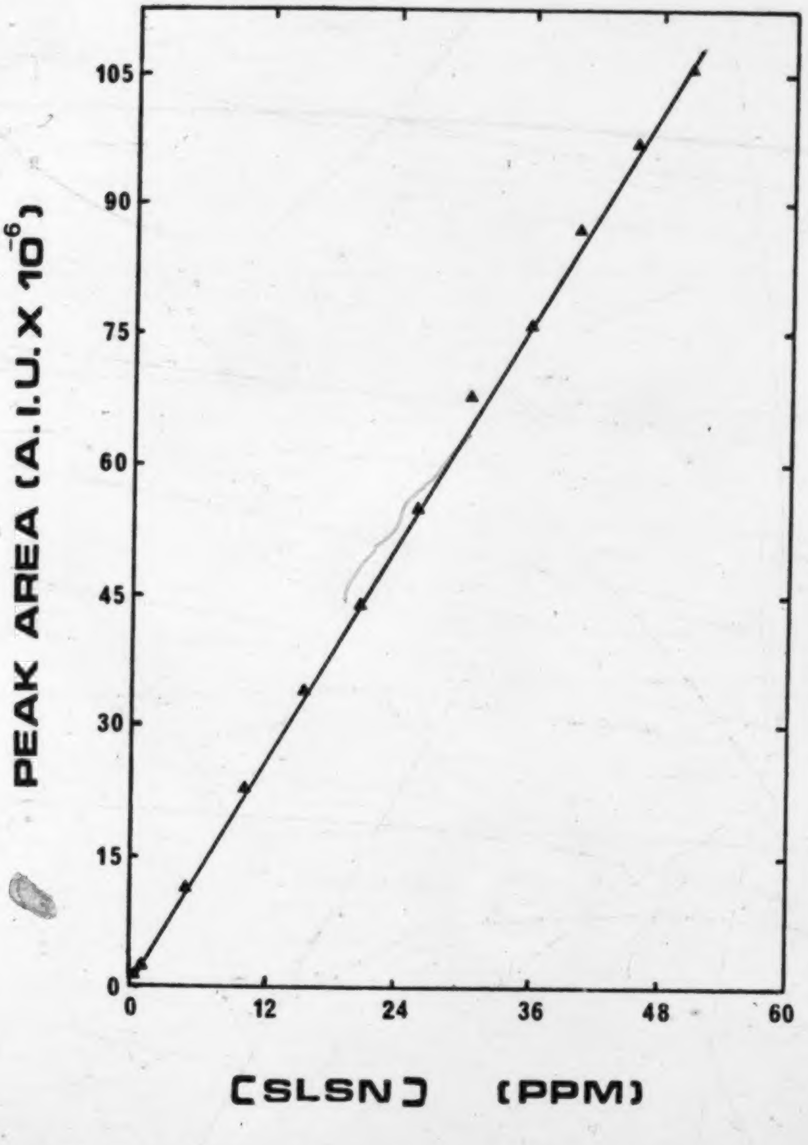

Figure 48. Sodium lauryl sulfonate calibration curve. Instrument parameters: As in table XXX.

samples 1A, 1B, 2A, 2B, 3A, and 3B, respectively. From these data, an average purity value of 30.2 ± 1.0% was obtained, in agreement with the two-phase titration value (29.5%).

3.3.3 Suntech IV

This sample is a mixture of natural petroleum sulfonates and synthetic sulfonates with an average molecular weight of 418. It is marketed as a seemingly homogeneous yellow liquid, from which 3 samples of approximately 2000 ppm were prepared. These were analyzed versus SLSN standards in the SE/FIA system presented in figure 45 under the conditions utilized in section 3.3.1. As was the case of Enordet, a discrepancy of results between the SE/FIA and the two-phase titration methods was found to exist: 0.64 ± 0.01% using the former against 14.98% utilizing the latter. This was attributed to the fact that the standard is less surface active than the sample.The explanation was thought to be as follows: Since SLSN is less surface active, the SLSN-dye ion pair is also less active than the Suntech IV-dye ion pair and the SLSN-dye ion pair is adsorbed to less extent at the organic-aqueous interface. As a consequence, the concentration of SLSN-dye ion pair in the bulk organic phase is disproportionally high. This, in turn, produces abnormally "high" response factors which, when compared to the "normal" response factors of surfactant samples, yield artificially low results. However, when the determination of Suntech IV was performed utilizing as reference the TRS 10-80 standard, which was believed to be more surface active than SLSN, the result obtained (5.52 ± 0.11%) was still quite far from the accepted value (14.98%). Therefore, it was thought that this discrepancy might arise from a different relative amount of interfacial adsorption, and that a more detailed and quantitative investigation of interfacial adsorption was required.

Interfacial adsorption was measured on the following materials: TRS 10-80 standard material, SLSN, Enordet, and Suntech IV. The study involved the creation and disappearance (using stirring and non-stirring conditions) of a large amount of interface between a toluene-water system containing a surfactant-dye ion pair, while monitoring the absorbance of the organic phase. A typical plot of absorbance versus time is presented in figure 49. The fact that there is a dependence of organic phase absorbance upon degree of agitation in this type of systems has been reported before [19]. During vigorous stirring, the organic-aqueous interfacial area is increased by several orders of magnitude. If the bulk organic phase contains an ion pair prone to be adsorbed at the interface, then this increase in the amount of interface causes a decrease in the concentration, and hence the absorbance, of such an ion pair in the bulk solution. Conversely, in the absence of vigorous stirring, the multitude of droplets present in the aqueous-organic system coalesce and give rise to a state of minimum interfacial area; thereby forcing the ion pair into the bulk solution again, and causing its absorbance to increase. The results obtained for the four samples are presented in table XXXII.

If the absorbance values obtained in this study are utilized in conjunction with the concentrations of each sample, the assay values presented in table XXXIII are obtained. From the data of these two tables it can be inferred that all four samples are adsorbed onto the interface to approximately the same extent (since all four samples have roughly the same absorbance decrement and this reflects the extent of interfacial adsorption); that in this system, as opposed to the SE/FIA system, the use of TRS 10-80 or SLSN as reference material produces essentially the same result; and that the reason for having different results when different standard materials are used in the SE/FIA system is not primarily due to the degree of adsorption at the interface.

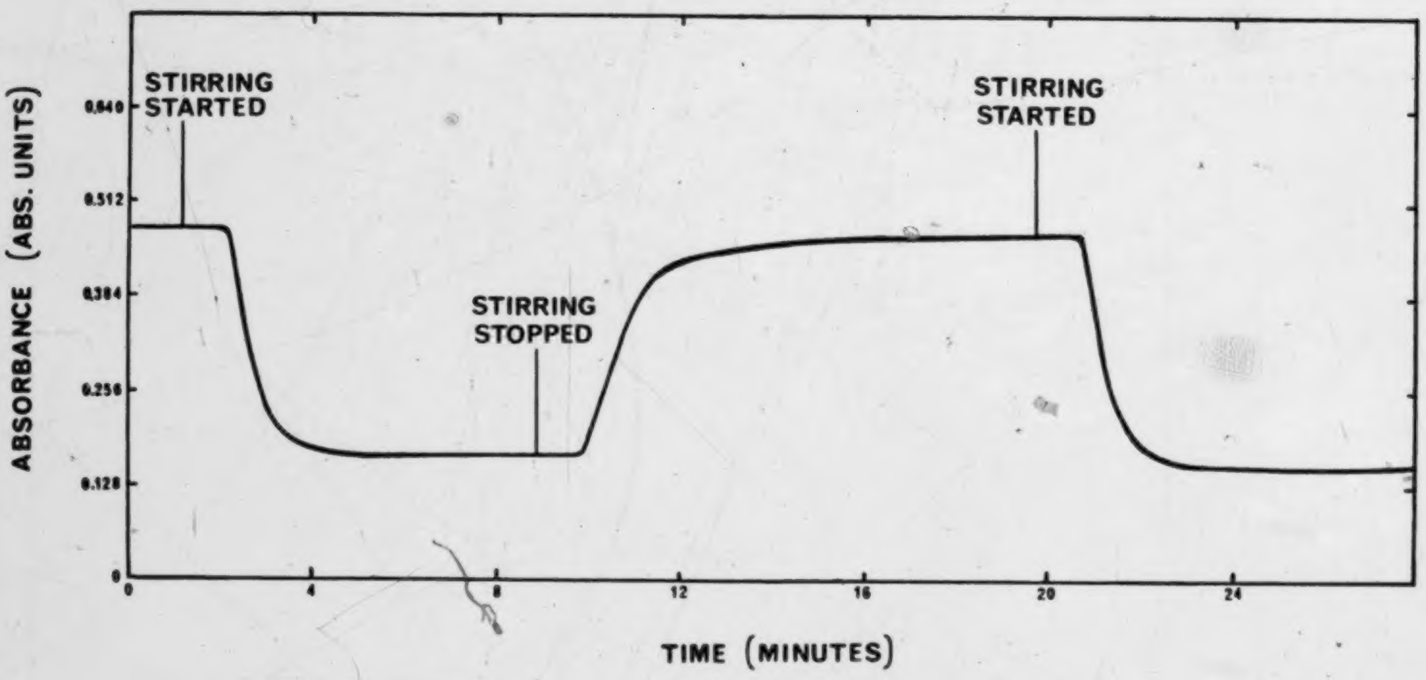

Figure 49. Spectrophotometric recorder tracing for the determination of interfacial adsorption of TRS 10-80. Instrument parameters: As in table XXXII. See text for details of the procedure.

Table XXXII. Interfacial adsorption data. Instrument parameters: Wavelength of detection, 546 nm; dye concentration, 6×10^{-5} M (dissolved in 99.5 % toluene and 0.5 % methanol); buffer composition, 0.18 M sodium acetate and 0.16 M acetic acid; sodium sulfate concentration, 0.6 M; volume ratio of organic to aqueous phase, 1.8; molar ratio of dye to surfactant, 6. See text for details of the procedure.

Sample	[ion pair](a) (M)	Absorbance under non-stirring conditions (abs. units)	Absorbance under stirring conditions (abs. units)	Absorbance decrement(b) (%)
TRS 10-80	9.93×10^{-6}	0.56	0.21	62
SLSN	9.65×10^{-6}	0.58	0.19	67
ENORDET	10.2×10^{-6}	0.59	0.13	78
SUNTECH	9.74×10^{-6}	0.60	0.24	60

(a) In the bulk organic phase assuming quantitative (100 %) extraction.

(b) Calculated as follows:

[1 - (abs. under stirring cond. / abs. under non-stirring cond.)] 100

Table XXXIII. Assay values under non-stirring/stirring conditions. Instrument parameters as in table XXXII.

Standard	Sample	Assay under non-stirring conditions[(a)] (%)	Assay under stirring conditions[(a)] (%)	SE / FIA assay value[(b)] (%)
TRS10-80	SLSN	107	93.1	—
TRS10-80	ENORDET	30.8	18.1	30.2
TRS10-80	SUNTECH	16.4	17.5	5.5
SLSN	TRS 10-80	93.8	107	—
SLSN	ENORDET	28.9	19.4	6.6
SLSN	SUNTECH	15.4	18.8	0.6

(a) Assay values were calculated using equation 3.1 but absorbance values were utilized instead of peak areas.

(b) SE/FIA values are shown for comparison purposes.

Note: The two-phase titration assay data are: 80.0% for TRS 10-80, 29.5% for Enordet, and 15.0% for Suntech IV.

A possible explanation for the differences observed in the SE/FIA system for SLSN and TRS 10-80 may be ascribed to a different extent of coalescence of the two phases in the chamber of the phase separator. If coalescence is faster for one of these compounds than for the other, then the amount of interface at the time of phase separation, and thus the concentration of sample in the bulk organic phase, would be different thereby causing different response factors.

Considering the above results, it was clear that the reason for the discrepant assay values had not yet been discovered. Consequently, several experimental variables were investigated in order to find a clue to the reason for this discrepancy.

3.3.3.1 Extraction coil length.

The behavior of the SE/FIA system shown in figure 45 as a function of extraction coil length was studied on chapter 2 under the same ("initial") conditions that are currently being utilized. In those experiments, it was found that a coil length of 450 cm was enough to attain distribution equilibrium. However, this was done utilizing sodium lauryl sulfate as a model compound and it was thought that, perhaps, the experiment could not be extrapolated to the other surfactants that are being used in this part of the project. Consequently, the extraction coil length was increased from 450 to 750 cm and the assay of Suntech IV repeated using SLSN as a standard. The assay value was found to increase from 0.64 ± 0.01% for the shorter coil to 1.25 ± 0.03% for the longer coil. Even though this may seem to indicate that equilibrium had not been attained using the extraction coil length of 450 cm (the assay value increased presumably because a longer coil allows a closer approach to extraction equilibrium), the fact that the purity value was still much too low in comparison with the expected two-phase titration value (14.98%) clearly indicated that coil length was not the main factor causing low assay values.

3.3.3.2 Insufficient ethyl violet concentration.

Since the last test suggested that equilibrium was not being attained, it was postulated that perhaps our low purity values were caused by an insufficient amount of ethyl violet in the system. Therefore, the Suntech IV samples were reanalyzed versus SLSN under the conditions utilized in sub-section 3.3.3.1 but with the concentration of dye doubled. The new assay value increased slightly to 1.60 ± 0.03%, suggesting again that equilibrium may not have been achieved yet. However, the increment was so slight that it suggested the dye concentration was not the major cause of low purity values.

3.3.3.3 pH.

Another possible explanation for the disagreement observed between the SE/FIA and the titration methods was thought to be pH. As indicated in chapter 2, the range of maximum absorbance for the surfactant-ethyl violet ion pair occurs when the pH is between 3 and 6. Since the pH of Suntech IV in the original sample was found to be 8.6 (9.7 for Enordet), a new hypothesis was postulated. If the pH of the sample were outside the maximum absorbance range and the amount of buffer present in the system were not enough to overcome it and bring the sample into this range, then a "reduced" absorbance would be obtained for the sample and a "normal" absorbance for the standard, thereby causing low assay values. To check this hypothesis, the following tests were performed. (i) A measurement of the pH of the standard and sample solutions utilized for the preceding analyses (prepared by diluting the original compounds with distilled water) gave as a result 5.8 and 6.3 for SLSN and Suntech IV, respectively. (ii) If instead of using distilled water to dilute the sample, a mixture of acetate buffer and sodium sulfate at the concentration levels used in the SE/FIA system was employed, the observed pH values were 4.6 for both the standard and the sample. Upon analysis of these solutions in the SE/FIA system under the conditions utilized on sub-section 3.3.3.1, a decreased assay value of 0.70 ± 0.03% was found. During the preparation of these solutions, it was noticed that the sample solution was very cloudy whereas the standard solution was clear. If no sodium sulfate was used to prepare the sample and standard solutions, but only the acetate buffer; cloudiness of the sample solution was still observed. (iii) When the sample and standard solutions were prepared using distilled water acidified with one drop of acetic acid, the pH of both solutions was found to be 3.9; and no cloudiness was observed in either solution. Analysis of these solutions under the conditions described in sub-section 3.3.3.1 gave an assay value equal to 1.30 ± 0.03%. The fact that the pH values of the standard and sample solutions were nearly within the range of maximum absorbance, and that low assay values were obtained even when such solutions were brought into this range; clearly indicated that pH was not responsible for the low-response problem.

3.3.3.4. Micelle formation.

The cloudiness observed when the sample was prepared in the acetate buffer or the mixture of buffer and sodium sulfate provided a new hypothesis based on the fact that the presence of salts in surfactant solutions lowers the critical micelle concentration [1]. If micelle formation occurs when the surfactant sample comes in contact with the buffer-sodium sulfate mixture in the SE/FIA system, the rate of reaction between the micellized sample and the dye would be slower than when the sample is not present in the form of micelles, thereby making the extraction incomplete in the time available. Since the standard solution did not show any cloudiness, micelle formation does not occur and, thus, its extraction is not affected. The fact that augmented assay values were obtained upon utilizing a longer extraction coil (sub-section 3.3.3.1) or a doubled dye concentration (sub-section 3.3.3.2) seems to corroborate this hypothesis since the inhibited dye-micellized surfactant reaction would have a longer time/higher probability to occur. Also, when the buffer-sodium sulfate mixture contained in the "buffer" cylinder in the SE/FIA system was replaced by distilled water, the sample and standard solutions prepared utilizing only distilled water, and the determination of Suntech IV repeated; the assay value increased to 4.44 ± 0.04%, in spite of the fact that in the absence of the buffer and sodium sulfate there was no "salting-out" of the ion pair. This enhanced recovery of surfactant is presumably due to the elimination of micelle formation prior to the mixing of dye with the surfactant.

3.3.3.5 Avoiding micellization.

In order to avoid micelle formation while still retaining the buffer and sodium sulfate which are necessary to control the pH and to "salt out" the ion pair, a rearrangement was made in the configuration of the instrument (see figure 45). So far, the sample-containing carrier stream has been mixed first with the emerging flow of the buffer-sodium sulfate solution and then with the reagent-containing organic phase. In order to minimize micelle formation, the buffer-sodium sulfate solution was combined with the carrier stream after the carrier had merged with the dye-containing organic phase. This was done by adding an extra tee, which allows the introduction of the buffer-sodium sulfate solution into the extraction coil at a point located downstream from the segmentor as shown in figure 50. Thus, the dye was transferred from the organic into the aqueous phase, where the sample was contained, and the ion pair formation occurred before the buffer-sodium sulfate mixture was incorporated. In this new configuration, the distance between T_2 and T_3 was expected to influence the results of the assay. On the one hand, if it were too small it would allow micellization to occur, while on the other hand, if it were too long it would cause incomplete salting out and pH control. Therefore, several tests were

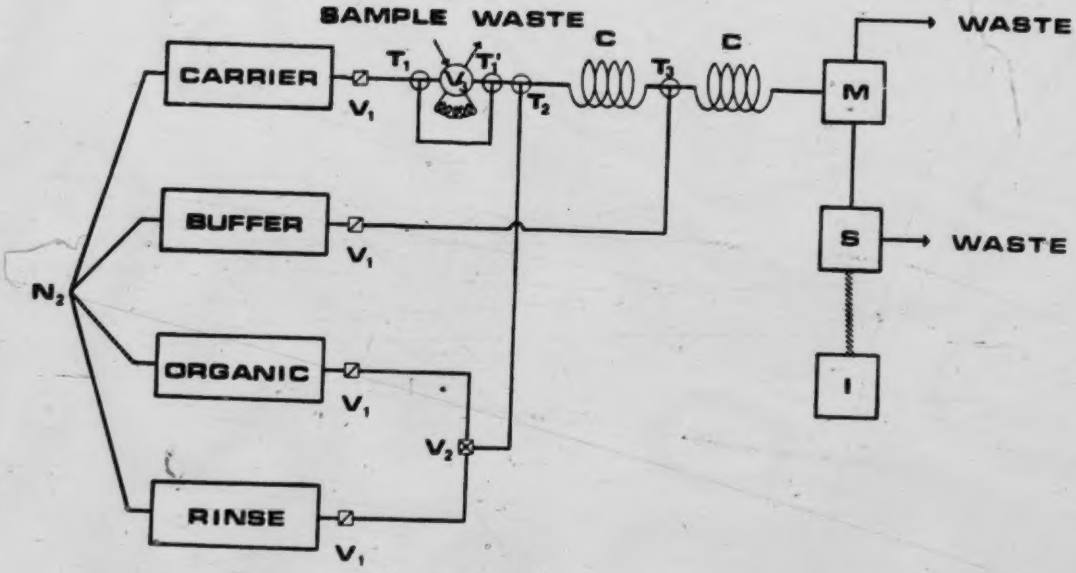
SAMPLE
WASTE
CARRIER
BUFFER
ORGANIC
RINSE
N_2
V_1
V_2
T_1
T_1'
T_2
T_3
C
C
M
S
I
WASTE
WASTE

Figure 50. Block diagram of the modified solvent extraction/flow injection analysis apparatus utilized for the analysis of surfactant sample.The contents of the cylinders are: Methanol in the "Rinse" cylinder; acetate buffer and sodium sulfate in the "Buffer" cylinder; distilled water in the "Carrier"; and an ethyl violet solution prepared with a mixture of 99.5% toluene and 0.5% methanol in the "Organic" cylinder. "C" is the extraction coil (which has now been divided); "M" the membrane phase separator; "S" a spectrophotometric detector; and "I" is an integrator.

performed using various lengths of tubing between T_2 and T_3 and from T_3 to the phase separator. The instrument conditions and the results obtained can be seen on table XXXIV. It was observed that a distance from T_2 to T_3 equal to 50 cm gave the highest assay value of Suntech IV yet obtained in the SE/FIA system when using SLSN as standard. However this value of about 6.8% was still too low when compared to the two-phase titration value of 14.98%. Increasing the distance between T_2 and T_3 (tests 1-4) did not further increase the assay values. Furthermore, if the distance from T_3 to the phase separator becomes shorter than 600 cm (tests 4 and 5), the assay values drop, pressumably due to incomplete salting out and pH control. It was only when TRS 10-80 standard was substituted for SLSN (test 6), that the content of active matter in Suntech IV evaluated via SE/FIA was finally consistent with the results of the two-phase titration. The assay values were: 14.96, 14.91, 14.34, 14.84, 15.01, and 15.18%; which produced an average value of 14.88 ± 0.29%.

3.3.3.6 Final conditions versus initial conditions.

Even though the TRS 10-80 and Enordet samples had at this point already been successfully analyzed via SE/FIA, the fact that the Suntech IV sample could only be analyzed satisfactorily under the conditions developed to avoid micellization suggested that all of our samples should be re-run under such conditions. The results of these analyses are presented in table XXXV, in which "initial conditions" refer to the ones utilized previously (see sections 3.3.1 and 3.3.2) and "final conditions" refer to the ones developed to avoid micellization utilizing a distance of T_2 to T_3 equal to 50 cm.

The use of the so-called final conditions made it possible to quantitatively determine all three samples (TRS 10-80, Enordet, and Suntech IV) with results in agreement with the values obtained via the two-phase titration method. Nevertheless, the fact that satisfactory results for Suntech IV could only be

Table XXXIV. Avoiding micellization of Suntech IV. Instrument parameters: Dye concentration, 6 x 10^{-5} M (dissolved in a mixture of 99.5% toluene and 0.5% methanol); sodium sulfate concentration, 0.6 M; buffer composition, 0.18 M sodium acetate and 0.16% M acetic acid; total extraction coil length, 750 cm (see figure 50); injection volume, 50 microliters; wavelength, 546 nm; nitrogen pressure, 20 psig.

Test	Standard	T_2- T_3 distance (cm)	T_3- PS distance (cm)	Assay$^{(a)}$ (%)	r.s.d. (%)
1	SLSN	50	700	6.8	1.6
2	SLSN	100	650	6.2	3.3
3	SLSN	150	600	6.9	3.5
4	SLSN	300	450	3.7	4.0
5	SLSN	150	300	3.6	5.5
6	TRS10-80	50	700	14.9	2.2

Note: PS stands for phase separator.

(a) Assay by two phase titration= 15.0%

Table XXXV. Assay of samples under "initial conditions" (instrument parameters as in table XXX) and "final conditions", instrument parameters: Injection volume, 50 microliters; wavelength, 546 nm, nitrogen pressure, 20 psig; sodium sulfate concentration, 0.6 M; buffer composition, 0.16 M acetic acid and 0.18 M sodium acetate; dye concentration 6 x 10^{-5} M (batch N-2 dissolved in 99.5% toluene and 0.5% methanol); total extraction coil length, 750 cm (T_2-T_3 distance= 50 cm, T_3-phase separator distance=700 cm. See figure 50.

		TRS 10-80(a)	ENORDET(b)	SUNTECH IV(c)
INITIAL CONDITIONS				
Using SLSN as std.	(%)	—	6.6 ± 0.1	0.6 ± 0.0
Using TRS 10-80 as std.	(%)	76.3 ± 1.4	30.2 ± 1.0	5.5 ± 0.1
FINAL CONDITIONS				
Using SLSN as std.	(%)	—	—	6.8 ± 0.1
Using TRS 10-80 as std.	(%)	79.9 ± 1.6	29.7 ± 0.5	14.9 ± 0.3

(a) The two-phase titration assay was equal to 80.8%.

(b) The two-phase titration assay was equal to 29.5%.

(c) The two-phase titration assay was equal to 15.0%.

obtained when the TRS 10-80 standard material was used (and not when using the SLSN standard material), clearly indicated that the choice of an appropriate standard is of utmost importance for obtaining correct assay values. When a particular sample is to be analyzed, and a reference material of the same compound is available, the analysis can be readily performed without complications. If, however, the same material is not available in pure form for use as a standard, then a very careful selection of a standard material has to be made by trial-and-error experiments involving a comparison of results to those determined by a reliable, though less convenient method, such as the two-phase titration. Further study is required to fully understand the cause of the non-equivalence of different standard materials and to develop SE/FIA conditions under which various standards are equivalent.

3.3.4 Comments

In summary, a set of SE/FIA conditions is now available for the determination of anionic surfactants by ion pair formation with ethyl violet, with all the inherent advantages of an automated method. This method follows logically from Motomizu's manual method [131] and from the semi-automated version based on a combination of manual and FIA techniques proposed by Hirai et al. [142].

Several rather "unique" features of the behavior of surfactants in SE/FIA determinations by ion pair extraction have been examined, and their effect on the efficiency of extraction has been evaluated. Among these features, the adsorption of dye, surfactant, and ion pair onto the liquid-liquid and liquid-solid interfaces of the system; the formation of charged colloidal ion pairs; and the micellization of surfactant in the aqueous phase at high ionic strength, have proved important.

The method can be used to determine about 30 samples/h with a precision of 2%, evaluated from the relative standard deviation of the slope in several calibration curves, and from the relative standard deviation among samples observed during their analyses. The dynamic range is estimated to go from about 1 to 100 ppm, thereby allowing the determination of surfactants in enviromental samples without pre-concentration or in more concentrated samples upon appropriate dilution.

The fact that standard materials are not equivalent indicates that further work is still required. Some recommended future studies are the following:

(1) The extent of coalescence of the phases in the phase separator chamber should be examined as a function of the type of surfactant employed. It may be that coalescence is faster with some surfactants, thereby causing higher concentrations in the bulk phase present in the phase separator.

(2) A study of the mass transfer processes in segmented flow involving reagents, solutes, and products that may form micelles or colloidal ion pair precipitates, and which are surface active, would be extremely useful.

(3) Long term future work should probably focus on interfacing the SE/FIA system with separation techniques to allow the determination of each surfactant in complex mixtures.

BIBLIOGRAPHY

1. D. Attwood & A. T, Florence, "Surfactant Systems", Chapman, New York (1983).

2. J. Cross, "Anionic Surfactants-Chemical Analysis", Marcel Dekker Inc., New York (1977).

3. R. Wickbold, Seifen, Ole, Fette, Wachse 86, 79 (1960).

4. K. Bey, Fette, Seifen, Anstrichmittel 67, 25 (1965)

5. H. Koing, Z. Anal. Chem. 254, 337 (1971).

6. A. E. O'Donnell, Soap Chem. Specialities 47, 26 (1971).

7. W. H. Houff, D.F. Christie, R. H. Beaumont, Anal. Chem. 29, 1866 (1957).

8. E. A. Gribova, Ind. Lab. 27, 155 (1961).

9. R. K. Maurmeyer & M. Rafalowits, Mikrochim. Acta 561 (1964).

10. R. R. Parmar & B. M. Sahukar, Ind. Lubr. Tribol. 28, 192 (1976).

11. S. K. Chhibber & O. N. Anad, Indian J. Technol. 14, 355 (1976).

12. D. Jeffries & J. Fresco, Can. J. Chem. 59, 1497 (1981).

13. J. Chlebicki & W. Garncarz, Tenside deterg. 17, 13 (1980).

14. R. Wickbold, Tenside deterg. 9, 173, (1972).

15. D. J. Fenwick, Ind. Lubr. Tribol. 23, 201 (1971)

16. I. P. Brewer, J. Inst. Pet. (London), 58, 41 (1972).

17. K. L. Wang & J. K. Yang, Water Resour. Bull. 11, 267 (1975).

18. Z. Li & M. J. Rosen, Anal. Chem. 53, 1516 (1981).

19. H. Y. Mohammed & F. F. Cantwell, Anal. Chem. 52, 553 (1980).

20. A. Braun & B. Czajkowska, Chem. Abs. 96: 183193 g.

21. V. V. Nekrasova & L. K. Mukhin, Chem. Abs. 96: 96821 z.

22. J. Longwell & W. D. Maniece, Analyst 80, 167 (1955).

23. E. H. Bradli & R. M. Kelley, J. Am. Oil Chem. Soc. 47, 200 (1970).

24. T. Tanaka, K. Hiiro, and A. Kawahara, Japan Anal. 24, 320 (1970).

25. L. K. Wang & R. G. Ross, Int. J. Environ. Anal. Chem. 4, 285 (1976).

26. S. Taguchi, I. Kasahara, Y. Fukushima, and K. Goto, Talanta 28, 616 (1981).

27. K. Higuchi, Y. Shimoishi, and K. Toei, Bull. Chem. Soc. Jpn. 55, 621 (1982).

28. N. H. Anderson & J. Girling, Analyst, 107, 836 (1982).

29. L. Farreto, B. Stancher, and F. Tunis, Analyst 105, 833 (1980).

30. K. Toei, S. Motomizu, and T. Umano, Talanta 29, 103, (1982).

31. Z. Marzenko & H. Kalowska, Anal. Chim. Acta 123, 279 (1981).

32. J. R. Crawford & C. R. Robbins, J. Soc. Cosmet. Chem. 31, 273 (1980).

33. J. Kawase, Anal. Chem. 52, 2124 (1980).

34. A. Heywood, A. Mathias, and A. E. Williams, Anal. Chem. 42, 1272 (1970).

35. K. C. Schreiber, Anal. Chem. 21, 1168 (1949).

36. H. Alter & M. Bit-Alkhas, Text. Res. J. 39, 479 (1969).

37. J. L. Boyer, J. P. Canselier, and V. Castro, J. Am. Oil Chem. Soc. 59, 458 (1982).

38. H. Cerfontain, A. Koeberg-Telder, and C. Kruk, Anal. Chem. 46, 72 (1974).

39. N. Ishabashi, J, Kohara, and K. Horinouchi, Talanta 20, 867 (1973).

40. A. Craggs, G. J. Moody, J. D. R. Thomas, and B. J. Birch, Analyst 105, 426 (1980).

41. G. C. Dilley, Analyst 105, 713, (1980).

42. A. Hulanicki, M. Trojanowics, and E. Pobozy, Analyst 107, 1356 (1982).

43. H. Shiraishi, A. Otsuki, and K. Fuwa, Bull. Chem. Soc. Jpn. 55, 1410 (1982).

44. K. Takeshita, N. Jinnai, and H. Yoshida, J. Chrom. 123, 301 (1976).

45. J. Franc, V. Pikes, and M. Hajkova, J. Chrom. 119, 616 (1976).

46. M. Koehler & B. Chalupka, Chem. Abs. 97: 25530 p.

47. C. Yonese, T. Shishido, T. Kaneko, and K. Maruyama, J. Am. Oil Chem. Soc. 59, 112, (1982).

48. O. R. Adlof & E. A. Emken, J. Am. Oil Chem. Soc. 58, 99 (1981).

49. S. Anquera, D. J. J. Garcia, L. J. Sanchez, and M. Dalman, Invest. Inf. Text. Tensoactivos 24, 305 (1981).

50. J. J. Kirkland, Anal. Chem. 32, 1388 (1960).

51. S. Siggia & L. R. Whitlock, Anal. Chem. 42, 1719 (1970).

52. R. D. Swisher, J. Am. Oil Chem. Soc. 43, 137 (1966).

53. J. S. Parsons, J. Gas Chromatogr. 5, 254 (1967).

54. P. Thackeray & D. Hoar, Methodology Surv. 10, 161 (1981).

55. G. Goretti, L. Zoccolillo, F. Greaci, and S. Gravina, Chromatographia 15, 361 (1982).

56. J. L. Boyer, J. P. Canselier, and V. Castro, J. Am. Oil Chem. Soc. 59, 458 (1982).

57. L. Farkas, J. Margos, P. Sallay, I. Rusznak, B. Bartha, and C. Veress, J. Am. Oil Chem. Soc. 58, 650 (1981).

58. S. Kawase, K. Kirose, and S. Ukai, J. Chrom. 213, 265 (1981).

59. K. Weber, K. Leusen, G. V. Louter, A. J. H. Boerboom, and P. J. Haverkamp, Anal. Chem. 54, 1458 (1982).

60. P. Daehling, F. W. Roellgen, J. J. Zwinselman, R. H. Fokkens, and N. M. M. Nibbering, Fresenius' Z. Anal. Chem. 312, 335 (1982).

61. W. R. Ali & P. T. Lawrence, Anal. Chem. 45, 2426 (1973).

62. J. C. Kraak & J. F. K. Huber, J. Chrom. 102, 333 (1974).

63. C. P. Terweij-Groen & J. C. Kraak, J. Chrom. 138, 245 (1977).

64. K. G. Wahlund, J. Chrom. 115, 411 (1975).

65. J. J. Kirkland, Anal. Chem. 43, 37A (1971).

66. J. H. Knox & G. R. Laird, J. Chrom. 122, 17 (1976).

67. D. J. Pietrzyk & C. H. Chu, Anal. Chem. 49, 860 (1977).

68. D. E. Linder & M. C. Allen, J. Am. Oil Chem. Soc. 59, 152 (1982).

69. C. P. Terweij-Groen, J. C. Kraak, W. M. A. Niessen, J. Lawrence, C. F. Werkhoven-Goewie, U. A. T. Brinkman, and R. W. Frei, Int. J. Environ. Anal. Chem. 9, 45 (1981).

70. F. Smedes, J. C. Kraak, C. F. Werkhoven-Goewie, U. A. T. Brinkman, R. W. Frei. J. Chrom. 247, 123 (1982).

71. K. Nakamura, Y. Morikawa, and I. Matsumoto, J. Am Oil Chem. Soc. 58, 72 (1981).

72. K. Nakamura & Y. Morikawa, J. Am. Oil. Chem. Soc. 59, 64, (1982).

73. J. D. Willett, E. P. Brody, M. M. Knight, J. Am. Oil Chem. Soc. 59, 273 (1982).

74. M. C. Allen & D. E. Linder, J. Am. Oil Chem. Soc. 58, 950 (1981).

75. J. D. McClure, J. Am. Oil Chem. Soc. 59, 364 (1982).

76. A. Nozawa & T. Ohnuma, J. Chrom. 187, 261 (1980).

77. M. Kudoh, S. Fudano, and S. Yamaguchi, J. Chrom. 205, 473 (1981).

78. E. Fernandez & J. Marzo, Fis.-Quim. Apl. Jrn. Com. Esp. Deterg. 11, 543 (1980).

79. S. L. Abidi, J. Chrom. 213, 463 (1981).

80. V. T. Wee & J. M. Kennedy, Anal. Chem. 54, 1631 (1982).

81. A. Nakae, K. Tsuji, and M. Yamanaka, Anal. Chem. 53, 1819 (1981).

82. J. Ruzicka & E. H. Hansen, "Flow Injection Analysis"; Wiley, New York (1981).

83. K. K. Stewart, G. R. Beecher, P. E. Hare, Anal. Biochem. 70, 167 (1976).

84. R. Tijssen, Anal. Chim. Acta 114, 71, (1980).

85. L. T. Skeggs, Anal. Chem. 38, 31A (1966).

86. B. Karlberg & S. Thelander, Anal. Chim. Acta 98, 1 (1978).

87. F. H. Bergamin, J. X. Medeiros, B. F. Reiss, and E. A. G. Zagatto, Anal. Chim. Acta 101, 9 (1978).

88. F. F. Cantwell & J. A. Sweileh, Anal. Chem. 57, 329 (1985).

89. B. Karlberg, S. Thelander, P. A. Johansson, Anal. Chim. Acta 104, 21 (1979).

90. J. Kawase, A. Nakae, and M. Yamanaka, Anal. Chem. 51, 1640 (1979).

91. L. Nord & B. Karlberg, Anal. Chim. Acta 118, 285 (1980).

92. T. Imasaka, T. Harada, and N. Ishibashi, Anal. Chim. Acta 129, 195 (1981).

93. L. Nord & B. Kalberg, Anal. Chim. Acta 125, 199 (1981).

94. L. Fossey & F. F. Cantwell, Anal. Chem. 54, 1693 (1982).

95. P. A. Johansson, B. Karlberg, and S. Thelander, Anal. Chim. Acta 114, 215 (1980).

96. A. H. M. T. Scholten, U. A. T. Brinkman, and R. W. Frei, J. Chrom. 205, 229 (1981).

97. L. Snyder, J. Levine, R. Stoy, and A. Conetta, Anal. Chem. 48, 942A (1976).

98. L. Snyder & H. J. Adler, Anal. Chem. 48, 1022 (1976).

99. O. Astrom, Anal. Chim. Acta 105, 67 (1979).

100. E. H. Hansen & J. Ruzicka, J. Chem. Educ. 56, 677 (1979).

101. J. B. Landis, Anal. Chim. Acta 114, 155 (1980).

102. B. F. Reiss, H. F. Bergamin, E. A. G. Zagatto, and J. F. Krug, Anal. Chim. Acta 109, 45 (1979).

103. J. W. B. Stewart, J. Ruzicka, H. F. Bergamin, and E. A. G. Zagatto, Anal. Chim. Acta 81, 371 (1976).

104. B. Karlberg & S. Thelander, Anal. Chim. Acta 114, 129 (1980).

105. K. Kina, K. Shiraishi, and N. Ishibashi, Talanta 25, 295 (1978).

106. O. Klinghoffer, J. Ruzicka, and E. H. Hansen, Talanta 27, 169 (1980).

107. M. Bengtsson and G. Johansson, Anal. Chim. Acta 158, 147 (1984).

108. K. Backstrom, L. G. Danielsson, and L. Nord, Analyst 109, 323 (1984).

109. L. Nord & B. Karlberg, Anal. Chim. Acta 145, 151 (1983).

110. J. A. Sweileh & F. F. Cantwell, Anal. Chem. 57, 420 (1985).

111. E. H. Hansen & J. Ruzicka, Anal. Chim. Acta 87, 353 (1976).

112. H. Baadenhuijsen & H. E. H. Seuren-Jacobs. Clin. Chem. 25, 443 (1979).

113. J. F. Lawrence, U. A. T. Brinkman, and R. W. Frei, J. Chrom. 185, 473 (1979).

114. J. F. Lawrence, U. A. T. Brinkman, and R. W. Frei, J. Chrom. 171, 73 (1979).

115. C. Van Buuren, J. F. Lawrence, U. A. T. Brinkman, I. L. Honigberg, and R. W. Frei, Anal. Chem. 52, 700 (1980).

116. R. J. Reddingius, G. J. de Jong, U. A. T. Brinkman, and R. W. Frei, J. Chrom. 205, 77 (1981).

117. K. Tsuji, J. Chrom. 158, 337 (1978).

118. C. E. Werkhoven-Goewie, U. A. T. Brinkman, and R. W. Frei, Anal. Chim. Acta 114, 147 (1980).

119. C. Ranger, Anal. Chem. 53, 20A (1981).

120. D. Betteridge, Anal. Chem. 50, 832A (1978).

121. J. Ruzicka & E. H. Hansen, Chemtech. Dec., 756 (1979).

122. C. Ranger, Am. Lab. 14, 56 (1982).

123. B. Rocks & C. Riley, Clin. Chem. 28, 409 (1982).

124. J. Ruzicka & E. H. Hansen, Anal. Chim. Acta 145, 1 (1983).

125. B. Karlberg, Am. Lab. 15, 73 (1983).

126. J. H. Jones, J. Assoc. Offic. Agric. Chem. 28, 398 (1945).

127. J. Longwell & W. D. Maniece, Analyst 80, 167 (1955).

128. D. C. Abbott, Analyst 87, 286 (1962).

129. A. Sodergren, Analyst 91, 113 (1966).

130. APHA-AWWA-WPCF "Standard methods for examination of water and wastewater", 15th edition, Washington, D. C. (1980).

131. S. Motomizu, S. Fujiwara, A. Fujiwara, and K. Toei, Anal. Chem. 54, 392, (1982).

132. R. Hux & F. F. Cantwell, Anal. Chem. 54, 1279 (1982).

133. E. Bishop, "Indicators", Pergamon Press LTD, Torónto (1972).

134. The Society of Dyers and Colorists, and the Association of Textile Chemists and Colorists, "Color Index", 3th ed., vol. 4, Yorkshire, England (1971).

135. Beilsteins Handbuch der Organischen Chemie 13, 2075 (1973).

136. H. E. Fierz-David, "Dyes and Coloring Matters", Allen's Commercial Organic Analysis, vol. VI, 5th ed., Blakiston's son & Co., Phil., Pa (1928).

137. I. Saenz Lascano Ruiz and C. La Roche, Bull. Soc. Chim. Fr. 1963, 1594.

138. H. Schweppe "Thin Layer Chromatography" 2nd ed., Springer-Verlag Inc. New York (1969).

139. M. B. Naff & A. S. Naff, J. Chem. Educ. 40, 534 (1963).

140. R. Takeshito, N. Itoh, and Y. Sakagami, J. Chrom. 57, 437 (1971).

141. F. F. Cantwell & H. Y. Mohammed, Anal. Chem. 51, 218 (1979).

142. Y. Hirai & K. Tomokuni, Anal. Chim. Acta 167, 409 (1985).

143. L. Nord & B. Karlberg, Anal. Chim. Acta 164, 233 (1984).

144. L. Anderson, Anal. Chim. Acta 110, 123 (1979).

145. M. F. Gine, H. F. Bergamin, F. A. G. Zagatto, and B. F. Reiss, Anal. Chim. Acta 114, 191 (1980).

146. "Journal of Flow Injection Analysis" vol. 1 and 2, Kyushu University, Fukuoka, Japan (1984 and 1985).

147. J. A. Sweileh & F. F. Cantwell, Can. J. Chem. 63, 2559 (1985)

148. V. W. Reid, G. F. Longman, and E. Heinerth. Commission Internationale d' Analyses (CIA) Report, Tenside 4, 292 (1967).

149. D. Hummel, "Identification and analysis of surface-active agents" Vol.1, Interscience, New York (1962).

150. S. R. Epton, Nature 160, 795 (1947).

151. S. R. Epton, Trans. Faraday Soc. 44, 226 (1948).

152. W. B. Smith, Analyst 84, 77 (1959).

153. T. Barr & W. V. Stubbings, J. Soc. Chem. Ind. 67, 45 (1948).

154. H. Y. Lew, J. Am. Chem. Soc. 41, 297 (1964).

155. F. F. Cantwell & H. Freiser, personal communication.